VERMONT
AGENCY OF TRANSPORTATION

ACOUSTIC EMISSION MONITORING OF PREFABRICATED AND PRESTRESSED REINFORCED CONCRETE BRIDGE ELEMENTS AND STRUCTURES

Dryver R. Huston, Principal Investigator
The University of Vermont
College of Engineering and Mathematical Sciences

November 2018

Research Project
Reporting on VTRC 16-3

Final Report 2018-02

The University of Vermont

1. Report No. 2018-02	**2. Government Accession No.**	**3. Recipient's Catalog No.**
4. Title and Subtitle Acoustic Emission Monitoring of Prefabricated and Prestressed Reinforced Concrete Bridge Elements and Structures		**5. Report Date** November 7, 2018 **6. Performing Organization Code**
7. Author(s) Huston, Dryver R; Dewoolkar, Mandar; Xia, Tian; Worley II, Robert		**8. Performing Organization Report No.**
9. Performing Organization Name and Address College of Engineering and Mathematical Sciences The University of Vermont 33 Colchester Ave. Burlington, VT 05405		**10. Work Unit No.** **11. Contract or Grant No.** VTRC 16-3
12. Sponsoring Agency Name and Address Vermont Agency of Transportation Research Section One National Life Drive Montpelier, VT 05633		**13. Type of Report and Period Covered** Final Report(2016-2018) **14. Sponsoring Agency Code**

15. Supplementary Notes
Conducted in cooperation with the U.S. Department of Transportation, Federal Highway Administration.

16. Abstract
Prefabricated and pre-stressed reinforced concrete beams and girders are integral components of many highway structures, including those build by rapid construction techniques. Concerns exist regarding the development of cracks during curing, form removal, detensioning, transport, installation, and operation. Non-destructive, Acoustic Emission (AE) sensing techniques have the potential for detecting and locating cracking in prefabricated, pre-stressed concrete girders used as Prefabricated Bridge Elements and Systems (PBES) in rapid construction practices as part of a Quality Assurance/Quality Control (QA/QC) program. AE sensing records transient elastic waves produced by the release of stored elastic energy resulting in plastic deformations (i.e., crack nucleation and growth) with an array of point sensors. The AE instrument system is relatively portable which can allow for it to be an option for both off-site fabrication QA/QC as well as on-site field QA/QC. This report presents a multi-stage research initiative on acoustic emission measurements of prefabricated and pre-stressed concrete beams used in highway bridge construction during detensioning, craned removal from formwork and transport to bridge sites, along with supporting laboratory tests and numerical analysis.

The project objectives are: 1. Identify suitable instruments to monitor pre-stressed and/or post-tensioned concrete girders for cracking activity; 2. Design and develop a reusable instrumentation package; 3. Measure performance and condition of concrete girders during fabrication and transport; 4. Identify test protocols and possible accept/fix/reject criteria for structural elements based on information from monitoring system; and 5. Develop plans for reusing monitoring instruments on multiple bridge projects. Presented are results from laboratory, full-scale girder fabrication, and transport monitoring, along with recommendations for future testing procedures and quality assurance protocol development.

17. Key Words Pre-stressed Concrete, Prefabricated Girders, Acoustic Emission, Quality Control	**18. Distribution Statement** No restrictions. This document is available through the National Technical Information Service, Springfield, VA 22161.

19. Security Classif. (of this report)	**20. Security Classif. (of this page)**	**21. No. Pages**	**22. Price**
Unclassified	Unclassified	139	

ABSTRACT

Prefabricated and pre-stressed reinforced concrete beams and girders are integral components of many highway structures, including those built by rapid construction techniques. Concerns exist regarding the development of cracks during curing, form removal, detensioning, transport, installation, and operation. Non-destructive, Acoustic Emission (AE) sensing techniques have the potential for detecting and locating cracking in prefabricated, pre-stressed concrete girders used as Prefabricated Bridge Elements and Systems (PBES) used in rapid construction practices as part of a Quality Assurance/Quality Control (QA/QC) program. AE sensing records transient elastic waves produced by the release of stored elastic energy resulting in plastic deformations (i.e., crack nucleation and growth) with an array of point sensors. The AE instrument system is relatively portable which can allow for it to be an option for both off-site fabrication QA/QC as well as on-site field QA/QC. This report presents a multi-stage research initiative on AE measurements of prefabricated and pre-stressed concrete beams used in highway bridge construction during detensioning, craned removal from formwork and transport to bridge sites, along with supporting laboratory tests and numerical analysis.

The project objectives are: 1. Identify suitable instruments to monitor pre-stressed and/or post-tensioned concrete girders for cracking activity; 2. Design and develop a reusable instrumentation package; 3. Measure performance and condition of concrete girders during fabrication and transport; 4. Identify test protocols and possible accept/fix/reject criteria for structural elements based on information from monitoring system; and 5. Develop plans for reusing monitoring instruments on multiple bridge projects. Presented are results from laboratory, full-scale girder fabrication, and transport monitoring, along with recommendations for future testing procedures and quality assurance protocol development.

ACKNOWLEDGMENTS

This work was funded by the Vermont Agency of Transportation (VTrans)

The authors would like to thank VTrans personnel who assisted in various stages of conception, planning and management of this project, including Nick van den Berg, Jonathan Razinger, Emily Parkany, Rob Young, Ian Anderson, Douglas Bonneau and Bill Ahern.

The authors would like to thank J P Carrara and Sons, Inc. of Middlebury, VT who granted access to their concrete facilities and transport processes and provided invaluable insights to regarding the behavior of pre-stressed concrete.

Several University of Vermont graduate and undergraduate students assisted with the preparation of the software and databases, and assisted with collecting data at bridge sites, including Dylan Burns, Daniel Orfeo, Robert Farrell and Mauricio Pereira

Table of Contents

CHAPTER 1
PROBLEM STATEMENT AND RESEARCH FOCUS

1.1 Introduction and Motivation

This research project addresses Quality Assurance/Quality Control (QA/QC) of prefabricated pre-stressed concrete girders used as Prefabricated Bridge Elements and Systems (PBES) with attention paid to monitoring and controlling cracking in the girders. Preventing and mitigating such problems early on may be possible with the use of a properly designed reusable condition monitoring instrumentation system, when combined with effective QA/QC practices. Solving these problems has significant implications for the construction of highway structures in Vermont and nationwide.

PBES techniques make extensive use of manufacturing bridge components off site and shipping as needed to accelerate bridge construction, including prefabricated pre-stressed concrete girders. Advantages of these girders include strength and the ability to be lifted into place with a crane, thereby avoiding the complexity of lateral slide in place maneuvers. The girders can come with wide top flanges and top side studs to enable casting in place an integral concrete deck immediately following girder placement. Such construction can quickly produce a strong integrated pre-stressed and reinforced deck-girder configuration.

During this process many problems could occur that may damage the concrete/beam at different stages of manufacturing and construction process, including:

1) Rapid load transfers from pre-stress tendon cuts,

2) Cutting the tendons before the concrete fully sets,

3) Improper lifting of the beam for transport, shipping the component,

4) Placing it in its final position, and

5) Post installation cracking often due to misalignment poor materials or miscalculated dimensions.

A significant potential drawback to using prefabricated and pre-stressed concrete girders is cracking. A recent report by Head et al. for the Maryland State Highway Administration found that many prefabricated and pre-stressed concrete bridge girders suffered from cracking, with most of the cracks appearing as diagonal cracks at the ends (Head et al., 2015). These cracks were deemed unlikely to be of structural concern but were of sufficient concern to warrant further observation. Controlling camber during fabrication and delivery were also important concerns. Camber is an important component to ensuring timely placement of the girders on site. In terms of QA/QC a major issue was lack of automated inspection processes to aid in streamlining paperwork and data management.

An example of notable concrete cracking in a PBES bridge has been recently observed in Vermont. The bridge crossing Gold Creek on VT 100 near Moscow and Stowe has extensive cracking in the girders

and cast-in-place integral deck. The source of these cracks has not been firmly established. It is also not certain if the cracks are stable or are still growing. While these cracks may not pose a serious structural threat to the bridge, they do present aesthetic, serviceability and long-term maintenance concerns.

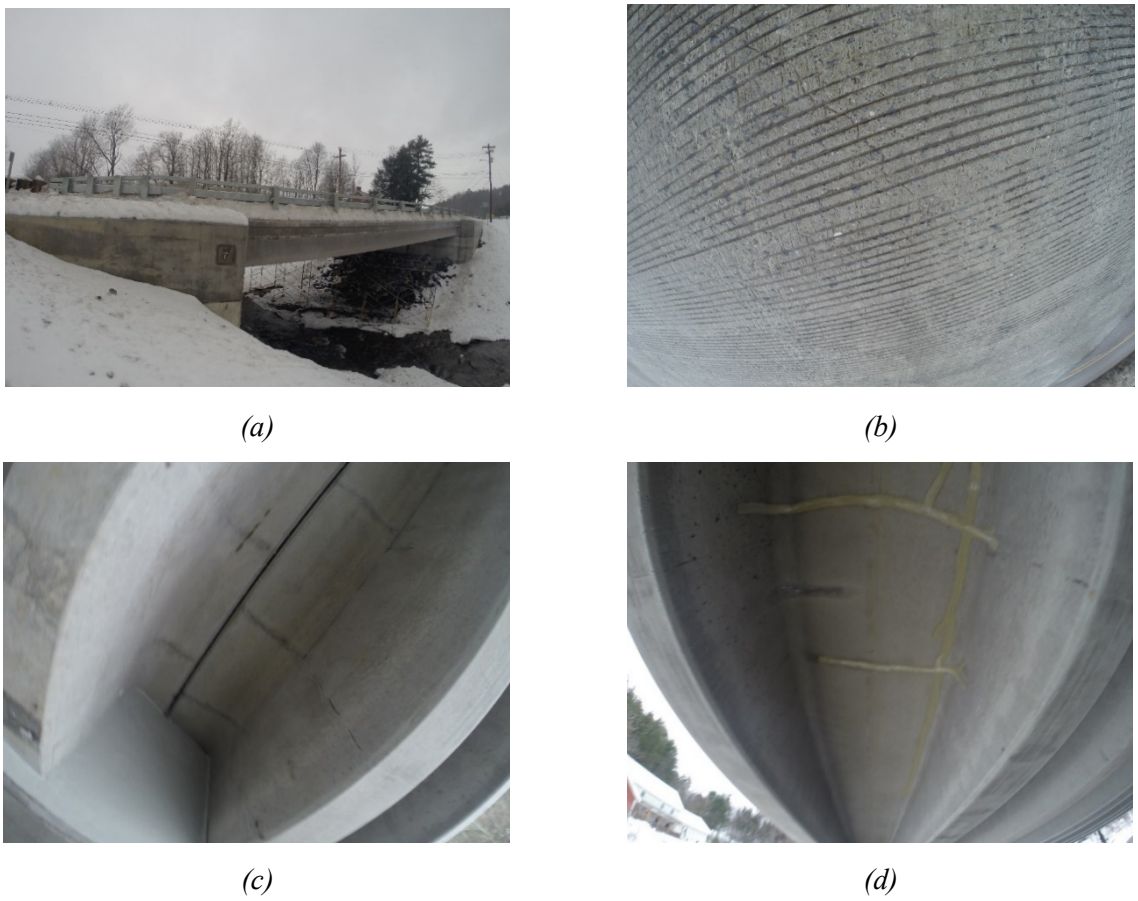

(a) *(b)*

(c) *(d)*

Figure 1.1: VT 100 Gold Creek Bridge near Moscow and Stowe with girder and deck cracks (a) bridge side view, (b) deck with multiple cracks, (c) girder with cracks in the flanges near to the end, and (d) some of the cracks repaired

The VT 100 Bridge along with the reports of cracking in similar girders in Maryland provides an impetus for monitoring cracks in these girders as part of a QA/QC system to minimize and mitigate this cracking problem. An ideal monitoring system would have the following traits: 1. Identify the occurrence, location and severity of cracking – including non-visible subsurface cracks, 2. Provide test results in a sufficiently timely and understandable format to enable accept/reject QA/QC decision, 3. applicable to multiple types of beams, girders and bridges, 4. not damage the elements under test, 5. not disrupt the construction process, 6. be of sufficiently mature technology that it is reliable and easy-to-use with turn-key instruments, 7. operate over a fairly short test cycle, and 8. affordable.

Structural sensing and health monitoring technologies are widespread and encompass many types of sensors (Huston, 2011). Acoustic emission (AE) monitoring appears to be the best technique for this application. AEs are short-duration high-frequency elastic waves in solids caused by incipient micro-fractures and other localized events detecting the strength, shape and timing of elastic waves emanating from cracks as they form is the basis of the AE technique. Analysis of the signals can determine the location and type of cracking, as well as the overall level of cracking, i.e. whether the cracks are stable or are growing. When applied to concrete girders, the simplest signal processing measures the rate of AE events. If the production rate is relatively low and steady or dropping, the amount of new crack generation is small. If the AE rate is high or growing, then the cracks are growing. Concrete AE testing has encompassed: Maturity level of concrete – as concrete cures it produces micro cracking which is detectable by AE. Once the curing slows, the beam would be stable enough to move; Impact to concrete members as it is moved to its final location – AE can detect and locate Impacts to the members; Continuous cracking; Reaction of beams and components to loading; Wire break in pre-stressing; and Estimating load values using b-Values, CALM Ratio (Landis and Baillon, 2012; Chen and He, 2001).

Advantages of AE monitoring are: 1. The sensors easily attach to the surface of the structure, are removable and reusable (Figure 1.2); 2. AE can detect, locate and assess subsurface nonvisible cracks; 3. The technology is mature with applications across a variety of structure types, including concrete; 4. Software and data analysis procedures are available for a variety of conditions, including those specific to concrete cracking; 5. AE-based codes, standards, test and continuous monitoring procedures (ASME, RILEM, ASTM), have been in place since the 1980s (Huang and Nissen, 1997); and 6. Certain industries, in particular pressure vessel manufacturing, use accept/reject criteria based on the level of AE signal production. The pre-stressed character of pressure vessels and pre-stressed girders are similar enough to lend credence to the possibility of developing similar accept/reject criteria for girders.

Disadvantages of AE testing are: 1. Data must be collected continuously, otherwise important AE events may go undetected, including those occurring prior to instrument installation; 2. The standard setup requires cables connecting AE sensors to the AE monitoring instrument. Running these cables along girders without damage requires skill and some expense. An alternative is to use wireless data transmission and incurring the associated increased costs and complexity; and 3. The monitoring instruments consume modest amounts of power (~20 W).

Figure 1.2: *Acoustic emission sensor attached to a concrete girder (reference)*

Relation to VTrans Strategic goal(s) and objective(s): This project tracks the confluence of PBES QA/QC alignment with VTrans Strategic Goals 1, 2, 3 and 5 (VTrans, 2015) as follows:

• **Goal 1:** *Provide a safe and resilient transportation system that supports the Vermont economy* – PBES QA/QC offers the possibility of rapidly upgrading bridges on a network level.

o *Reduce the number of major crashes* - The reduced construction times reduces traffic restrictions and redirections and the associated increased risk of crashes.

o Increase the resilience of the transportation network to floods and other extreme weather and events - The use of longer span bridges with high-performance girders moves the piers further out of stream beds and reduces the risk of scour, flanking and other flood-related damage. Increased quality control reduces the potential for unexpected repairs throughout the lifetime of a bridge.

• **Goal 2:** *Preserve, maintain and operate the transportation system in a cost effective and environmentally responsible manner.*

o *Maintain pavement, structures and other transportation system assets in a state of good repair* – Increased use of PBES in rapid bridge construction is a possible framework for rapidly upgrading the bridges in VTrans' inventory. Quality control during construction and monitoring efforts holds out the possibility of significantly reducing maintenance costs throughout the lifetime of a bridge structure.

o Implement an Asset Management System and integrate it with Planning and Programming – The monitoring and quality control data collected during use of PBES in rapid bridge construction may prove useful in an Asset Management System, especially if problem conditions are identified and mitigated early on.

- *o Minimize the environmental impacts of the transportation system* – Success with the use of high-performance girders, as this project may enable, will allow for longer spans that remove piers and abutments further away from river beds, thereby reducing the environmental impact of construction and non-natural disruptions of flow during high-water events.

• **Goal 3:** *Provide Vermonters energy efficient, travel options.*

- o *Minimize traveler delay* – Quality control practices during use of PBES in rapid bridge construction have the potential of operating the construction pace at a high speed while reducing the risk of unexpected delays. This can reduce traveler delay during the construction cycles.

• **Goal 5:** *Develop a workforce to meet the strategic needs of the Agency.*

- o *Retain and develop excellent and diverse employees* – A key part of this project is to develop a turnkey quality control monitoring system that can be used by VTrans personnel. Training and gaining of experience in the use of this instrumentation will be part of the ongoing personnel skills development underway for VTrans personnel engaged in the use of PBES in rapid bridge construction.

Studied in this project are Northeast Extreme Tee (NEXT) beams and Northeast Bulb Tee (NEBT) girders during specific prefabrication processes including; detensioning and craned lifting from form beds. The evaluation of the efficacy of AE technology, as part of this study, begins with laboratory proof of concept testing before moving on to field testing of the highly stressed end zone regions of pre-fabricated and pre-stressed reinforced concrete NEXT beams and Bulb Tee girders. The end zone regions of the pre-fabricated and pre-stressed reinforced concrete NEXT beams and Bulb Tee girders are the major region of stress transfer from the pre-tensioning strands to the surrounding concrete, which is approximately 60 times the pre-tensioning strand diameter, per 5.11.4.1 of AASHTO Bridge Design Specifications (PCINE-14-ABC, 2014).

The current state of practice for pre-cast manufacturers, is to use empirical data and a trial and error approach to reduce the development of end zone cracking while achieving the required girder load capacity, with minimal specific guidance from codes and standards. This has led to a variety of end zone reinforcement procedures for the reduction of end zone cracking, unique to each pre-cast manufacturer. In addition to limited guidance on the prevention of end zone cracking there is also limited guidance on the acceptance/rejection criteria for end zone cracks. Instead decisions to accept or reject a girder due to end zone cracking are often subjective based on the experience and knowledge of the pre-cast manufacturers

and inspectors. A long-term goal of this line of research is to develop a set of accept/reject criteria based on structural and serviceability considerations.

NEXT beams are widely used and have become a standard bridge construction element in the northeastern United States. These double-tee beams provide for rapid PBES construction similar to box and hollow-core beams but have the additional benefits of ease of inspection and no void space for water to accumulate (Tuan et al., 2004; Okumus et al., 2016; Arancibia and Okumus, 2017; Ronaki et al., 2017). NEXT beams also have an integral deck such that laying sections of NEXT beams together create a bridge deck and girder system that only needs a foundation and surface finishing (PCINE-14-ABC, 2014).

The evolution of designs of NEBT girders is towards deeper and more slender sections to allow for an increased number of pre-tensioning strands to induce larger amounts of pre-stress into the Bulb Tee (Hasenkamp et al., 2008). This results in end zone cracking patterns similar to the NEXT beams. Although small end zone cracking may not make the beam structurally deficient, it can cause durability issues by allowing water and de-icing solutions to be in contact with the reinforcing steel or pre-tensioning strands, leading to corrosion and eventually to structural deficiencies.

The three major types of characteristic end zone cracking appearing in NEXT beams and NEBT girders include; horizontal web cracking, inclined web cracking, and Y cracking. Eccentric loading is a common source of horizontal web cracking. Pre-tensioning strand distributions are typical sources of inclined web cracking and Y cracking. Both horizontal and inclined web cracking are typically small enough that they close under service loading. Y cracking does not normally close under service loading and therefore has the greatest potential for durability issues (Okumus and Olivia, 2013). Figure 1.3 shows examples of horizontal web cracks observed during this study.

Figure 1.3: Recorded end zone cracking of bulb tee

The most common end zone cracking control method modifies the end zone reinforcing bar pattern. Typical end zone reinforcing steel patterns were developed based on experimental data, linear analytical studies, and finite element analysis and were mostly developed based on analyses of vertical flange cracking (Okumus and Olivia, 2013). While current end zone reinforcement pattern practices have mostly eliminated vertical flange cracking, the issues of horizontal, inclined and Y cracking of the web remain as challenges that require further research.

1.2 Objectives

This project designs and implements a reusable instrumentation system for evaluating the condition of structural elements during the use PBES in the construction of transportation structures in Vermont. Quality control of the processes is an opportunity for improved final delivery of the product at reduced cost. This project focuses on developing reusable instrumentation for monitoring pre-stressed concrete girders during fabrication, transport, installation and initial traffic-bearing phases. The instrumentation should be reusable for multiple bridge projects. Potential instruments include AE sensors to measure incipient cracking, strain gages, accelerometers, tilt/orientation sensors, and 3-D imaging.

Objective 1. Identify suitable instruments to monitor pre-stressed and/or post-tensioned concrete girders for cracking activity.

Objective 2. Design and develop a reusable instrumentation package.

Objective 3. Measure performance and condition of concrete girders, specifically to measure the performance of one concrete girder PBES/ABC bridge throughout fabrication and installation.

Objective 4. Identify test protocols and possible accept/fix/reject criteria for structural elements based on information from monitoring system.

Objective 5. Work with VTrans to develop plans for reusing monitoring instruments on multiple bridge projects.

1.3 Methodology

The proposed tasks align with the objectives.

Objective 1. Identify suitable instruments to monitor pre-stressed and/or post-tensioned concrete girders for cracking activity.

Task 1. ***Select a suitable instrument configuration.*** The instruments must be capable of monitoring cracking activity in prefabricated pre-stressed concrete girders during the following stages: 1. In the factory following pre-stressing, 2. During transport, 3. During placement, and 4. Following placement, including proof and traffic loading. Initial considerations have indicated that a portable and reusable AE monitoring system supplemented with other sensors (acceleration, strain, temperature and/or tilt) continuously using up to 8 AE sensors deployed along a bridge girder with a portable power supply that can run for 48 hours is nominally the desired instrument configuration for this application. A consideration is to determine whether it is better to use a completely reusable system or to use one with sensors permanently mounted on the girders.

Objective 2. Design and develop a reusable instrumentation package.

Task 2. Design the instrumentation package. The plan is for the instrumentation to operate in a turnkey manner and be reusable on multiple bridge girders. The instruments need to run continuously and require portable power, such as with marine or lithium-polymer battery. The estimated power consumption is 20 W. The system configuration will likely be a wired-sensor version instead of wireless due to benefits of simplicity and reduced cost. This instrument should accommodate taking measurements during these stages: 1) Cutting of the pre-stressing tendons; 2) During lifting out of the formwork, storage on site, lifting onto trucks and transport to the bridge site; 3) During lifting and assembly into the bridge structure; and 4)

During usage of the structure, including traffic loads.

Task 3. Acquire and assemble the instrumentation package. Acquire the equipment and supplies in a timely manner.

Task 4. Verify performance of instrumentation package with preliminary laboratory tests. Conduct modest scale laboratory tests at UVM to verify that the monitoring instruments work as designed, while paying close attention to mounting details.

Objective 3. Measure performance and condition of concrete girders throughout PBES construction processes. Measure performance and condition of concrete girders. The goal is to measure the performance of one concrete girder PBES bridge throughout fabrication and installation, and in-service performance following installation.

Task 5. Measure performance of girders during fabrication. The first step is to select a suitable PBES construction process in Vermont. Use the monitoring instrumentation at girder fabrication site, especially prior to pre-stress loading. This will likely be at a commercial facility and will require cooperation and coordination with the fabricator and VTrans.

Task 6. Measure performance of girders during transport. Use the monitoring instrumentation to measure girders during transport. This will likely involve a commercial contractor and will require cooperation and coordination with the fabricator and VTrans.

Task 7. Measure performance of girders during placement. Use the monitoring instrumentation during girder placement. This will likely be a commercial facility and will require cooperation and coordination with the fabricator and VTrans.

Task 8. Measure performance of girders following installation. Use the monitoring instrumentation at girder fabrication site. This will likely be a commercial facility and will require cooperation and coordination with the fabricator and VTrans.

Objective 4. Identify test protocols and possible accept/fix/reject criteria for structural elements based on information from monitoring system.

Task 9. Synthesize literature on using acoustic emission monitoring as acceptance criteria in structural elements. This involves examining the literature and standards on fiber reinforced polymer pressure vessels, and similar structures that use AEs measurements as accept/reject QA/QC criteria during fabrication.

Task 10. Combine state of the art techniques with data collected during AE monitoring to formulate accept/reject criteria. Measurements collected during the tests in this project and combined with the synthesis results of Task 9 will lead to proposed accept/reject criteria.

Objective 5. Work with VTrans to develop plans for reusing monitoring instruments on multiple bridge projects.

Task 11. Plan for reuse of instruments. The goal is to reuse the instruments on other bridges. This requires coordination and guidance of VTrans personnel that may use the instruments in these follow-on tests. VTrans personnel will participate in the assessment of the technology for implementation purposes.

Task 12. Reporting. Preparation and submission of quarterly, draft final report, final report and presentation of final results as required by programmatic guidelines.

Technology Transfer and Implementation Plan – A key goal of this research is to develop a monitoring system for PBES construction QA/QC for use by VTrans personnel on multiple bridges following the end of this project. Success requires: 1. The technology works and is suitable for VTrans needs; 2. The system is turnkey in setup and data processing so that it is easy to use and does not require extensive expertise and experience to operate; and 3. The system is reliable.

The plan for transferring this technology includes: 1. Use commercially-available off-the-shelf components when available; 2. Include VTrans personnel in all key aspects of the project; 3. Develop a user manual for use of the equipment, along with drawings, technical documentation, parts list and recommendations for improving the system; 4. Provide training to VTrans personnel on the use of the equipment; 5. Transfer the equipment to VTrans, if desired; 6. Provide guidance for future research and design activities that use the collected data to improve design, fabrication and installation practices that reduce cracking and improve the overall quality of the completed bridge structures.

1.4 Organization of this Report

This report follows with Chapter 2 that presents a concise literature review on prefabricated and pre-stressed, reinforced concrete Northeast Extreme Tee (NEXT) beams and Northeast Bulb Tee (NEBT) girders, AE data collection techniques and methodologies, along with statistical and empirical methods for AE event source locating, differentiation, and damage assessment.

Chapter 3 provides the rational for the selection of AE monitoring as a possible technique for development as a quality control/quality assurance (QA/QC) procedure during the fabrication and transport of pre-stressed, reinforced concrete beams and girders.

Chapter 4 presents the selected AE instruments and rationale for selections. The chapter also presents pricing details for the selected equipment and recommendations from the manufacturer. Additionally, Chapter 4 presents some initial and preliminary tests performed to verify the functionality of the acoustical emission monitoring equipment.

Chapter 5 describes the multiple laboratory tests performed to verify the performance of the acoustical emission development as a Quality Control/Quality Assurance (QA/QC) procedure during the fabrication and transport of pre-stressed, reinforced concrete beams and girders as well as to develop a base methodology and input parameters for future field testing on full-scale beams and girders.

Chapter 6 provides fabrication process observations, methodologies, data collected, and results of field testing on full-scale pre-stressed, reinforced concrete Northeast Extreme Tee (NEXT) beams and Northeast Bulb Tee (NEBT) girders. This chapter also describes some of the challenges with data collection and correlations established between beam features and clustering of AE events.

Chapter 7 describes the transport process observations, methodologies, data collected, and results of field testing on full-scale pre-stressed, reinforced concrete Northeast Bulb Tee (NEBT) girders from J.P. Carrara and Sons, Inc. in Middlebury, VT to the I-91 bridge construction site located in Rockingham, VT. This chapter also describes some of the challenges with data collection and correlations established between travel conditions and AE event clustering as well as finite element stress modeling and AE event clustering.

Chapter 8 details current damage assessment techniques and procedures for reinforced concrete and discusses their relevance to the unique loading scenarios of fabrication and transport testing. Due to the general development of current damage assessment techniques with a cyclic loading regime; this chapter describes possible alterations of existing damage assessment tools to work with the unique loading conditions of fabrication and transport along with hypothesizes a new approach for damage assessment in pre-stressed, reinforced concrete beams and girders.

Chapter 9 lists the capabilities of the acoustical emission monitoring equipment as proven during this study and lists additional potential capabilities along with repeat testing scenarios that would provide for a large enough data set for further development of the use of AE technology as a quality control/quality

assurance (QA/QC) procedure during the fabrication and transport of pre-stressed, reinforced concrete beams and girders.

Chapter 10 provides with overall conclusions and recommendations.

CHAPTER 2

LITERATURE REVIEW

The foci of the literature review are pre-tensioned and post-tensioned reinforced concrete Northeast Bulb Tee (NEBT) girders and Northeast Extreme Tee (NEXT) beams, end-zone cracking, an overview of AE monitoring, AE sensor types, AE wave modes and propagation, AE source locating, AE source differentiation, and AE damage assessment.

2.1 Pre-Tensioned and Post-Tensioned Reinforced Concrete

Concrete technologies date back to antiquity and continue to advance to this day. A significant modern development is composite technologies with the introduction of reinforcing followed by pre-stressing to accommodate the inherently weak strength of concrete. The first patent filing for pre-stressing of concrete was in 1886 (NJIT, 2018). There are three main types of structural elements used in modern construction; structural steel, reinforced concrete, and pre-stressed concrete. Figure 2.1 is a flow chart of the varieties of structural materials and specifically the varieties of pre-stressed concrete.

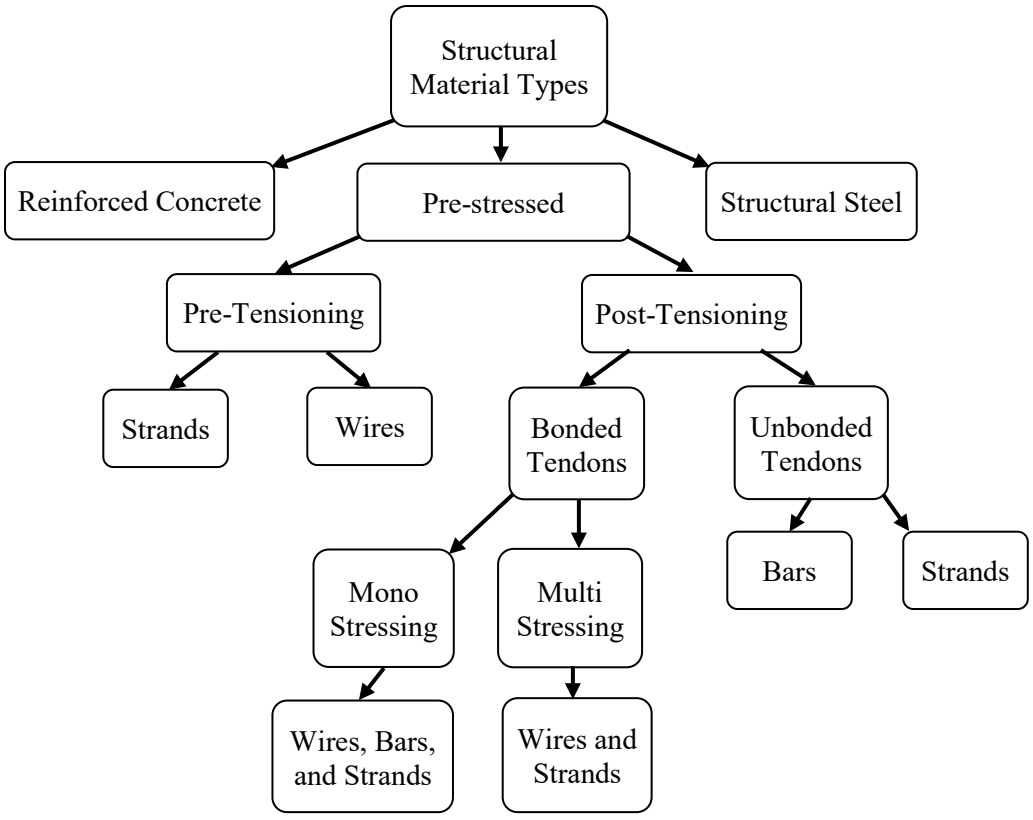

Figure 2.1: Structural material and pre-stressed concrete types flow chart (Steel Auto Industries, 2018)

Pre-stressed concrete uses either a pre-tensioning and/or post-tensioning technique to induce compression in the concrete element prior to service loading. The introduction of compressive stress prior to service loading counteracts some tensile loading which allows for the pre-stressed concrete to carry more tensile forces than non-pre-stressed concrete (Vejvoda, 2018). Figure 2.2 is a schematic of the typical process for pre-tensioning and post-tensioning of concrete..

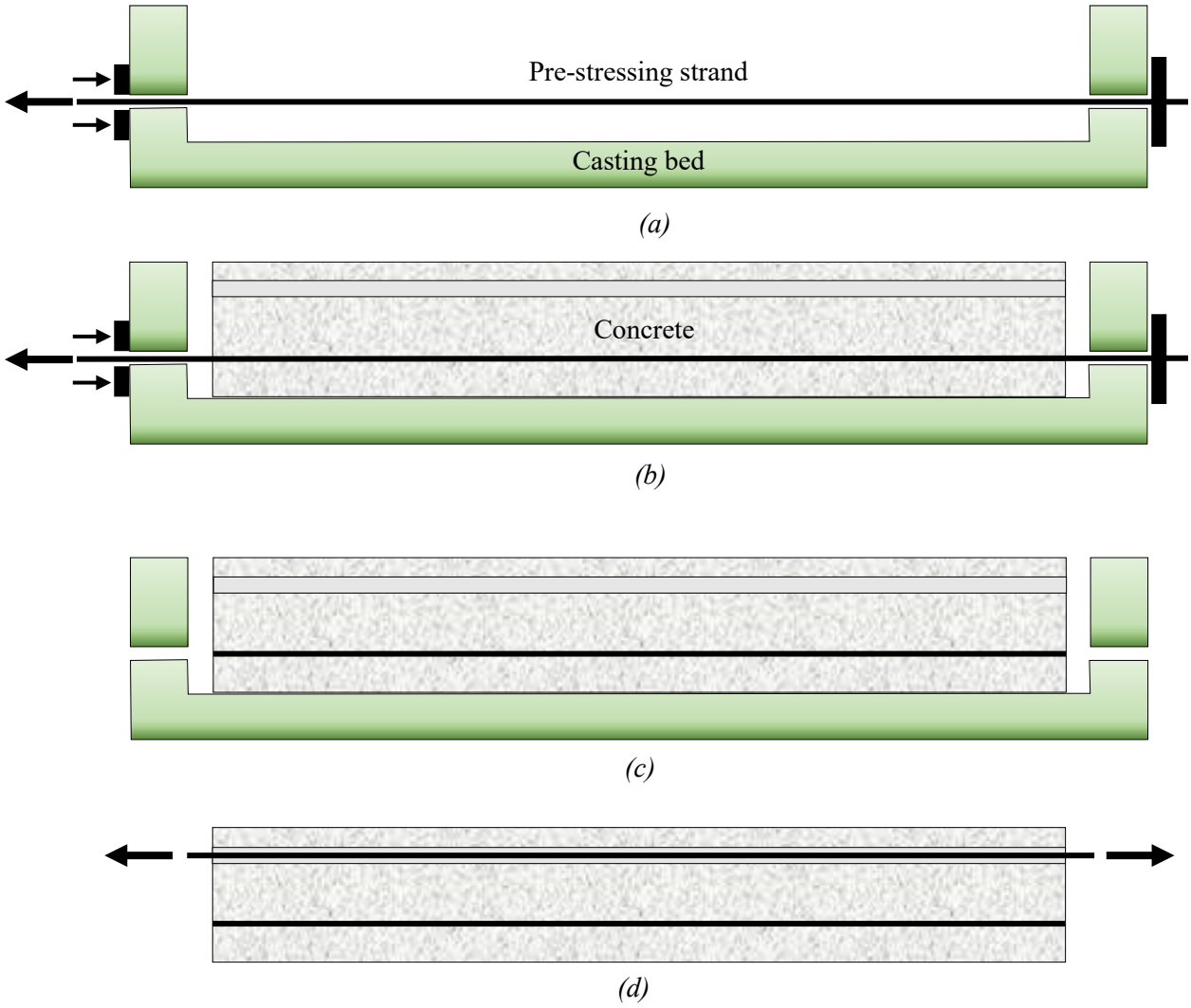

Figure 2.2: Pre-tensioned and post-tensioned concrete (a) tensioning of the pre-stressing strands against the end abutments, (b) casting of the reinforced concrete beam, (c) detensioning of the pre-tensioning strands, and (d) post-tensioning of the reinforced concrete beam

Typically, the pre-tensioning and post-tensioning tendons are steel but may also be made of various other materials such as nylon and fiberglass depending on the application. The pre-tensioning strands can be sleeved to control the spatial distribution of the pre-stressing, or not sleeved. A typical loading configuration uses hydraulic jacks pulling against a frame with bulkheads and deadman anchors to stretch the cable without applying any load to the concrete, steel reinforcing or formwork. Placing the concrete

into the formwork encapsulates the pre-tensioning strands. Setup and curing of the concrete bonds the concrete to the pre-stressing strands. Once the concrete has cured to a sufficient compressive strength, cutting the pre-tensioning strands compresses the structural concrete element by a transfer of the tension through the shear developed on the outer surface of the strands.

Post-tensioning is an alternative method of pre-stressing concrete, often as a supplement to pre-tensioning. Post-tensioning offers a wide variety of advantages. Perhaps most importantly is the introduction of compressive force between individual structural elements to allow for continuity of longer spans. Post-tensioning strands may be either unbonded or bonded as seen in Figure 2.3.

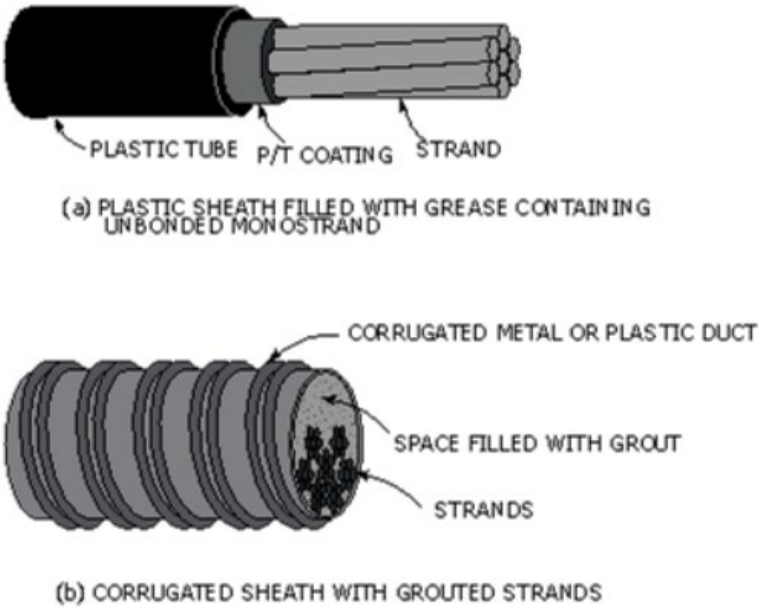

Figure 2.3: Post-tensioning strands (typical) (a) unbonded post-tensioning strand and (b) bonded post-tensioning strand (Vejvoda, 2018)

Disadvantages of post-tensioning include the development of secondary moments when combined with pre-tensioning. Post-tensioning has the potential for pre-stress loss due to friction, wedge set, elastic shortening of concrete, concrete shrinkage, concrete creep, or steel relaxation (Vejvoda, 2018).

2.2 End-Zone Cracking

Although there are standard designs for Northeast Extreme Tee (NEXT) beams and Northeast Bulb Tee (NEBT) girders, the designs continually evolve to meet project specific requirements that include deeper and more slender sections with increased pre-stressing, which in some cases have been attributed to an increase in frequency and magnitude of end zone cracks; most notably in NEBT girders (Hasenkamp et al., 2008). The three most common types of end zone cracking in NEBT girders are; horizontal web cracking, inclined web cracking, and Y cracking. The source of horizontal and inclined web cracking is

typically eccentric loading or pre-tensioning strand distribution. A primary source of Y cracks is pre-tensioning strand distribution. Horizontal and inclined web cracks often close during in-service loading. Y cracks tend to not close and are of greater concern (*Okumus and Olivia, 2013*).

Current end zone cracking control methods for reinforcement bar pattern designs were developed with respect to vertical flange cracking and have been largely effective as vertical flange cracking is now a rare occurrence (*Okumus and Olivia, 2013*). These same reinforcement bar patterns, however, have not been as effective in the reduction of horizontal web cracking, inclined web cracking, and Y cracking, supported by observations made during this study. The only cracks observed during this study were horizontal web cracks, Figure 2.3.

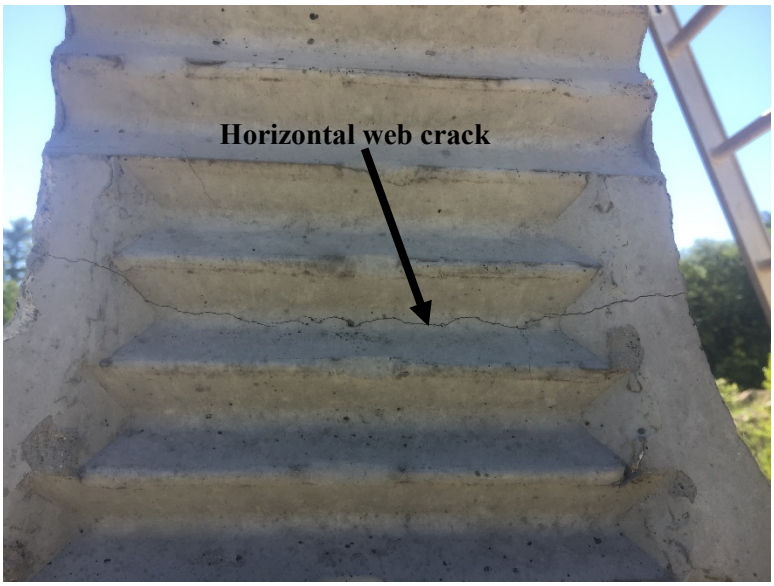

Figure 2.3: Horizontal end-zone web cracking of a Northeast Bulb Tee (NEBT) girder

2.3 Acoustic Emission Monitoring

2.3.1 Overview and History

AE sensing by ear has been used for thousands of years with potters as early as 6,500 B.C. listening to for the audible "tings" of crack nucleation during the kiln firing stage of creating their ancient ceramics (NDT Resource Center, 2018). These AE signals from the initiation of a crack coupling with the air create the audible "tings" alerting the potter to a structural deficiency with their creation that could lead to its rejection. Modern AE technology appeared in the early 1950's with the completion of the "Results and Conclusions from Measurements of Sound in Metallic Materials under Tensile Stress," doctoral thesis of Joseph Kaiser of the Technical University Munich (TUM) (Tensi, 2004). Kaiser built equipment using piezo-crystal microphones that relayed signals to an oscilloscope where they could be recorded and

analyzed. Schofield coined the term "acoustic emission" in 1961 (Grosse and Ohtsu, 2008), The first known practical application of AE technology was in 1964 with the testing and development of rocket motor casings (Kaphle, 2012a). Although early research and uses of AE technology examined steel and aluminum alloys (Tensi, 2004) it was not long until AE technology expanded to use with concrete and the U.S. Federal Highway Administration (FHWA) started research on the use of AE in bridge strength testing.

An Acoustic Emission (AE) is a transient elastic wave produced by the release of stored elastic energy resulting in plastic deformations, typically associated with damage. The release of stored elastic energy or redistribution of stresses can be cause by a wide variety of sources such as loading, pressure changes, temperature changes, or chemical reaction processes (NDT Resource Center, 2018). These AE event sources can be as small as micro and nano-scale cracking to catastrophic failures of full-scale bridge beams and girders. AE testing is nominally a non-destructive test (NDT) method. AE differs from many other NDT test methods in that it requires the material being monitored to crack or have some sort of plastic deformation. This arguably makes AE testing a destructive and not a non-destructive test procedure. AE testing is also a passive technique that relies on a release of stored energy from the material instead of introducing energy into the material such as with ultrasonic testing.

There are many modern and commercially available AE detection systems that can record AE wave forms and record specific parameters related to the wave forms. These systems employ surface-mounted sensors that detect the propagating acoustical emission and convert the analog signal to a digital signal. Once in a digital format, it becomes convenient to filter signals with user identified inputs for setting thresholds and for pre-amplification of acoustical signals, amplitude thresholds, event duration thresholds, material wave mode velocities, etc. AE signals are typically weak. Some materials, including concrete, quickly attenuate AE waves with distance from the source emission location. It is common to use multiple amplifiers in a ganged configuration with a pre-amplifier and a main amplifier. Additional signal conditioning reduces background noise with a band-pass filter using a nominal pass band of several kHz to 1 MHz (Grosse and Ohtsu, 2008). Most civil infrastructure produces AE signals with an operating frequency range of 100 kHz to 300 kHz which is an achievable range of modern AE test equipment (Kaphle, 2012b).

2.3.2 Acoustic Emission Sensors

Although there are a variety of non-contact AE sensors such as fiber optic and laser interferometers, the optical AE sensors are limited in the physical area they are able to monitor as the distribution properties of light create the need to focus the light to a small area. Most AE sensors that operate with a surface contact configuration use the piezoelectric effect in lead zirconate titanate (PZT) for transduction. The piezoelectric effect is a reversible process. At the macroscopic scale piezoelectricity appears as the creation

of a voltage across a solid as it deforms and vice versa the piezoelectric substance will deform in response to an applied voltage (Aysal, 2018). At the molecular scale piezoelectricity acts in anisotropic crystals in which a crystal lattice deformation leads to the polarized movement of electric charge and vice versa. At the micro to meso scales, sintering-type manufacturing processes cause PZT to take on a polycrystalline structure with random polar orientations of the piezoelectricity as illustrated in Figure 2.4.

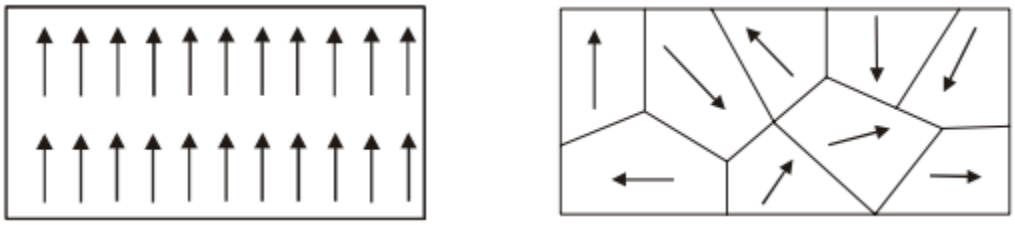

Mono-crystal with Single Polar Axis Polycrystal with Random Polar

*Figure 2.4: Mono-crystals vs. Poly-crystals (*Aysal, 2018*)*

Applying an electric field is applied to the PZT polycrystal at a suitably elevated temperature biases the dipole molecules of the PZT line up to some extent as illustrated in Figure 2.5 (Aysal, 2018).

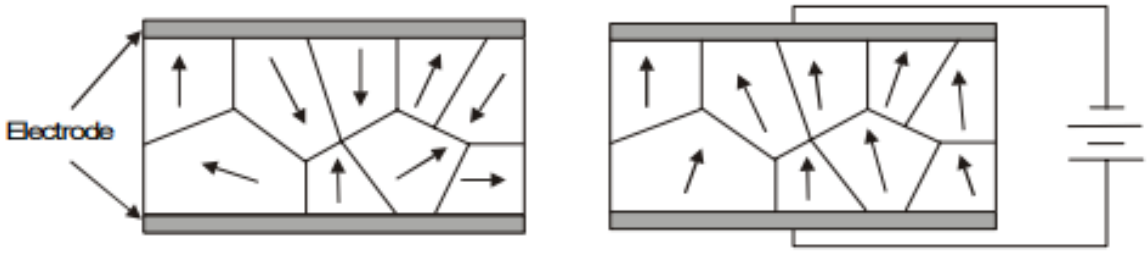

Random Dipole Polarization

*Figure 2.5: Polarization of Ceramic Material to Generate Piezoelectric Effect (*Aysal, 2018*)*

The polycrystalline approach enables the manufacture of PZT elements into various shapes and sizes to achieve different vibration modes and range of operating frequencies. Figure 2.6 shows the different piezoelectric responses to different loading scenarios with Figure 2.6.f being a common configuration for use in AE testing.

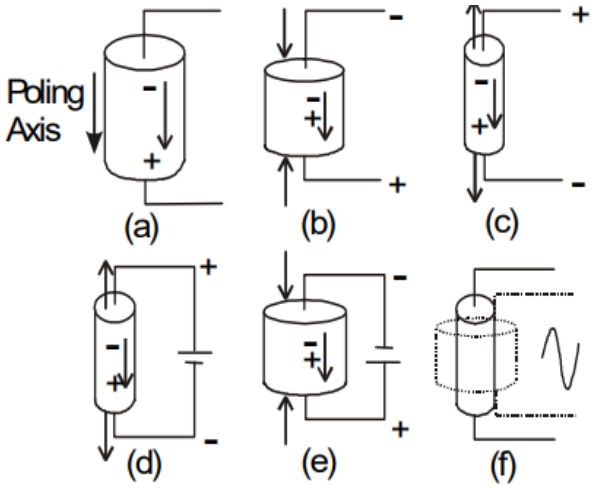

*Figure 2.6: Piezoelectric effect under different circumstances (a) no stress or charge, (b) compression, (c) tension, (d) applied voltage opposite polarity, (e) applied voltage same polarity, and (f) applied AC signal (*Aysal, 2018*)*

The surface mounted AE sensor experiences the vibration of the AE which excites and deforms the piezoelectric element and produces a voltage. Specific to PZT elements; a 0.1% deformation generates a measurable piezoelectric response, often in the microvolt range (J. Krautkrämer et al., 1990). Since the mechanical deformations and piezoelectric transduction sensitivities are small, the initial analog signals require multiple layers of amplification during transmission and digitization. This overall process eventually converts the analog AE signal to a digital signal for interpretation with the AE monitoring equipment and displayed to the end user.

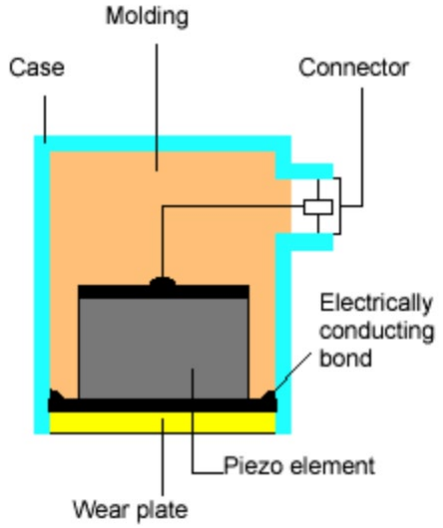

Figure 2.7: Typical piezoelectric sensor schematic (Vallen, 2009)

There are two primary variants of piezoelectric sensor; resonant and broadband. The main difference is the transfer of the AE signal to the piezoelectric element. In a resonant sensor, a small proof mass mechanically

couples to the piezoelectric element through a flexible mount and vibrates freely around resonance in response to the AE signal. A broadband sensor has a stiff support connected to the piezoelectric element that directly applies deformations to the piezoelectric element. Each sensor has advantages and disadvantages which can make for best use scenarios for each sensor type. As illustrated in Figure 2.7, resonant sensors are more sensitive and better at detecting timing and event counts but can distort the recorded AE signal since the AE signal is transferred from the solid to the proof mass and then to the piezoelectric element. The broadband sensors are less sensitive but have a high-fidelity direct transduction of the AE signal to the piezoelectric element. Since with a broadband sensor there is not a proof mass but instead a stiff support the sensor can be used in reverse as described previously where the application of a suitable oscillating voltage produces ultrasonic vibrations.

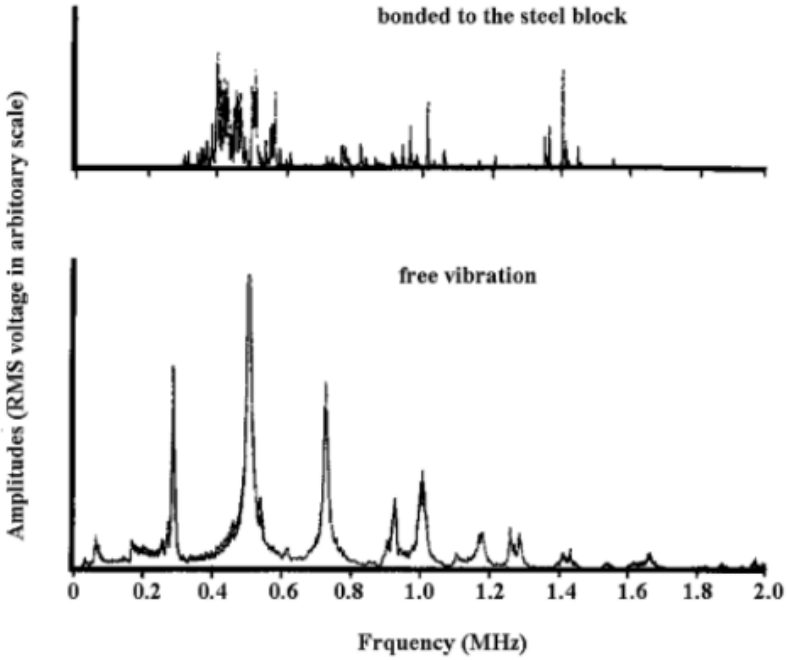

Figure 2.8: Broadband (top) vs. resonant (bottom) sensitivity comparison (Grosse and Ohtsu, 2008)

2.3.3 Acoustic Emission Wave Modes and Propagation

The nucleation of a crack, crack growth, rubbing, loading, and other irreversible deformative processes that emit an AE do so through multiple different wave modes. The three main wave modes measures for AE monitoring include; longitudinal waves (body wave/P-wave), transverse waves (shear wave/S-wave), and surface waves (Rayleigh wave). Longitudinal waves or P-waves are where particles oscillate in the direction of the wave propagation. Transverse wave or S-waves are where particles oscillate transverse to the direction of the wave propagation. P- and S-waves travel through bulk solids, with the P-waves having the higher velocity. Surface waves travel along the surface of a solid. Surface waves can

result from P- and S- waves interacting at a surface (Kaphle, 2012a). The typical earthquake has P-waves, S-waves and surface waves, with the S-waves usually being the strongest and being the primary source of damage.

The AE waveform released from the source location propagates in all directions in a pulse-like manner. Anisotropy at the AE source can lead to a preferred directionality associated with the waveform. The pulses can be very short in time duration such as is the case with microcracking which releases AE signal pulses with durations lasting anywhere from a fraction of a microsecond to a few microseconds. The signal eventually measured by the AE sensor is not the same as that from the AE source. Extracting information for the measured signal requires additional signal conditioning, such as filtering, and post-processing. The AE signal detected at the AE sensor is a combination of the initial AE signal, and reflected and refracted signals, background signals, and the coupling of different signals at the same phase.

2.3.4 Acoustic Emission Source Locating

The pulse-like transmission of AE signals from crack nucleation, crack growth, and other events emanate in all directions from the source point. Measuring the time of arrival (TOA) of a signal with an array of point sensors enables locating the emission source through triangulation, Figure 2.9.

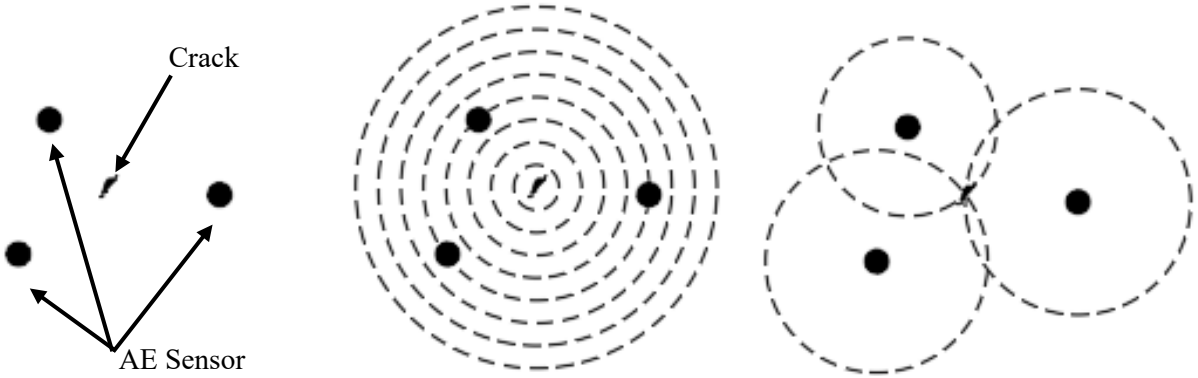

Figure 2.9: AE signal triangulation schematic (a) crack nucleation and AE sensors, (b) acoustical emission of transient elastic wave, and (c) AE source location by triangulation (Huston, 2010)

Locating an AE source with accuracy requires recording AE signals with microsecond precision. The accuracy of the source location also depends on the wave propagation velocities of the solid. A concern with concrete is the attenuative nature of the material in the range of 40 dB/meter and scatter of the AE signal due to wave interaction with natural air voids or existing cracks. Nonhomogeneous wave speeds due to reinforcing, differing states of cure and damage can all contribute to distorting the wave propagation and confounding source location estimates.

2.3.5 Acoustic Emission Source Differentiation

The AE signals carry additional information beyond TOA, largely in the detailed shape of the waveform. Such information correlates to the details of the AE source and the path traveled. There are two main types of AE source differentiation techniques (Kaphle, 2012b). The first is a feature-based analysis where an analysis of the specific waveform extracts and records a set of features, also known as parameters, describing the wave form. Typical features include amplitude, duration, counts-to-peak, and peak frequency as illustrated in Figure 2.10. Others are available. Subsequent processing of waveform features extracts information.

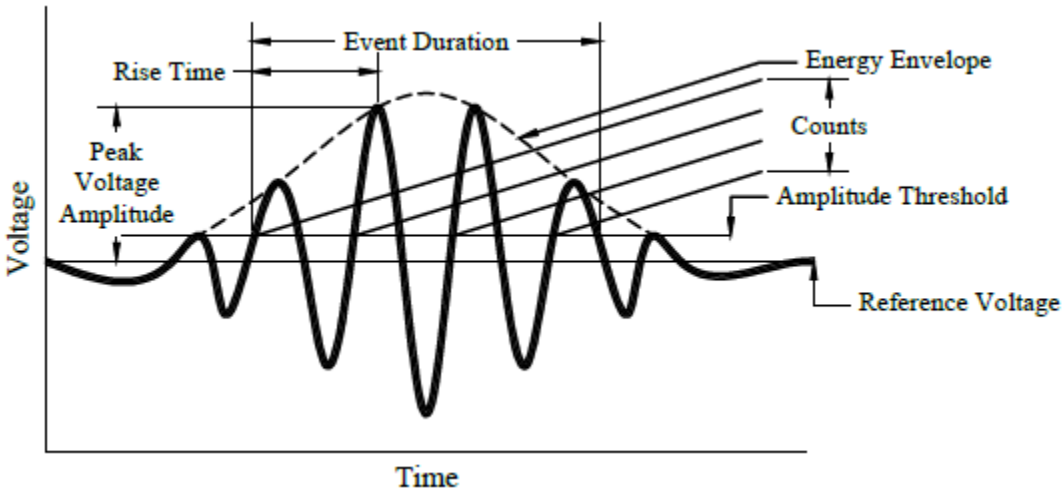

Figure 2.10: Parametric analysis of typical measured waveform features

The second AE source differentiation method begins by recording entire AE waveforms for a more detailed post-data collection analysis. Success requires sampling at a sufficiently high frequency to avoid Nyquist and related under-sampling problems. This creates a far larger volume of data (Kaphle, 2012a). Two primary emission types are burst and continuous, Figure 2.11. A burst emission is typically the result of crack nucleation or growth with a characteristic short-duration burst of waveform wiggling. Continuous emissions produce a steady stream of merged bursts that appear as stationary noise. The kinetic nature of all solids produces a low-level of continuous emissions. Many macroscopic processes also produce continuous emissions. Selecting the appropriate amplitude filter can pre-filter these non-interesting continuous emissions prior to post-processing.

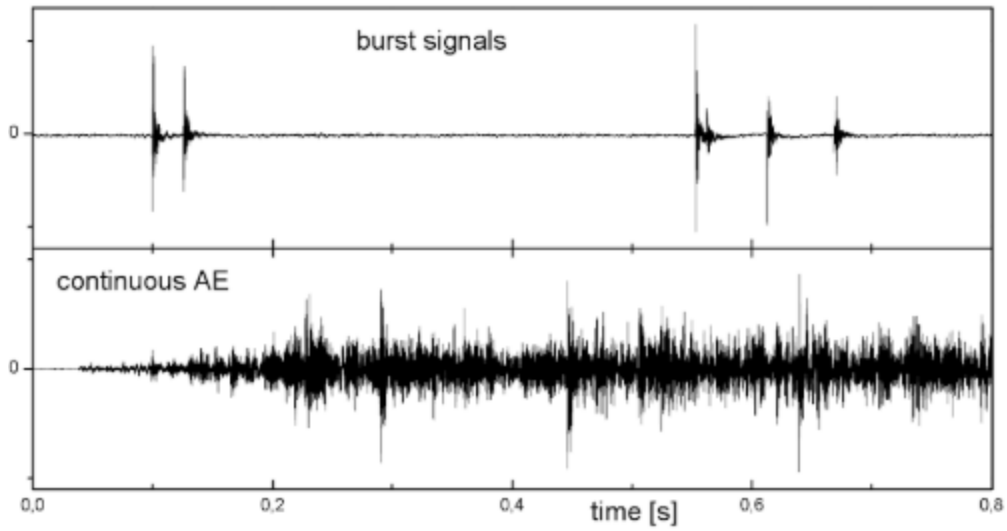

Figure 2.11: Burstt emission (top) vs. continuous emission (bottom) (Grosse and Ohtsu, 2008)

Multi-sensor spatial filters provide additional capabilities, such as the identification and rejection of anomalous situations, including simultaneous events, remote events outside the region of interest and secondary reflections from surface boundaries and the rubbing of newly formed cracks (Kaphle, 2012b).

A study by ElBatanouney et al., 2014, used an amplitude and duration filter to eliminate AE events not correlated to crack formation during a laboratory test of cyclically loading a reinforced concrete beam to failure. Figure 2.12 shows how a careful choice of filter settings can reduce AE event location estimates from a diffuse swath of points centered on the cracks, Figure 12.b, to a smaller set of points that provide a superior alignment with the observed cracks, Figure 12.c.

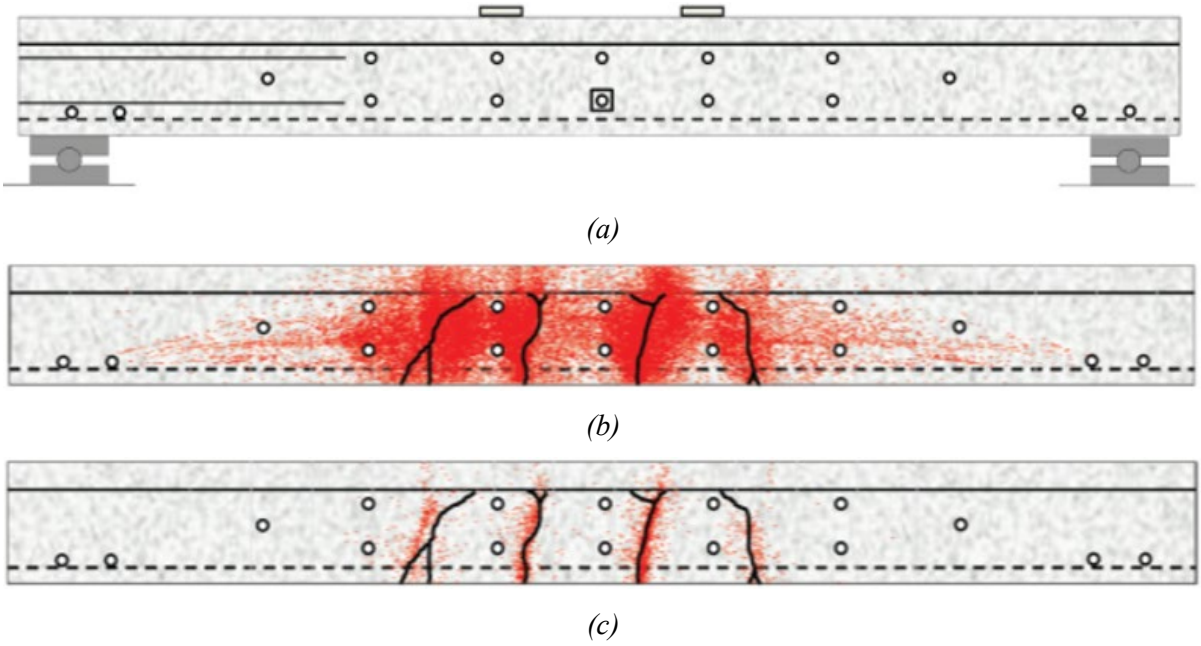

Figure 2.12: AE event amplitude and duration filtering for crack correlation (a) laboratory beam and AE sensor array, (b) unfiltered AE event location, and (c) filter AE event locations correlated to observed cracking (ElBatanouney et al., 2014)

2.3.6 Acoustic Emission Damage Assessment

Damage assessments and quantification typically account for the stress level at which AE events occur, peaks in amplitude of AE events, number of AE events, spatial clustering of AE events, and rate of accumulation of AE events (Arches, 2009). The technical literature contains multiple published damage assessment techniques, with the majority looking at conventional non-pre-stressed reinforced concrete Additionally, most of the available damage assessment methods use cyclical loading scenarios that lend themselves to serve use monitoring of bridges that experience cyclical loading and unloading from traffic. Some of the most common damage assessment techniques for reinforced concrete are:

1. Felicity ratio;
2. Parametric analysis;
3. Load-Calm ratio;
4. B-value analysis;
5. Frequency analysis.

These damage assessment techniques and quantification metrics all use data obtained from the recorded AE waveform or parametric data representative of the AE waveform to relate the AE event with a crack event or to relate the AE event to a severity of damage.

2.3.7 Felicity Ratio

The basis of the Felicity ratio is the load history dependent Kaiser effect. The test protocol uses a sequence of loading and unloading cycles with an amplitude that increases at each cycle. The Kaiser effect is where no AE events occur until the load levels exceed the previous maximum loads. The Felicity effect is the opposite case where AE events occur a load levels below the previous maximum loads. This indicates the occurrence of damage.

$$\text{Felicity Ratio} = \frac{\text{Load at AE restart}}{\text{Previously applied maximum load}}$$

A Felicity Ratio of 1 or greater indicates no damage, whereas, a Felicity Ratio of less than 1 indicates damage. The lower the Felicity ratio the greater severity of damage. Figure 2.13 illustrates the Felicity Ratio concept.

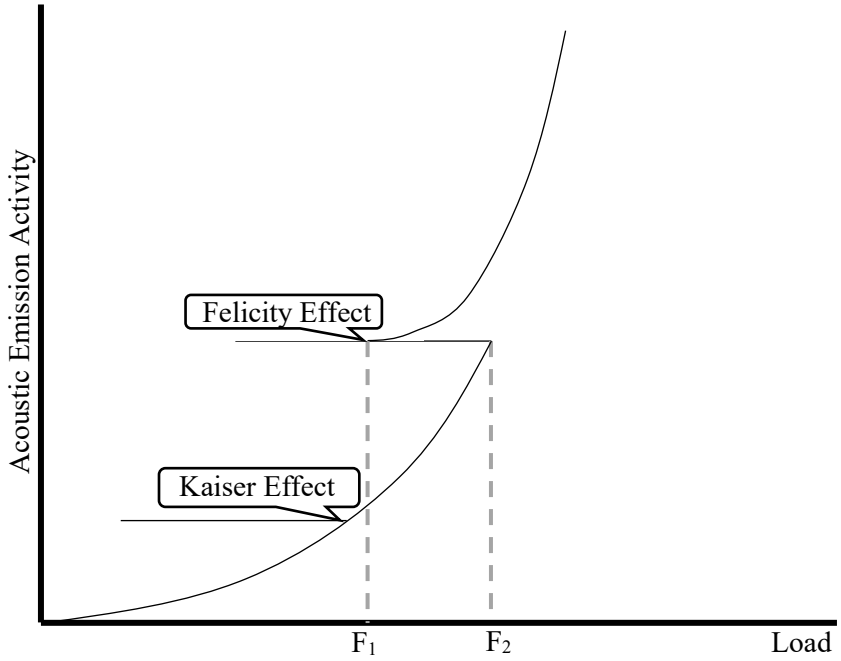

Figure 2.13: Felicity effect and ratio illustration (typical) (Arches, 2009)

2.3.8 Parametric Analysis

A parametric analysis uses parameters determined from the AE event waveform and observed damage features, such as cracking, to establish correlations between AE event parameters and damage. An example is to plot the RA values (rise time/peak amplitude) versus the average frequency (kHz). AE events above the y=1/10x boundary indicate tensile cracking, whereas, AE events below the y=1/10x boundary indicate other types of cracking (Arches, 2009).

2.3.9 Load-Calm Ratio

The Load-Calm ratio damage assessment technique plots the Load Ratio and Calm Ratio of a loading-unloading cycle to classify the AE events as; minor damage, intermediate damage, or heavy damage. The Load Ratio is the same as the Felicity ratio. The Calm Ratio is the ratio of AE activity during the unloading process compared to the AE activity during the last loading cycle. Plotting the Load Ratio versus the Calm Ratio can then indicate minor, intermediate, or heavy damage, Figure 2.14.

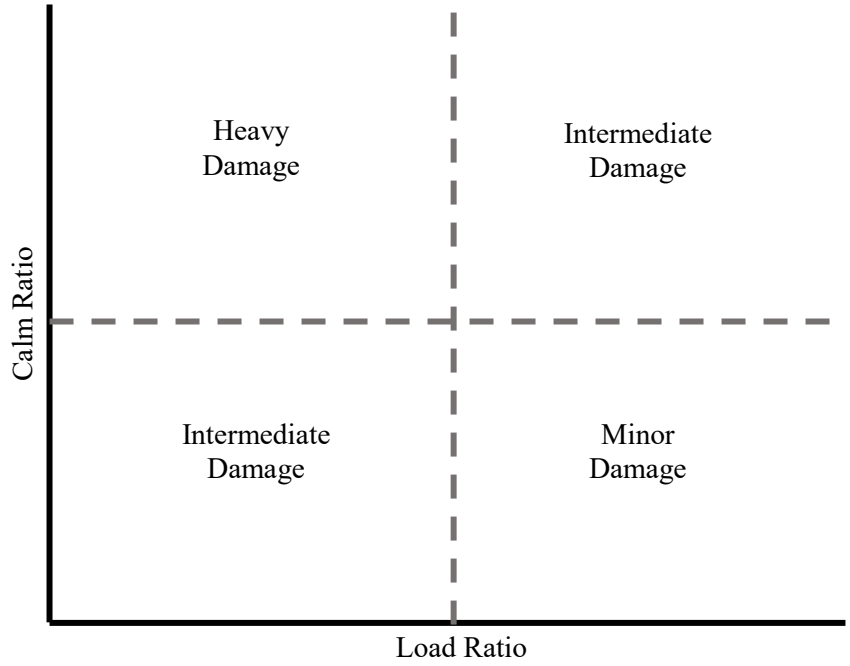

Figure 2.14: Load-calm ratio illustration (typical) (Arches, 2009)

2.3.10 B-value Analysis

The b-value analysis is a statistical regression of the AE event peak amplitudes. The technique requires a complete loading-unloading cycle for calculation. The basis of the b-value analysis is the seismic Gutenberg-Richter formula:

$$\log_{10} N = a - b'(A_{dB})$$

$$B - value = 20b'$$

Where,

N = number of AE events with amplitude above A_{dB}

A_{dB} = AE signal amplitude (decibels)

a = empirical constant (background noise)

b’ = empirical constant

An abrupt decrease of the calculated b-value indicates the occurrence of damage. This method is sensitive to the attenuative nature of concrete. Appropriate sensor placement is critical for accurate results. The sensor array must be near to or encompass the area of damage. The sensor spacing must be close enough to register AE events accurately, nominally a spacing of 2 m or less.

2.3.11 Frequency Analysis

The frequency analysis uses a flow chart, Table 2.1, to categorize concrete damage based on frequency and energy of the AE event. This method is specific to reinforced concrete and has a high potential to mis- categorize damage if the sensor placement is not close enough to read AE events accurately before severe attenuation by the concrete.

Table 2.1: Frequency analysis flow chart (Arches, 2009)

AE Source	High frequency	High energy	Steel wire breaking or stress corrosion cracking
		Low energy	Steel corrosion
	Medium frequency	High energy	Concrete cracking
		Low energy	Steel/concrete interface damage
	Low frequency	Changes in nonlinear acoustic behavior of concrete	Structure damage under loading

CHAPTER 3
SELECTED INSTRUMENTS AND RATIONALE

3.1 Overview

The goal is to select an instrumentation package to measure the occurrence and location of cracking in prefabricated and pre-stressed bridge girders during fabrication and during transport to bridges sites. AE testing is the primary measurement technique. The method attaches sensors onto the surface of the girder with adhesives, connects the sensors to the data acquisition unit with coaxial cables and collects data continuously throughout the cycle. Figure 3.1 show a typical sensor installation.

Figure 3.1: Acoustic emission sensor attached to a concrete girder (Figure courtesy Mistras Group)

3.2 Acoustic Emission Sensing

AEs are short-duration high-frequency elastic waves that propagate in solids following micro-fractures and other localized events. In many situations the elastic waves propagate with sufficient strength for detection at remote locations. Analysis of the detected signals can determine the location, type, and overall level of cracking, including whether the cracks are stable or are growing. A simple, but effective,

technique measures the rate of AE events. If the AE production rate is relatively low and steady, or dropping, the amount of new crack generation is small. If the AE production rate is high or growing, then the cracks are growing. More sophisticated processing estimates the locations of the sources of the AE waves, and identifies the types of events that created the wave.

Advantages of AE monitoring are: 1. The sensors attach to the surface of the structure, are removable and reusable; 2. AE can detect, locate and assess subsurface nonvisible cracks. The technology is mature with applications across a variety of material and structure types, including concrete. Software and data analysis procedures are available for a variety of conditions, including those specific to concrete cracking. 3. Certain industries, in particular pressure vessel manufacturing, use accept/reject criteria based on the level of AE signal production. The in-plane-stressed character of pressure vessels and that of pre-stressed girders are similar enough to lend credence to the possibility of eventually developing similar accept/reject criteria for pre-stressed girders.

Disadvantages of AE testing are: 1. Data must be collected continuously otherwise important events may go undetected; 2. The standard setup requires cables to connect the sensors to the data acquisition instrument. Running these cables along girders without damage requires skill and some expense. A wireless alternative is possible but increases costs and complexity; and 3. The monitoring instruments consume moderate amounts of power (~20 W), which can be a concern for off-grid continuous battery-powered monitoring.

3.3 Methodology

Instrument configuration: Initial considerations indicated that a portable and reusable AE monitoring system supplemented with other sensors (acceleration, strain, temperature and/or tilt) with a portable battery power supply that can run for 48 hours continuously using up to 8 AE sensors deployed along a bridge girder is a preferred configuration.

Phase 1 – Measure AEs during curing and formwork stripping –The presence of formwork on the bottom and sides of the girder will likely lead to placement of the sensors in an array on top of the girders. AE data will be collected continuously throughout the cure cycle. It is anticipated that the amount of AE activity will be small during curing but will pick up during formwork stripping operations.

Phase 2 – Measure AEs during pre-stress release by cutting tendons – Measure AE activity during tendon release and immediately afterwards. The release transfers the forces that held the tendons in tension from and external frame onto the concrete. This may be the source of a large level of AE activity. If the

formwork has been stripped prior to tendon release, a preference is to reposition the sensor array into a configuration to better capture AE events, such as around the tendon clusters near to the end of the girder.

Phase 3 – Measure AEs during transport – (Optional) Measure AE activity during transport of the girder from the fabrication facility to the bridge site. Considerations include positioning the array and data acquisition system to minimize the possibility of damage and providing portable power.

Additional consideration – ***Use of tendons as waveguides*** – Steel tendons can be excellent waveguides for carrying AEs from remote sources throughout the girder. There may be advantages to attaching the AE sensors to one or more tendons during testing.

CHAPTER 4
DETAILED DESIGN OF INSTRUMENT PACKAGE

4.1 Overview

The plan is to measure AEs on concrete girders in the factory, during transport, during installation and for a short period following installation. The following is a listing of the proposed AE monitoring system, justification and description of the parts, drawings of the system, potentially useful add-on options, a description of the difference between what was originally proposed and what is now recommended, and quotes from the vendors.

4.2 Planned Parts List

The key components of the planned AE monitoring system appear in Table 4.1. The total cost is $22,997.

Table 4.1: Planned parts list

Item No	Description	Vendor	Unit Cost	Quantity	Total Cost
1	SHIII-8, Smart Remote Monitoring, 8-channel Sensor Highway III	Mistras	$13,372	1	$13,372
2	AE-WIN 2D-LOC, FULL PLANAR, 2 DIMENSION LOCATION	Mistras	$1,369	1	$1,369
3	Low Power, Preamplified Sensor, 60kHz, with 26 dB gain, AST, coate	Mistras	$628.00	8	$5,024
4	Signal Cable, RG58 SMA-BNC 30 Meters	Mistras	$124.00	8	$992
5	AE WIN 3D-LOC, 3 DIMENSIONAL LOCATION SOFTWARE OPT	Mistras	$1,369	1	$1,369
6	ASUS T102HA-D4-GR Transformer Mini 10.1-Inch 2 in 1 Touchscreen	Amazon	$391.90	1	$392
7	12v 100AH Deep Cycle AGM Battery	Amazon	$159.49	2	$319
8	12V Battery Charger	Amazon	$27.55	1	$28
9	Power Center	Amazon	$57.58	1	$58
10	Battery Inverter Cable Set	Amazon	$8.87	1	$9
11	Auto Battery Disconnect Knife Blade Switch	Amazon	$20.99	2	$42
12	8-Gauge Maxi Fuse Holder	Amazon	$5.95	4	$24
	Total				$22,997

4.3 Details on Parts List and Justification

Part 1

Description: Mistras SHIII-8, Smart Remote Monitoring, 8-channel Sensor Highway III system is a full, stand-Alone AE system for unattended monitoring in outdoor environments. System Includes; Outdoor weatherproof case (18" x 12" x 6"), one 8-channel AE board, 8 single-ended parametric inputs, remote reboot, Windows 7 Operating system, AEwin installed and licensed for 8 channels, Ethernet connectivity to a factory network or Internet, 110/220VAC or 9 - 28 VDC power at 15 watts. Unit price is $13,372, a quantity of 1 and total cost of $13,372

Justification: This is base unit for AE monitoring. It can collect and distribute up to 8-channels of AE data, along with up to 8 other channels. It is designed for use outdoors in field testing. The vendor

(Mistras) has other systems, but this one is the simplest and most cost-effective of the options for the planned tests. Previous experience with laboratory-based AE systems from Mistras lends confidence in the selection of this type of system for the planned testing.

Part 2

Description: Mistras pn# 9380-7003-2, AE-WIN 2D-LOC, full planar, 2 dimension location. Unit price is $1,369, a quantity of 1 and total cost of $1,369.

Justification: AE-WIN is the basic Windows-based operating software for the Mistras AE systems. It is capable of manipulating and processing AE signals. It enables event location on 2D planar surfaces.

Part 3

Description: Mistras pn# R6IC LP-AST, Low Power, Preamplified Sensor, 60kHz, with 26 dB gain, AST, coated for outdoor use, 5meter coaxial RG-58A/U cable, and connector. Unit price is $628, a quantity of 8 and total cost of $5,024.

Justification: These are the AE sensors. This model is ruggedized for outdoor use. The total of 8 sensors should provide an adequate coverage of the girder for event detection and location.

Part 4

Description: Mistras PN# 1234-4002-30, 1234-SMA/BNC-30, Signal Cable, RG58 SMA-BNC 30 Meters. Unit price is $124, a quantity of 8 and total cost of $992.

Justification: These are the signal cables for the sensors in Part 3. They are needed to transmit the analog signals from the sensors back to the digitizer on the SHIII-8.

Part 5

Description: Mistras pn# 9380-7003-9, AE WIN 3D-LOC, 3 dimensional location software option. Unit price is $1,369, a quantity of 1 and total cost of $1,369.

Justification: This is a software add-on to AE-WIN that enables location of events in 3-dimensional structures – an item of importance for girder testing.

Part 6

Description: ASUS T102HA-D4-GR Transformer Mini 10.1-Inch 2 in 1 Touchscreen Laptop (Intel Quad-Core, 128GB EMMC, Grey, pen and keyboard included) by Asus. Unit price is $391.99, a quantity of 1 and total cost of $391.99

Justification: This is a mini laptop computer. It is used to configure and operate the SHIII-8, along with storing data. It is intended to leave this computer on-site inside the SHIII-8 box.

Part 7

Description: Universal UB121000-45978 12v 100AH Deep Cycle AGM Battery 12V 24V 48V(Black) by Universal Power Group Unit price is 2 $159.49 a quantity of 1 and total cost of $318.98

Justification: This is a deep draw rechargeable sealed lead-acid battery that will provide power to the SHIII-8. The duration between charges is estimated to be between 4 and 7 days. Two are selected so that it is possible to do a quick swap in the field.

Part 8

Description: Battery Tender 021-0123 Battery Tender Junior 12V Battery Charger by Battery Tender Unit price is 1 $27.55, a quantity of 1 and total cost of $27.55

Justification: This is a charger for the batteries in Part 8.

Part 9

Description: MinnKota Trolling Motor Power Center Unit price is $57.58, a quantity of 1 and total cost of $57.58

Justification: This is a case that surrounds the battery in Part 7 and provides some control over function.

Part 10

Description: EPAuto 20-Inch Battery Inverter Cable Set. Unit price is $8.87, a quantity of 1 and total cost of $8.87

Justification: This is a set of cables that connects the battery to the SHIII-8.

Part 11

Description: Auto Battery Disconnect Knife Blade Switch Top Post Top Terminal Car Battery Cut Off Shut Off. Unit price is $20.99 a quantity of 1 and total cost of $41.98

Justification: This is a set of switches for connecting and disconnecting the lines to the battery in Part 7.

Part 12

Description: 8-Gauge Maxi Fuse Holder Unit price is $5.95, a quantity of 1 and total cost of $23.80.

Justification: These are fuses for insertion into the electric power lines of the system and may prevent damage from electrical shorts and excessive current draws.

4.4 Drawings of the Systems

Figure 4.1 shows the cross section of a pair of typical bulb tee girders. The actual girder to be instrumented remains to be determined. This will also affect mounting details. Figure 4.2 shows the AE system on top of a girder. Figure 4.3 shows how an array of AE sensors would detect an incipient crack. Precise timing combined with triangulation methods produce the location estimate.

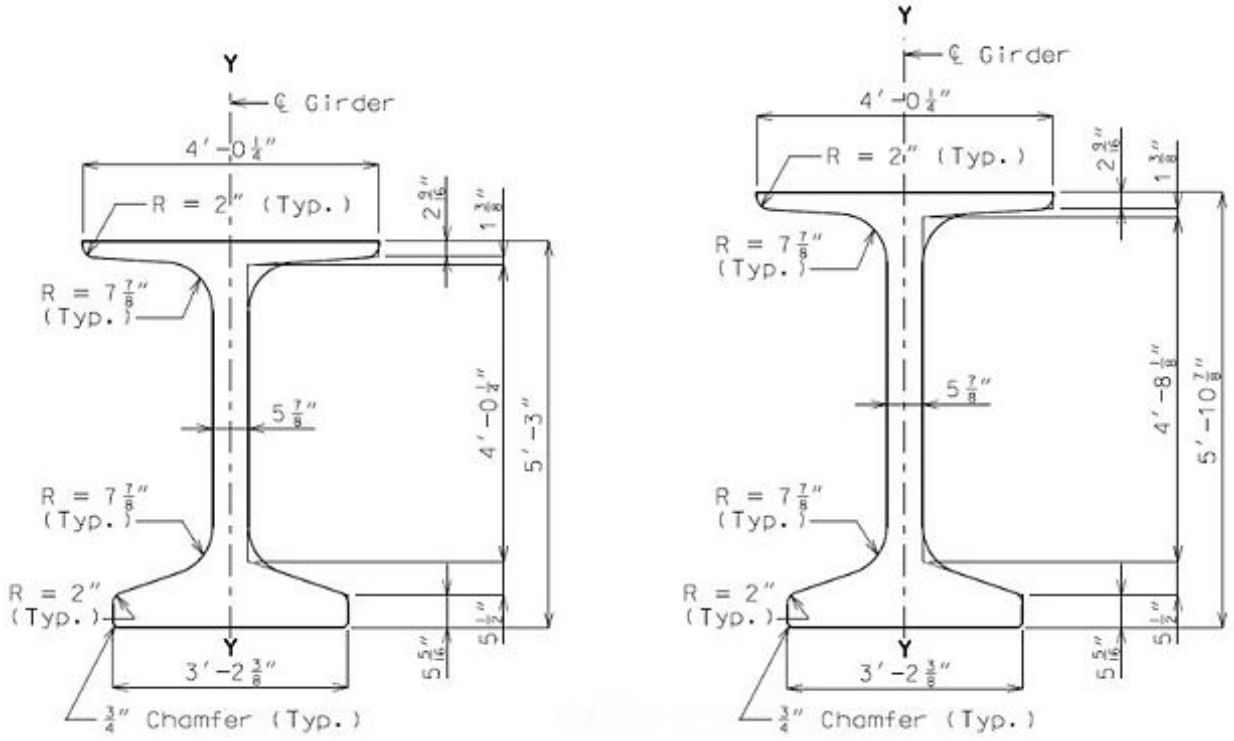

Figure 4.1 Typical Bulb Tee cross-section shapes for use in pre-stressed concrete girders (MoDOT, 2018)

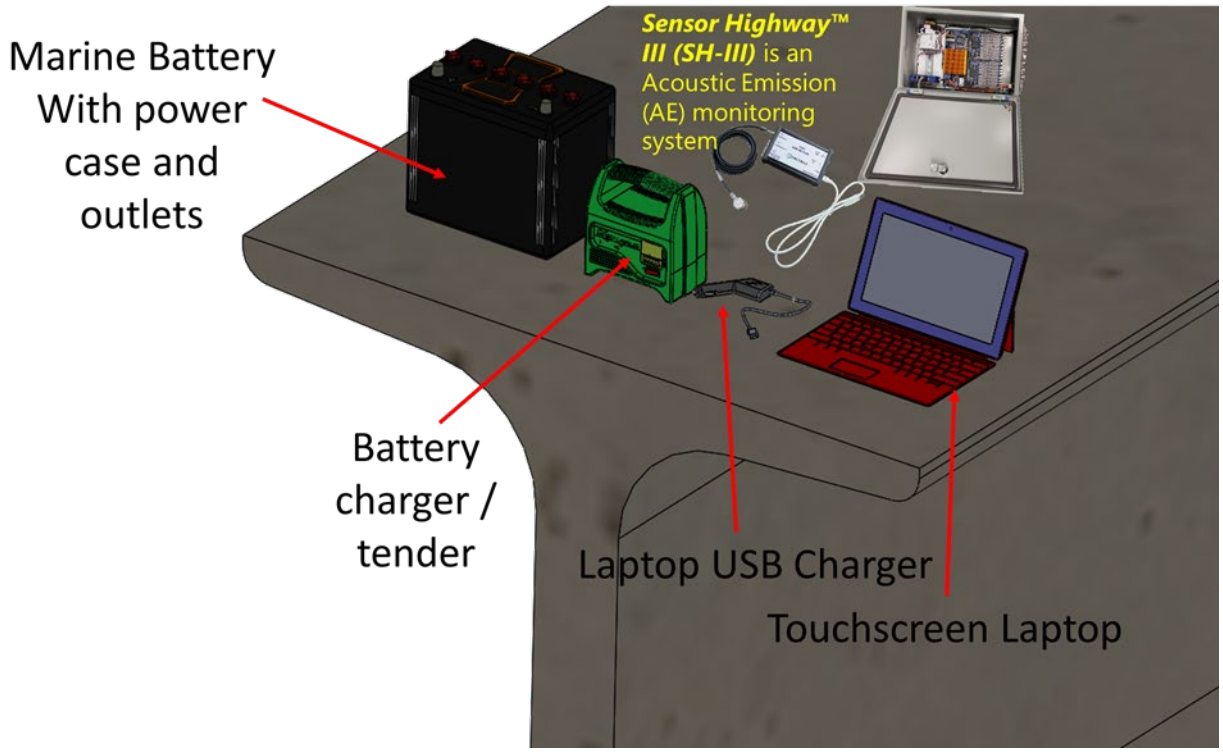

Figure 4.2 Main components of acoustic emission monitoring system sitting on top of a generic Bulb Tee girder

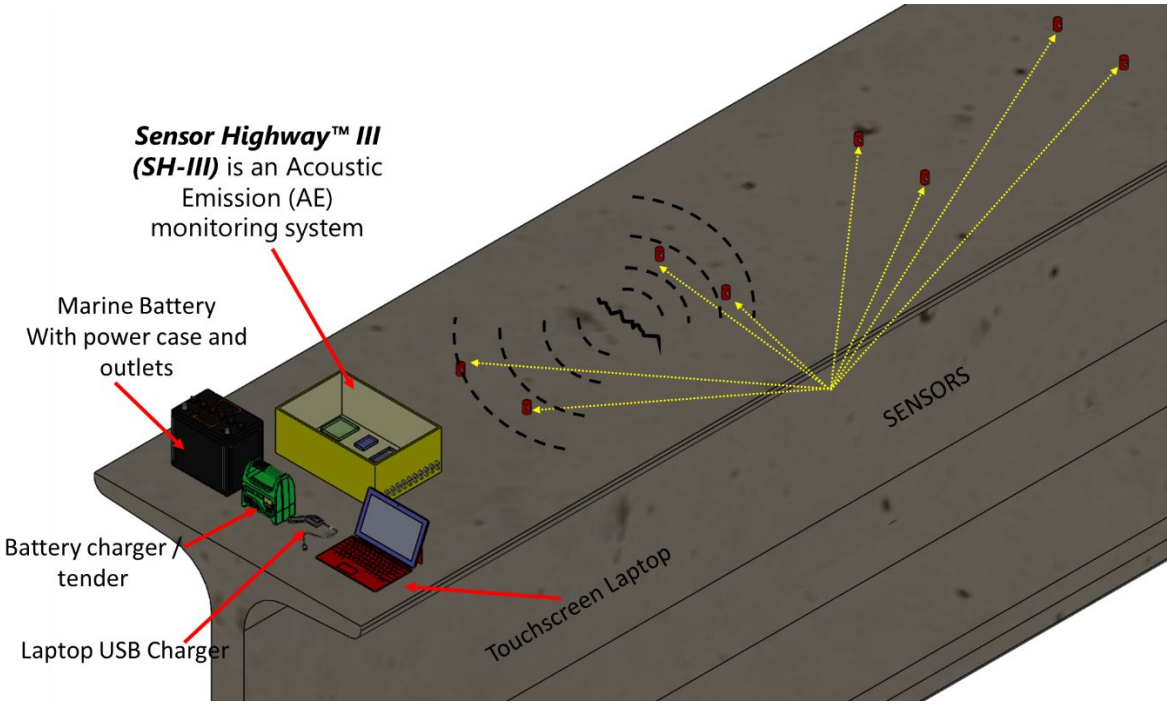

Figure 4.3 Acoustic emission system on top of girder with array configured to sense the elastic waves produced by an incipient crack

4.5 Potentially Useful Add-On Options

Option 1:

Description: Cellular Wireless Modem assembly, Wireless 3G modem with remote CPU reset capability. Hardware only. Needs a separate cellular contract provided by customer (For U.S. and Verizon service only). Includes Main Unit, DIN Rail mount, antenna, cable and install. Unit price is $2,506, a quantity of 1 and total cost of $2,506. A cellular plan is also needed

Comment: This may be the most useful of the optional add-ons. It will allow for remote access of the system while it is collecting data. It was not included in the original proposal.

Option 2:

Description: Mistras BaseStation Battery Backup, Outdoor BaseStation Battery Backup option installed into system. Up to 20 minutes operation. Unit price is $595, a quantity of 1 and total cost of $595.

Comment: This will provide an electrical backup in case of power loss. It may be useful in some cases for critical monitoring applications.

Option 3:

Description: OLM web site,Creation of an "On Line Monitoring" website, with server located at Mistras for posting a private, secure, website so that the customer can log in and see the status and activity on the structure, in terms of tables and graphs with selectable parameters such as Hits and events distribution and other parameters versus time or per channel. The website is typically updated every hour. Contact the factory for custom web site needs and quotes. Unit price is $2,950, a quantity of 1 and total cost of $2,950.

Comment: This may be useful if the testing moves to mostly remote site monitoring, rather than the more hands-on fabrication, transport and installation cases.

4.6 Difference from Original Proposed Plan

Table 4.1 lists the equipment items for the AE test system as originally proposed in September 2015. The primary difference is the sensors, Items 2 and 3, in Table 4.1. The original set of sensors, listing for $3,248, was the non-ruggedized version. The new set of sensors, listing for $5,024, is ruggedized with water resistant coating for outdoor use.

Table 4.1: *Equipment selection in the original proposal*

Item	Description	Qty	Unit Price	Total
1	SHIII-8, Smart Remote Monitoring, 8-channel Sensor Highway III system	1	13,372	13,372
2	PK6I, Low Power Sensor, 60 kHz with Integral Preamp and SMA Connector for Sensor Highway	8	406	3,248
3	1234-SMA/BNC-30, Signal Cable, RG58 SMA-BNC 30 Meters	8	124	992
4	AE-WIN 2D-LOC, FULL PLANAR, 2 DIMENSION LOCATION	1	1,369	1,369
5	DIMENSIONAL LOCATION SOFTWARE OPT	1	1,369	1,369
Total				**$20,350**

4.7 Vendor Quotes

MISTRAS

One Source for Asset Protection Solutions

PRODUCTS & SYSTEMS DIVISION

195 Clarksville Road :: Princeton Junction, NJ 08550 USA
Phone: +1.609.716.4000 Fax: +1.609.716.0706
www.mistrasgroup.com

1. - 5.

January 26, 2017

Dryver Huston
University of Vermont
E: dryver.huston@uvm.edu

Re: Sensor Highway III SRM Quotation
Quote # SH-15565 Revision B

Dear Mr. Huston:

The ***Sensor Highway™ III (SH-III)*** is an Acoustic Emission (AE) monitoring system with up to 32 high-speed channels and 16 standard parametric input channels (expandable to over 100). The system is designed for unattended and remote monitoring use in structural health, process and condition monitoring applications. It is rated for outdoor use and comes equipped in a rugged weatherproof NEMA 4 enclosure.

The key feature of the ***SH-III System*** is its highly flexible sensor fusion interface for input and processing, using a variety of sensors. The system is able to accept AE sensors (using the standard "phantom-power" coaxial connection for powering external preamplifiers), and various other sensors with current/voltage outputs.

This interface is accomplished through the use of standard industrial, DIN Rail Mounted Signal Conditioning Modules, with options for ICP Accelerometers, Proximity Probes, Tachometers, Pressure Transducers, Load Cells, Thermocouples, Environmental Sensors, Strain Gauges, Wireless Sensors and more.

The ***SH-III*** has several interfaces available for data communication and remote control. The principal interface is the built-in Ethernet 10/100/1000 BT port. Other available interfaces include: cellular modem and WiFi.

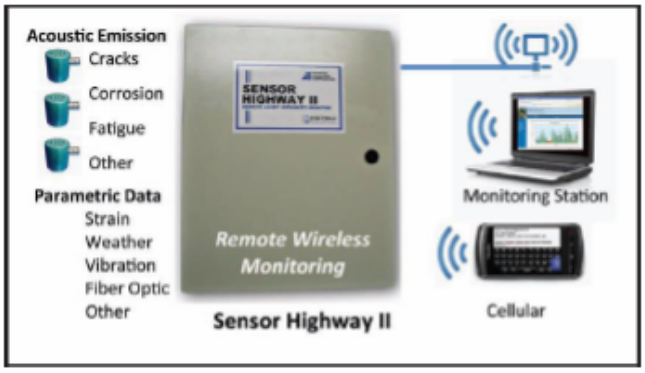

Designed to:

- Monitor effectiveness of repairs/retrofits
- Monitor pre-existing/known active defects
- Monitor "hidden areas" where visual
- inspection is difficult or impossible
- Monitor high stressed areas showing flaw-like activity
- Wire break monitoring on suspension cable and cable stay bridges

The ***SH-III-SRM System*** performs all the tasks of data collection, full signal processing (including location determination, clustering capabilities), analysis and alarming for standalone, surveillance monitoring, 24 hours a day, all within the SHII-SRM unit. This extra capability is achieved by incorporating a more powerful, industrial temperature range CPU inside the unit, running Windows XP and AEwin™ with all its features and capabilities. It is capable of making complex, on-line asset integrity decisions while interfacing to the user, the internet or to a control room.

Basic, built-in features common to all Sensor Highway™ Systems include:

- Data Acquisition: Full AE feature and waveform data acquisition to a data file, with ability to be downloaded through Ethernet connection
- Status and Trending Capabilities: Ability to generate timed STA files for individual and web based system status reporting and trending
- AE System Set-up and Control: Client program to remotely setup the system, generating a layout (set-up) file that can be uploaded to the Sensor Highway™ III
- Data File Upload and Download: Available through an FTP server with an MS Windows™ Explorer interface for transferring files
- Alarm Capability: Built-in alarms, based on Hit/Event activity or feature based (location or cluster based is available on the SHII-SRM)
- Communications: Ethernet networking built-in for walk-up, plug-in operation and remote Ethernet/Internet communications
- AE Software Analysis Compatibilities: Fully compatible with AEwin™ for SH-III (AEwin™SH). Remote user must have AEwin™SH installed on analysis workstation to analyze AE data files downloaded from the SH-III

The SH-III is a standalone, remote AE system capable of operating our high performance real time AEwin™ software. In addition to its basic capabilities, the SH-III has the following advanced capabilities:

- On-line data collection and signal processing
- Communication of alarm and status information over the internet
- Ability to handle many different types of source location in real time
- Clustering of location data and ability to alarm on clusters/cluster rate
- Comprehensive alarm detection capability
- Remote Internet communications over the Ethernet and WiFi, cellular
  or telephone modem for remote monitoring and control
- Web based remote monitoring application (RMA) to summarize state
- of one or more Sensor Highway™ III units

R6IC LP-AST Sensor with weather resistant coating.

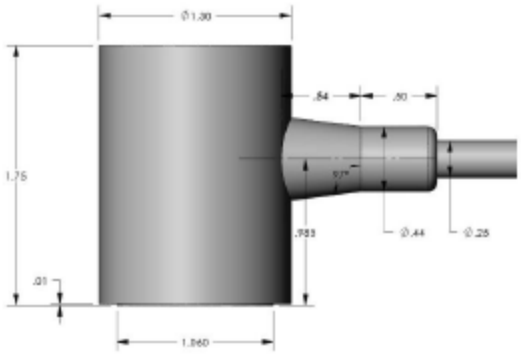

Battery for monitoring is not included. It can be supplied by the University.

Item	Model & Description	QTY	Unit Price	Total Price
001	*pn# SHIII-8, SHIII-8,* Smart Remote Monitoring, 8-channel Sensor Highway III system is a full, stand-Alone AE system for unattended monitoring in outdoor environments. System Includes; Outdoor weatherproof case (18" x 12" x 6"), one 8-channel AE board, 8 single-ended parametric inputs, remote reboot, Windows 7 Operating system, AEwin installed and licensed for 8 channels, Ethernet connectivity to a factory network or Internet, 110/220VAC or 9 - 28 VDC power at 15 watts.	1	$13,372.00	$13,372.00
002	*PN# 9800-7110-setup, OLM web site,*Creation of an "On Line Monitoring" website, with server located at Mistras for posting a private, secure, website so that the customer can log in and see the status and activity on the structure, in terms of tables and graphs with selectable parameters such as Hits and events distribution and other parameters versus time or per channel. The website is typically updated every hour. Contact the factory for custom web site needs and quotes.	1	$2,950.00	$2,950.00
003	*pn# 9380-5035,* Cellular Wireless Modem assembly, Wirless 3G modem with remote CPU reset capability. Hardware only. Needs a separate cellular contract provided by customer (For U.S. and Verizon service only). Includes Main Unit, DIN Rail mount, antenna, cable and install.	1	$2,506.00	$2,506.00
004	*pn# 9380-7003-2, AE-WIN 2D-LOC,* FULL PLANAR, 2 DIMENSION LOCATION	1	$1,369.00	$1,369.00
005	pn# R6IC LP-AST, Low Power, Preamplified Sensor, 60kHz, with 26 dB gain, AST, coated for outdoor use, 5meter coaxial RG-58A/U cable, and connector (specify BNC, BNCR, SMB, SMBR, or Pigtail on the order).d connector BNCR,	8	$628.00	$5,024.00
006	*PN# 1234-4002-30, 1234-SMA/BNC-30,* Signal Cable, RG58 SMA-BNC 30 Meters	8	$124.00	$992.00
	TOTAL			*$26,213.00*

Plus Sales Tax (Where Applicable) & Shipping

Item	Model & Description	QTY	Unit Price	Total Price
	Software Options for Sensor Highway			
001	*pn# 9380-7003-9,* ***AE WIN 3D-LOC,*** 3 DIMENSIONAL LOCATION SOFTWARE OPT	1	$1,369.00	$1,369.00
002	*pn# 9380-7003-10,* ***AE-WIN-SPHERE-LOC,*** Spherical location option for Aewin	1	$1,720.00	$1,720.00
003	*pn# 9380-7003-2,9,10,* ***AE-WIN-LOCwin-Suite,*** Full location suite including 2D-LOC, 3D-LOC and SPHERE-LOC software	1	$3,432.00	$3,432.00
004	*pn# 9380-7003-8,* ***AE-WIN-Supervisor-Mode,*** Supervisor/Operator mode provides a password protected supervisor mode for setting up AEwin and an operator mode for carrying out AE tests without the ability to change AEwin settings	1	$516.00	$516.00
005	*pn# 9380-7003-6,* ***AE-WIN 32 GROUPS,*** ENHANCEMENT TO 32 LOCATION GROUPS	1	$481.00	$481.00
006	*pn# 9380-7003-4,* ***AE-WIN-Smart-Threshold,*** Computer generated adaptive AE threshold control	1	$174.00	$174.00
007	*pn# 9380-7003-39,* ***AEwin-Intensity,*** Intensity Analysis module	1	$432.00	$432.00
008	*pn# 9380-7003-5L,* ***AEwin-Licensed-Replay-USB,*** Replay only AEwin License with all licensed options (Requires proof of existing AEwin license and options) and USB license key, for use on multiple analysis computers	1	$425.00	$425.00
	Additional Equipment Options for Sensor Highway			
009	*pn# 9380-5045,* ***BaseStation Battery Backup,*** Outdoor BaseStation Battery Backup option installed into system. Up to 20 minutes operation.	1	$595.00	$595.00
010	*pn# Weather Station,* ***Weather Station,*** Solid State Weather Station for use in SH-III Data Collector or SH-II Smart Remote, provides over 20 weather related parameters for direct input into AEwin software and parametrics	1	$6,005.00	$6,005.00
011	*pn# Weather Station Surge protector,* ***Weather Station Surge protector,*** Surge Protector for Weather station, highly recommended to prevent burnout from lightening strike	1	$1,305.00	$1,305.00

Validity:	*90 Days*
Payment Terms:	*Net 30 days upon approval by Accounting. We also accept credit cards, (VISA, MasterCard & American Express)* ***NOTE:*** *there will be a 3% processing fee levied on total of order when using a credit card for orders of $5000.00 or over.*
Tax Terms	**Mistras Group, Inc. is now adding all applicable sales tax, on equipment orders sold, on our invoices. Your local state, city or county tax will automatically be charged unless a tax exempt or re-sale certificate has been submitted**
Delivery:	*45-60 Days ARO*
FOB:	***Princeton Junction, NJ , Buyer understands that he/she is responsible for shipment, insurance and any damages caused by shipping, from the FOB Shipping Point.***
Ship Via:	*UPS Ground* ***PP & Add to invoice*** *or collect with customers account number*
Origin:	*Made in USA*
Minimum Order:	*$100*
Place an Order:	*Please submit documents to sales.systems@mistrasgroup.com or by fax to 609-716-0706*

"BUY AMERICAN"
"Help keep Americans Employed"

I trust that the specifications and options are clear, but if you have any questions or comments, please do not hesitate to call. We appreciate your inquiry and look forward to doing business with you in the near future. If you visit our website at www.mistrasgroup.com , there is some helpful information on our products.

Best regards,

Terry Tamutus

Terry Tamutus
Director Infrastructure Business Development
Products & Systems Division
Mistras Group, Inc.
P: 609-468-5737
E: terry.tamutus@mistrasgroup.com

<TAT/eg>

6.

Your Business: University of Vermont and State Agricultural Colle

Computers | Enter keyword or product number | Go | Dryver's Aoeount for Business | Lists

Departments | Today's Deals | Sell on Amazon Business | Help

Computers | Laptops | Tablets | Desktops | Monitors | Computer Accessories | PC Components | PC Gaming

Electronics › Computers & Accessories

Roll over image to zoom in

ASUS T102HA-D4-GR Transformer Mini 10.1-Inch 2 in 1 Touchscreen Laptop (Intel Quad-Core, 128GB EMMC, Grey, pen and keyboard included)

by Asus

80 customer reviews | 101 answered questions

Business Price $391.99 & Free Shipping. Details

Your cost could be $388.99: Qualified customers get $5 in Gift Card funds on first $100 reload of their Amazon Gift Card Balance. Learn more

In Stock.

Want it Thursday, Feb. 23? Order within **16 hrs 27 mins** and choose **One-Day Shipping** at checkout. Details

Ships from and sold by Amazon.

- Versatile Windows 10 device with keyboard and pen included, 2-in-1 functionality: use as both laptop and tablet
- All day battery life, rated up to 11 hours of video playback; 128GB EMMC storage
- Latest Intel Atom Quad Core x5-Z8350 Processor with 4GB RAM for fast and efficient performance
- One-touch login and enhanced security with fingerprint sensor supporting Windows Hello
- Magnesium Alloy body weighs less than 1.7 lbs with keyboard attached and only 0.6 inches thin

› See more product details

Used & new (63) from $309.22 & FREE shipping. Details

Report incorrect product information.

MICROSOFT

Save on Word, Excel & PowerPoint for Surface.

› Shop now

Microsoft Office 365

Ad feedback

Share

Buy new: $391.99

Qty: 1

Add to Cart

1-Click ordering is not available for this item.

Ship to:

Dryver R. Huston- Burlington - 05405

Buy used: $349.12

Add to List

Other Sellers on Amazon

$408.99 Add to Cart
+ Free Shipping
Sold by: OneDealOutlet Online

$417.22 Add to Cart
+ Free Shipping
Sold by: pcrush-outlet

$399.00 Add to Cart
& FREE Shipping on eligible orders. Details
Sold by: Amazon.com

Used & new (63) from $309.22 & FREE shipping. Details

Have one to sell? Sell on Amazon

Frequently Bought Together

Total price: $420.49

Add all three to Cart

These items are shipped from and sold by different sellers. Show details

- **This item:** ASUS T102HA-D4-GR Transformer Mini 10.1-Inch 2 in 1 Touchscreen Laptop (Intel Quad-Core, 128GB EMMC... $399.00
- KuGI Asus Transformer Mini T102HA screen protector - 9H Hardness HD clear Tempered Glass Screen... $9.50

Microsoft Surface

Save Now on Surface Book Devices.

Microsoft Surface Book (Intel Core i5, 8GB RAM, 256GB) with Windows 10 ...

43

~~$1,999.00~~ $1,848.00

Ad feedback

7.

Your Business: University of Vermont and State Agricultural Colle

All | deep cycle marine battery | Go | Dryver's Account for Business | Lists

Departments | Today's Deals | Sell on Amazon Business | Help

All Electronics | Deals | Best Sellers | TV & Video | Audio & Home Theater | Computers | Camera & Photo | Wearable Technology | Car Electronics & GPS

Health & Household › Household Supplies › Household Batteries › 12V

Roll over image to zoom in

Universal UB121000-45978 12v 100AH Deep Cycle AGM Battery 12V 24V 48V(Black)

by Universal Power Group

89 customer reviews | 107 answered questions

Price: $159.49 & FREE Shipping

Your cost could be $164.49: Qualified customers get $5 in Gift Card funds on first $100 reload of their Amazon Gift Card Balance. Learn more

Only 1 left in stock.

Get it as soon as Feb. 27 - March 2 when you choose Standard Shipping at checkout.

Business Seller Ships from and sold by First Web Sales .

- AGM design yields excellent Deep Cycle service Performance rating, Float Voltage: 13.6 to 13.8 V
- Less than 3% per month standing self discharge, Maintenance Free, Charge Voltage: 14.5 to 14.9 V
- Valve Regulated, Float and Cycle Use, Leak Proof/Spill Proof
- AGM design may offer greater reliability in extreme use applications
- Dimensions (LxWxH): 12.17 x 6.61 x 8.30 in, Weight: 63.93 lbs, 1 Year Warranty

New (3) from $159.49 & FREE shipping.

Report incorrect product information.

Share

$159.49 + Free Shipping
Only 1 left in stock. Sold by First Web Sales

Add to Cart

1-Click ordering is not available for this item.

Ship to:
Dryver R. Huston- Burlington - 05405

Add to List

Other Sellers on Amazon

$159.99 Add to Cart
+ Free Shipping
Sold by: Ace Comp Solutions

New (3) from $159.49 & FREE shipping.

Have one to sell? Sell on Amazon

Frequently Bought Together

Total price: $167.44

Add both to Cart

One of these items ships sooner than the other. Show details

This item: Universal UB121000-45978 12v 100AH Deep Cycle AGM Battery 12V 24V 48V(Black) $159.49

2PC 4 AWG Gauge Red Black Battery Post Inverter Cables Solar, Golf Car RV Boat $7.95

Sponsored Products Related To This Item (What's this?)

8.

Your Business: University of Vermont and State Agricultural Colle

All | trickle charger | Go | Dryver's Account for Business | Lists

Departments | Today's Deals | Sell on Amazon Business | Help

Automotive | Your Garage | Deals & Rebates | Best Sellers | Parts | Accessories | Tools & Equipment | Car Care | Motorcycle & Powersports | Truck

Shop by vehicle: Year | Make | Model | Go | Your Garage (0)

Automotive › Tools & Equipment › Jump Starters, Battery Chargers & Portable Power › Battery Chargers

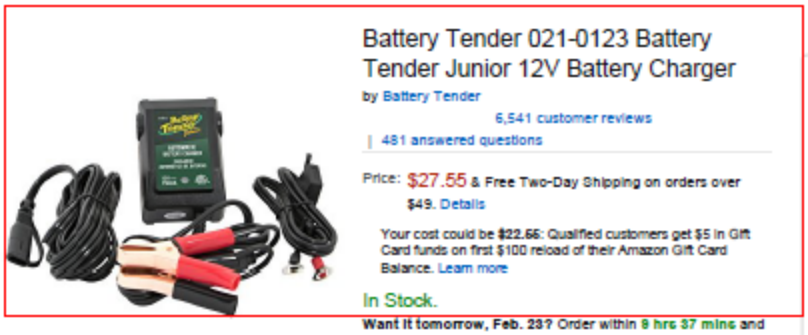

Roll over image to zoom in

Battery Tender 021-0123 Battery Tender Junior 12V Battery Charger

by Battery Tender

6,541 customer reviews | 481 answered questions

Price: $27.55 & Free Two-Day Shipping on orders over $49. Details

Your cost could be $22.66: Qualified customers get $5 in Gift Card funds on first $100 reload of their Amazon Gift Card Balance. Learn more

In Stock.

Want it tomorrow, Feb. 23? Order within 9 hrs 37 mins and choose **One-Day Shipping** at checkout. Details

Ships from and sold by Amazon.com.

- Spark proof during lead connection, reverse polarity protected and includes a 12-foot output cord and 5-year warranty
- Perfect for charging all 12-volt lead-acid, flooded or sealed maintenance free batteries (AGM and gel cell)
- Complete 4-step charging program (Initialization, Bulk Charge, Float Mode) allows for optimization of battery power, without overcharging
- Automatic charge cycle functionality switches to float mode after fully charging the battery
- Solid state two color LED indicates stage of charger.

› See more product details

Compare with similar items

Used & new (142) from $24.99 & FREE shipping.

Report incorrect product information.

Share 2K+ Shares

Qty: 1

Add to Cart

1-Click ordering is not available for this item.

Ship to:

Dryver R. Huston- Burlington - 05405

Add to List

Other Sellers on Amazon

$26.95 Add to Cart
+ Free Shipping
Sold by: WEGOTTHEGOODS4U

$26.99 Add to Cart
+ Free Shipping
Sold by: Autocare Depot

$27.42 Add to Cart
+ Free Shipping
Sold by: BAP0006

Used & new (142) from $24.99 & FREE shipping.

Have one to sell? Sell on Amazon

Frequently Bought Together

Total price: $42.31

Add both to Cart

☑ **This item:** Battery Tender 021-0123 Battery Tender Junior 12V Battery Charger $27.55

☑ Battery Tender 081-0148-25 25' Quick Disconnect Extension Cable $14.76

Sponsored Products Related To This Item (What's this?)

Page 1 of 25

OAK LEAF

Weatherproof, 50,000H Lighting, Low Consumption

LED Wall Pack Light,LuminWiz 70W 6000K Waterproof and Outdoor Light... 12

$99.99

Ad feedback

9.

Your Business: University of Vermont and State Agricultural Colle

All | battery box | Go | Dryver's Account for Business | Lists

Departments | Today's Deals | Sell on Amazon Business | Help | Website Feedback

Sports & Outdoors | Sports & Fitness | Outdoor Recreation | Sports Fan Shop | Sports Deals | Outdoor Deals

Sports & Outdoors › Sports & Fitness › Boating & Sailing › Boating › Boat Motors › Trolling Motors

Click to open expanded view

MinnKota Trolling Motor Power Center

by Minn Kota

879 customer reviews | 174 answered questions

Price: $57.58 & Free Two-Day Shipping. Details

Your cost could be $62.68: Qualified customers get $5 in Gift Card funds on first $100 reload of their Amazon Gift Card Balance. Learn more

In Stock.

Want it tomorrow, Feb. 23? Order within 7 hrs 10 mins and choose **One-Day Shipping** at checkout. Details

Ships from and sold by Amazon.com. Gift-wrap available.

- Battery Holder/Case ONLY. Battery NOT INCLUDED.
- Motor center ideal for small-boat transom applications
- Easy-access batter terminals for connecting leads
- Built-in battery meter displays current "state of charge"
- Designed to fit group 24- and 27-size batteries
- Offers pair of 12-volt accessory plugs and manual reset circuit breakers

Used & new (93) from $48.94 & FREE shipping. Details

Report incorrect product information.

Share

Recurring delivery
$57.58

One-time purchase:
$57.68

Qty: 1

Add to Cart

1-Click ordering is not available for this item.

Ship to:
Dryver R. Huston- Burlington - 05405

Add to List

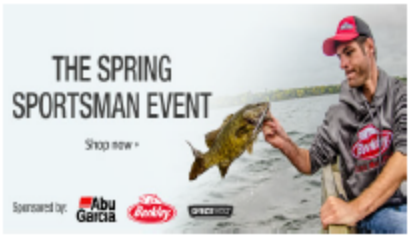

Other Sellers on Amazon

$63.04 Add to Cart
+ Free Shipping
Sold by: Northern Marine

$63.04 Add to Cart
+ Free Shipping
Sold by: BoxyBay [On Sale (ending soon) | Authorized]

$64.12 Add to Cart
+ Free Shipping
Sold by: my Goods

Used & new (93) from $48.94 & FREE shipping. Details

Frequently Bought Together

Total price: $209.66

Add all three to Cart

- ☑ **This item:** MinnKota Trolling Motor Power Center $57.58
- ☑ Minn Kota Endura C2 30 Freshwater Transom Mounted Trolling Motor (30" Shaft) $99.99
- ☑ MinnKota MK-105P Portable Battery Charger $52.09

Customers Who Bought This Item Also Bought

RENOGY, The Future of Clean Energy.

Renogy 100 Watts 12 Volts Polycrystalline Solar Starter Kit
189
~~$194.99~~ $184.37

Ad feedback

Your Business: University of Vermont and State Agricultural Colle

10.

All | battery cable | Go | Dryver's Account for Business | Lists

Departments | Today's Deals | Sell on Amazon Business | Help | Website Feedback

Automotive | Your Garage | Deals & Rebates | Best Sellers | Parts | Accessories | Tools & Equipment | Car Care | Motorcycle & Powersports | Truck

Shop by vehicle: Year | Make | Model | Go | Your Garage (0)

Automotive › Replacement Parts › Batteries & Accessories › Battery Accessories › Battery Jumper Cables

Roll over image to zoom in

EPAuto 20-Inch Battery Inverter Cable Set

by EPAuto

63 customer reviews

Price: $8.87 & Free Two-Day Shipping on orders over $49. Details

Your cost could be $8.87: Qualified customers get $5 in Gift Card funds on first $100 reload of their Amazon Gift Card Balance. Learn more

In Stock.

Want it tomorrow, Feb. 23? Order within 6 hrs 67 mins and choose **One-Day Shipping** at checkout. Details

Sold by EPAuto Direct and Fulfilled by Amazon. Gift-wrap available.

- A set of positive (Red) and negative (Black) small cables
- All copper conductor with nickel-plated copper terminals
- Heavy Duty 6 Gauge cables
- 1/4" & 3/8" round center hole
- Length: 20 inch

› See more product details

New (1) from $8.87 & FREE shipping on orders over $35.00. Details

Report incorrect product information.

Share

Qty: 1

Add to Cart

1-Click ordering is not available for this item.

Ship to:

Dryver R. Huston- Burlington - 05405

Add to List

Have one to sell? Sell on Amazon

RENOGY, The Future of Clean Energy.

Renogy 100 Watts 12 Volts Polycrystalline Solar Starter Kit

188

~~$194.89~~ $184.37

Ad feedback

Frequently Bought Together

Total price: $22.07

Add all three to Cart

These items are shipped from and sold by different sellers. Show details

- ☑ **This item:** EPAuto 20-Inch Battery Inverter Cable Set $8.87
- ☑ Shoreline Marine Battery Marine Terminal Kit $7.82
- ☑ Camco 55362 Standard Battery Box - Group 24 $5.38 Add-on Item

Sponsored Products Related To This Item (What's this?)

11.

Try Prime | All | auto knife switch

Departments | Browsing History | Dryver's Amazon.com | Hello, Dryver Account & Lists | Orders | Try Prime | 6 Cart

Automotive | Your Garage | Deals & Rebates | Best Sellers | Parts | Accessories | Tools & Equipment | Car Care | Motorcycle & Powersports | Truck

Shop by vehicle: Year Make Model Go | Your Garage (0)

Automotive › Replacement Parts › Batteries & Accessories › Battery Accessories › Battery Switches

ınect Knife Blade
p Terminal Car
ıt Off

r reviews

ping on orders over $35.

Your cost could be $15.89: Qualified customers get $5 in Gift Card funds on first $100 reload of their Amazon Gift Card Balance. Learn more

r within 16 hrs 26 mins and checkout, Details
d Fulfilled by Amazon. Gift-

and prevent theft or

ıan working on electrical

ost only;
ı power is cut;
electrical power on any

Share

Qty: 1

Add to Cart

Turn on 1-Click ordering for this browser

Ship to:
Dryver R. - Burl - 05405

Add to List

Other Sellers on Amazon

$21.99 Add to Cart
+ Free Shipping
Sold by: Penson & Co.

New (2) from $20.99 & FREE shipping on orders over $35.00. Details

Roll over image to zoom in

› See more product details

New (2) from $20.99 & FREE shipping on orders over $35.00. Details

Report incorrect product information.

Have one to sell? Sell on Amazon

Customers Who Bought This Item Also Bought

FIAMM 72112 Freeway Blaster Horn
617
$13.28

Cal-Hawk AZGA125 Rubber Grommet Assortment Set Electrical Gasket, 125 Piece
195
$7.76

WirthCo 20138 Battery Doctor Battery Disconnect for Top Terminal
112
$19.47

Sponsored Products Related To This Item (What's this?)

12.

Try Prime | All | weatherproof fuse box

Departments | Browsing History | Dryver's Amazon.com | Hello, Dryver Account & Lists | Orders | Try Prime | 6 Cart

Automotive | Your Garage | Deals & Rebates | Best Sellers | Parts | Accessories | Tools & Equipment | Car Care | Motorcycle & Powersports | Truck

Shop by vehicle: Year Make Model Go | Your Garage (0)

Automotive › Replacement Parts › Lighting & Electrical › Electrical › Fuses & Accessories › Fuse Boxes

8-Gauge Maxi Fuse Holder - Trucks,

Your cost could be $0.86: Qualified customers get $5 in Gift Card funds on first $100 reload of their Amazon Gift Card Balance. Learn more

roh 8 when you choose

Sales.

ory for trucks, semis, RVs and
lty - made in Taiwan
30V copper cable with thick

up to 80 amp (fuse not
ly)
st dirt and moisture; 6 in.
ting wiring
r high-draw 12V/24V/36V

Click to open expanded view

New (2) from $5.95 & FREE shipping.

Report incorrect product information.

Share

Qty: 1

$5.95 + Free Shipping
In Stock. Sold by Lecsoo Sales

Add to Cart

Turn on 1-Click ordering for this browser

Ship to:
Dryver R. - Burl - 05405

Add to List

Other Sellers on Amazon

$5.97 Add to Cart
+ Free Shipping
Sold by: FixFind

New (2) from $5.95 & FREE shipping.

Have one to sell? Sell on Amazon

Frequently Bought Together

Total price: $15.23

Add both to Cart

Add both to List

One of these items ships sooner than the other. Show details

This item: 8-Gauge Maxi Fuse Holder - Trucks, Semi, RV - Taiwan $5.95

Stinger SPFS680 Shoc-Krome Maxi Fuse 80 Amp 3-Pack $9.28

Brighter Road Ahead - HID Headlight Conversion Kit

Kensun HID Xenon 36W Headlight Conversion Kit

6,483

$129.99 $38.99

Ad feedback

Sponsored Products Related To This Item (What's this?)

Mistras shipped the Sensor Highway III AE test system to UVM on May 26, 2017. Upon arrival, personnel at UVM unpacked the boxes, checked items against the packing list (attached) and proceeded to conduct tests in the laboratory to verify the operational condition and capabilities of the equipment. The equipment performed in a satisfactory manner and seemed to be in good working order. The following is a summary of the test results.

1. ***Equipment*** – The Sensor Highway III, Figure 4.4, fits primarily in a steel electrical box, with cables extending to the transducers, controlling computer and power supply, Figure 4.4. This system can operate and collect data from 8 AE sensors and other voltage-type transducers.

(a) *(b)*

Figure 4.4: Sensor Highway III instrument box (a) lid closed and (b) lid open

2. ***Initial Tests and Transducer Mounting*** – The initial tests assessed the ability to measure AE signals produced on concrete slabs in the laboratory. Two standard nondestructive methods of exciting the structure are a pencil lead break and impact from a dropped steel ball. The testing indicated that the dropped ball provided more consistent data for the slabs tested. The initial method of a attaching the transducers to the concrete slab was to use a heavy silicone vacuum grease. This grease is remarkably sticky, but nonetheless did not provide a consistent and robust attachment to the concrete, largely due to the porous and rough nature of the surface. A workaround is to first attach small steel plates to the concrete with and adhesive and then to attach the transducer to the steel plate with vacuum grease, Figure 4.5. The testing examined four different commercially available adhesives. Three of the adhesives were single-part construction adhesives with an advertised capability of bonding metal to concrete. The fourth was a two-

part 5-minute cure epoxy. All four adhesives provided a strong grip. However, the two-part epoxy was the only one to setup in 5-10 minutes. The other three required an overnight cure cycle.

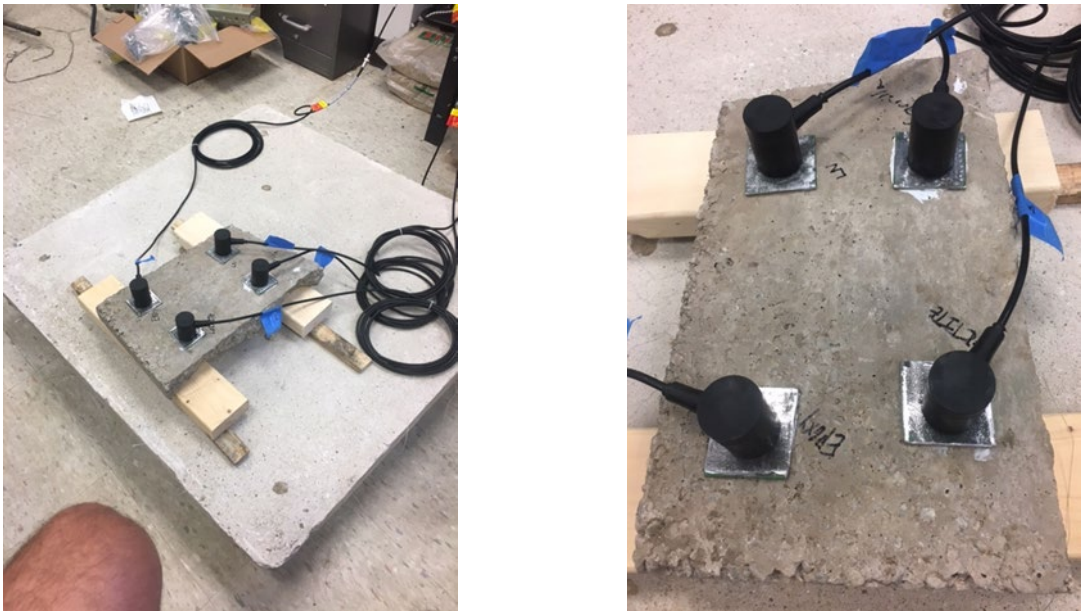

(a) (b)

Figure 4.5: Small concrete slab with adhesive-bonded steel plates and 4 acoustic emission transducers vacuum-grease attached to the steel plates

1. ***Steel Ball Drop Event Counting and Triangulation Tests*** – A series of tests evaluated the capability of the AE test equipment to detect and locate dynamic mechanical events. The tests used a 7/16 in. diameter steel ball dropped from a height of about 18 in. as the excitation source. The system logs hits as individual dynamic events. The system was consistently capable of detecting hits with the dropped steel ball using default settings. Determining the impact location required adjusting the transducer event threshold settings to obtain relatively consistent location information for the impacts, as shown in Figure 4.6 and Figure 4.7.

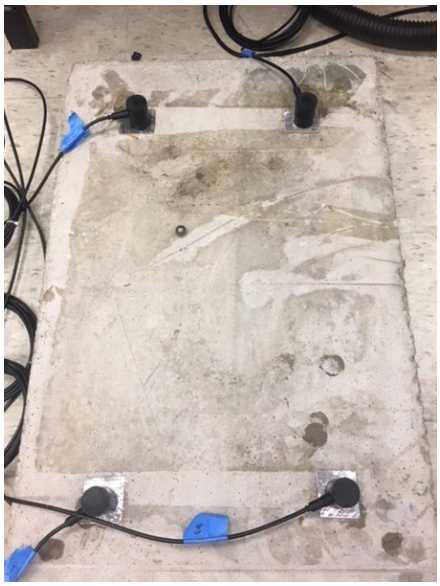

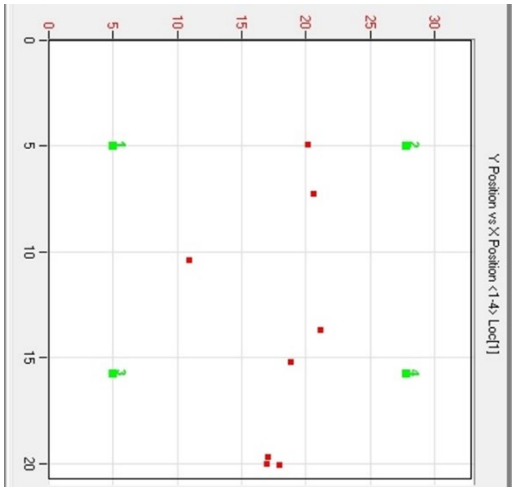

(a) *(b)*

Figure 4.7:

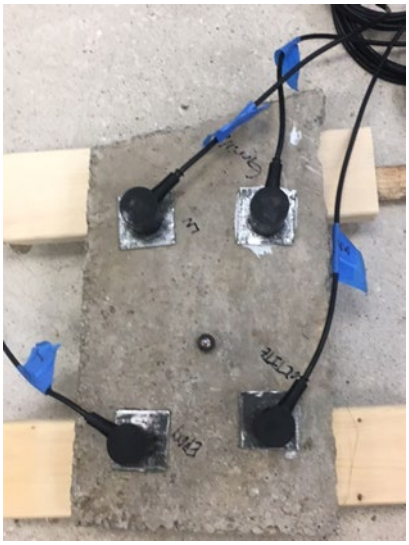

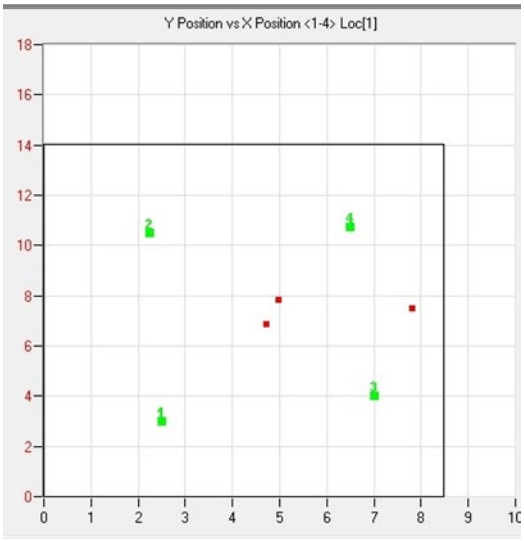

(a) *(b)*

Figure 4.6: Small concrete slab: (a) with steel ball, (b) with mapping of transducers (green dots), steel ball and sample location estimates (red dots)

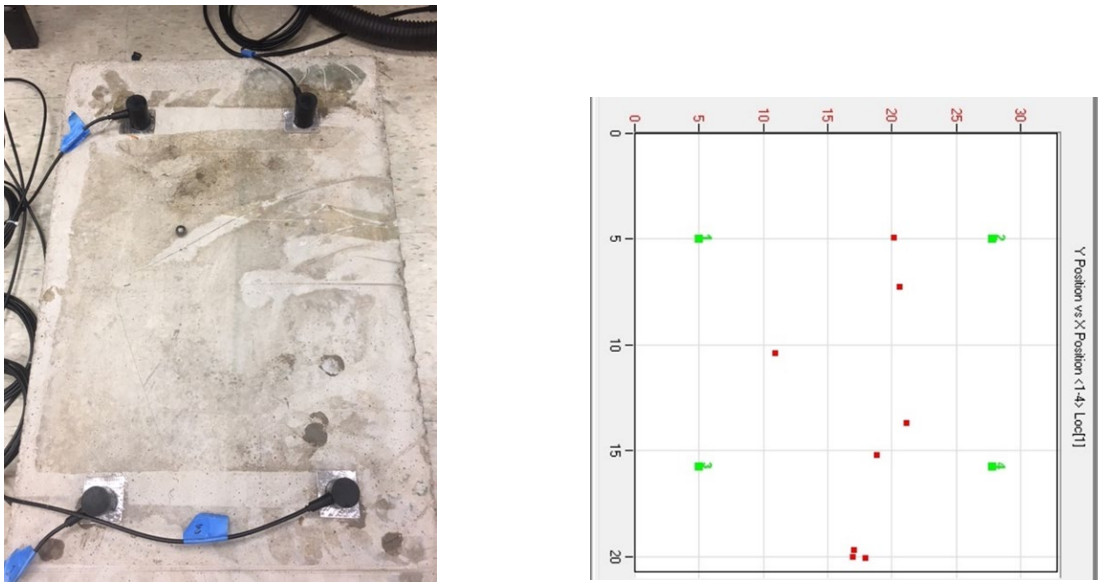

(a) *(b)*

Figure 4.7: Medium-sized concrete slab (a) with steel ball, (b) with mapping of transducers (green dots) and estimated ball impact locations (red dots)

4. ***Concrete Crush Test*** – The next series of tests examined the capability of the system to detect and locate damage to the concrete as it occurs. The first set of damage tests crushed the surface of a small concrete slab by pressing a steel ball into the surface. A large C-clamp with a missing articulated ball-foot and exposed ball provided the crushing action by turning the screw. Tight turning using a large wrench for leverage produced sufficient damage to be detected and located by the system. The estimated location of the damage with the AE system was reasonable, but did show some scatter, Figure 4.8.

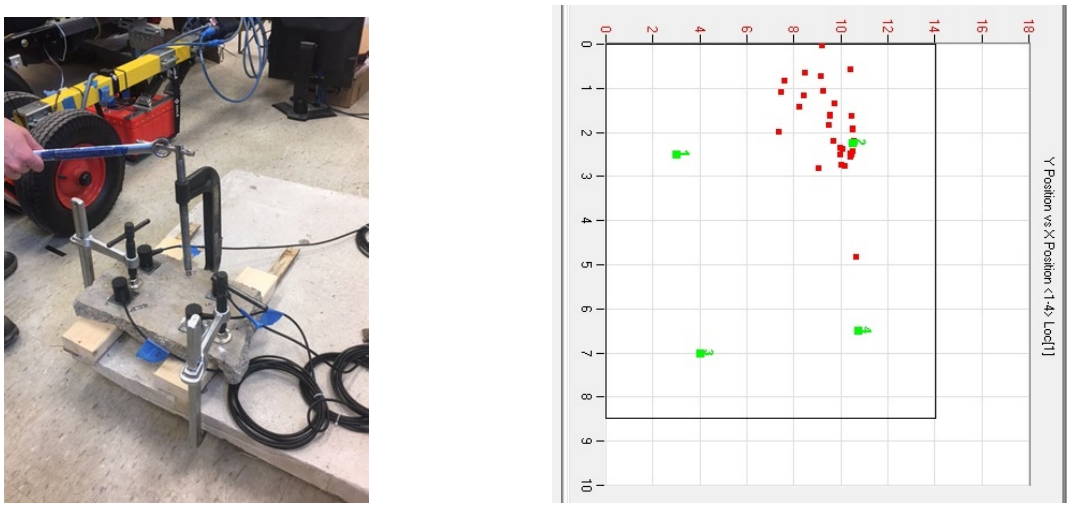

(a) *(b)*

Figure 4.8: C-clamp crush test: (a) setup, (b) detection and estimated location of damage site

5. ***Concrete slab fracture*** – This damage test applied a 3-point bending load to a small concrete slab, using a screw-driven adjustable length wood clamp. The slab contained no reinforcing and broke suddenly. This is a failure mode that should not occur often in transportation structures with conventional reinforcing, but nonetheless provided some useful data, including the detection of precursor microcracking before the major cracking, Figure 4.9.

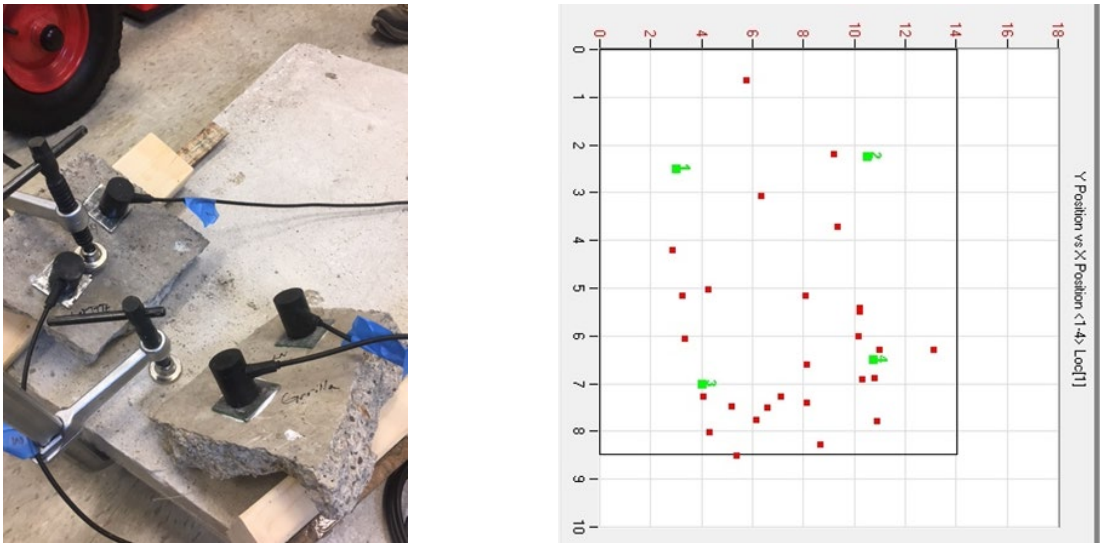

(a) *(b)*

Figure 4.9: Fracture test of small concrete slab: (a) broken slab, (b) test results with transducer location (green dots) and estimated damage location (red dots)

CHAPTER 5
ACOUSTIC EMISSION DATA COLLECTION AND RESULTS: LABORATORY TESTS

5.1 Overview

Laboratory testing helped to establish and adapt system setup input parameters for the field tests including: wave speed velocities, sensor array layouts, and amplification filters. Pull-out and three-point bending tests demonstrated the capability of AE sensing to detect cracks. Data from three-point bending tests provided the means to associate and correlate observed cracks and stress zones to AE event locations. The pull-out and three-point bending (flexure) tests followed the work of ElBatanouny, et al. (2014), but differed with smaller scale beams and the introduction of defects to control the failure locations are unique.

For pull-out tests the 5-inch x 5-inch x 12-inch (127 mm x127 mm x 305 mm) laboratory test beams used fast-setting QUIKRETE® and contained a single no. 4 reinforcing bar in the center of the beam, necked down off center from 0.5-inch (12.5 mm) diameter to 0.25-inch (6.25 mm) diameter to control the point of failure. The eight sensor arrays for the test beam employed a 3-D spatial array (Figure 5.1). Silicone vacuum grease secured the sensors to the concrete beam for the relatively short duration of the laboratory tests. A load frame applied center-span force to the beams with displacement control at a rate of 0.03 in/sec (0.762 mm/sec) until failure.

For the three-point bending tests the 5-inch x 5-inch x 24-inch (127 mm x127 mm x 610 mm) laboratory test beams used fast-setting QUIKRETE® and contained two no. 4 reinforcing bars spaced roughly 1.5-inches (38 mm) from the bottom and adjacent side and were necked down in the center from 0.5-inch (12.5 mm) diameter to 0.25-inch (6.25 mm) diameter to control the point of failure. The 8-sensor arrays for the test beams were either a 2-D planar array (Figure 5.2) or 3-D spatial array (Figure 5.4). Silicone vacuum grease secured the sensors to the concrete beam for the relatively short duration of the laboratory tests. A load frame applied center-span force to the beams with displacement control at a rate of 0.03 in/sec (0.762 mm/sec) until failure.

5.1.1 Laboratory Test Methodology

This section describes the methods for laboratory AE data collection using relatively small reinforced concrete beam specimens under pull-out and three-point bending to assess the efficacy of AE sensing in detecting cracks. This study employed a Mistras AEwin™ Sensor Highway III monitoring system, associated AEwin™ processing software, and an eight PK6I sensor array per manufacturers' recommendations and ASTM standards (ASTM E1316-18a, 2018; ASTM E3100-17, 2017; Physical Acoustics, 2018; Worley II et al., 2018). The PK6I sensor is a medium-frequency, resonant AE sensor with

an integral, ultra-low noise, low-power, filtered 26 dB preamplifier, which can drive signals through 200 meters of cable and operates at 60 kHz frequency (Physical Acoustics, 2018).

5.1.1.1 AE Instrumentation Input Parameters and Collection

Mistras AEwin™ Sensor Highway III monitoring system and associated AEwin™ processing software allows for user-defined inputs to refine the collected AE events. The acquisition setup parameters, as listed in Table 5.1, followed that specified by the manufacturer. Pencil lead break tests in controlled laboratory specimens confirmed the validity of these parameters (Sause, 2011).

Table 5.1: Mistras AEwin™ Sensor Highway III Input Parameters

Parameter		**Value**	**Units**
Threshold		60	decibel (dB)
Pre-amplifier Gain		26	decibel (dB)
Analog Filter	Lower Bounds	20	kilohertz (kHz)
	Upper Bounds	400	kilohertz (kHz)
Digital Filter	Lower Bounds	20	kilohertz (kHz)
	Upper Bounds	200	kilohertz (kHz)
Timing Parameters	Peak Definition Time (PDT)	200	microsecond (µs)
	Hit Definition Time (HDT)	800	microsecond (µs)
	Hit Lockout Time (HLT)	1,000	microsecond (µs)
	Maximum Hit Duration (MDT)	1,000	millisecond (ms)
Longitudinal Wave Velocity		13,083	feet per second (ft/sec)
Transverse Wave Velocity		7,833	feet per second (ft/sec)
Surface Wave Velocity		7,250	feet per second (ft/sec)

If the user-defined minimum sensor hits occur within the specified time duration parameters then the AEwin™ software collects fifteen features of the AE waveform signals including: 1) amplitude, 2) duration, 3) energy, 4) counts, 5) rise time, 6) peak frequency, 7) frequency centroid, 8) absolute energy, 9) signal strength, 10) initial frequency, 11) reverberation frequency, 12) counts-to-peak, 13) average signal level, 14) root mean square (RMS), and 15) average frequency.

5.1.2 Pull-out Test Data Collection

The pull-out test recorded ninety AE events. The concentration of AE events was around the observed cracking as seen in Figure 5.1. 48 of the 90 events led to anomalous location estimates with the estimated location appearing underneath one of the eight sensors. The recorded AE events, excluding the

on-sensor events, generally concentrated around the observed cracking. As mentioned earlier, the AE sensor connections to the beam were secured into prefabricated metal armored boxes made from hollow square stock and then attached to the beam simulate with 5-minute epoxy. Subsequent laboratory testing attempted to resolve the anomalous location behavior with a different sensor mount such as removing the metal boxes and use of different couplants (i.e. epoxy vs. silicone vacuum grease). The metal boxes cut from hollow stock may not fit truly flush to the sensor which would allow for a possible air gap between the sensor wear plate and steel box. This air gap could create for some disturbance or throw errors in the source location that could result in the AE event being located directly at the sensor. It should be noted that the investigators later learned that the underlying triangulation algorithm is prone to this anomaly when using rectangular arrays of sensors. A staggered triangular grid geometry tends to avoid these anomalies.

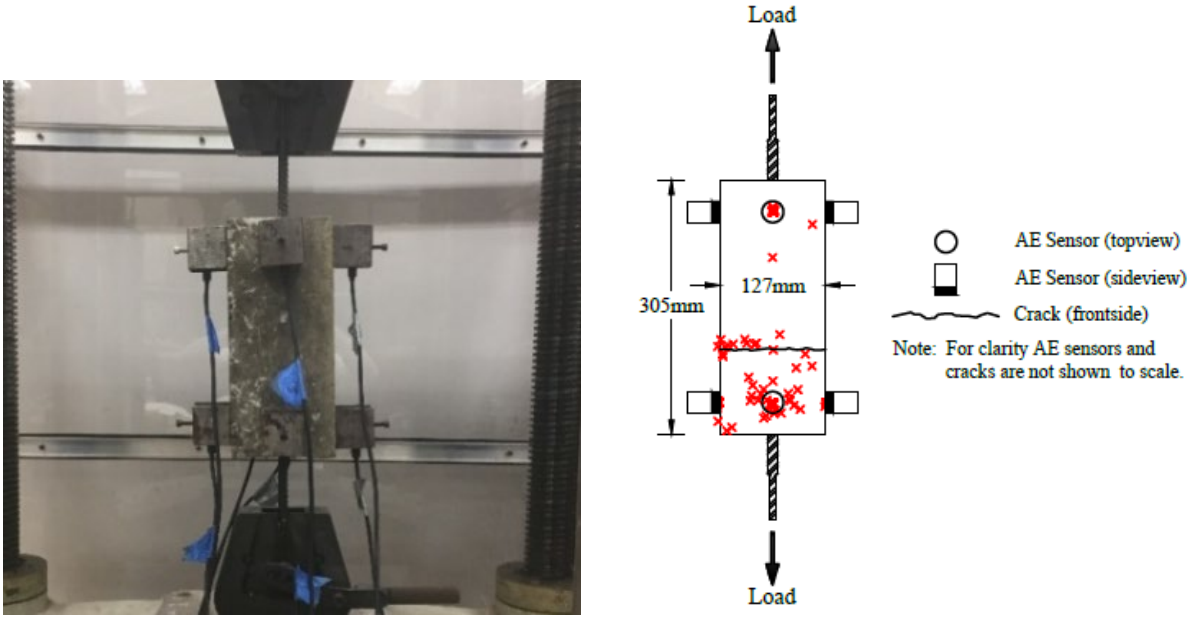

(a) *(b)*

Figure 5.1: Laboratory pull-out test of reinforced concrete beam with 3-D sensor array. (a) Photograph of 3-D sensor array prior to testing, (b) Schematic of 3-D sensor array including AE event locations, sensors, and observed cracks

5.1.3 Three-point Bending Test Data Collection

This section describes data collected from relatively small laboratory reinforced concrete beam specimens under three-point bending to evaluate the performance of AE sensing in detecting cracks.

5.1.3.1 2-D Sensor Array

The laboratory three-point bending test employing the 2-D planar sensor array recorded a total of 142 AE events when loaded to failure (Figure 5.2). Observed cracking took place in the middle of the beam, nearly in line with the point of loading. The recorded AE event locations were generally within 2 inches (50 mm) from the observed cracks. Recorded AE events with locations outside of this region may be due to other effects and events. Possibilities include internal cracking, anomalous under-sensor location estimates and guiding of the elastic waves by the crack surfaces.

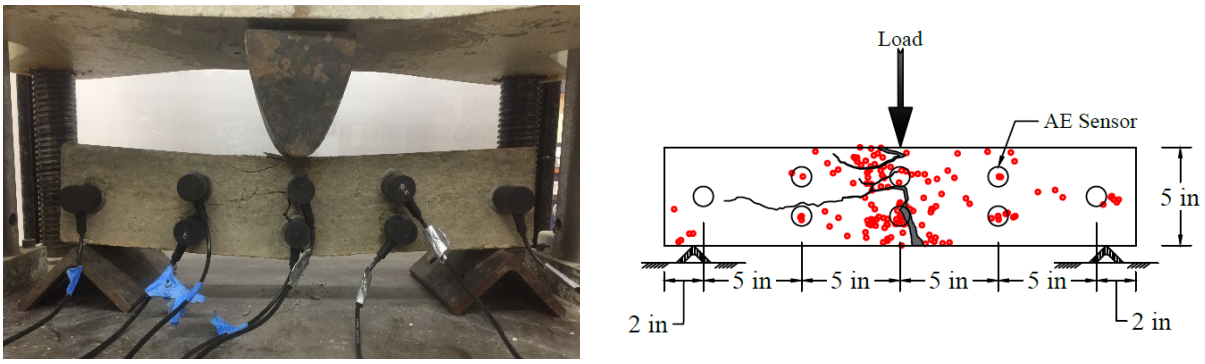

(a) *(b)*

Figure 5.2: Laboratory three-point bending test of reinforced concrete beam with 2-D sensor array. (a) Photograph of 2-D sensor array at the completion of testing, (b) Schematic of 2-D sensor array including AE event locations, sensors, and observed cracks

Categorization of the observed AE events based on location produced three groupings; 1) AE event on or near an observed crack, 2) AE event not on or near an observed crack, and 3) AE event directly at an AE sensor location. Analyzing the 15 waveform features collected from each AE signal. by the AEwin™ Sensor Highway III, provided a comparison of the three groups. Although a clear determination of the AE event features from the observed cracks was not identified immediately, of note is the linear distribution when plotting AE event amplitudes with respect to duration, Figure 5.3. A simple explanation of the linear relation may be that the larger events have longer durations, with the linear relation between the logarithm of the amplitude (dB) and duration explained by amplitude-dependent dissipative processes.

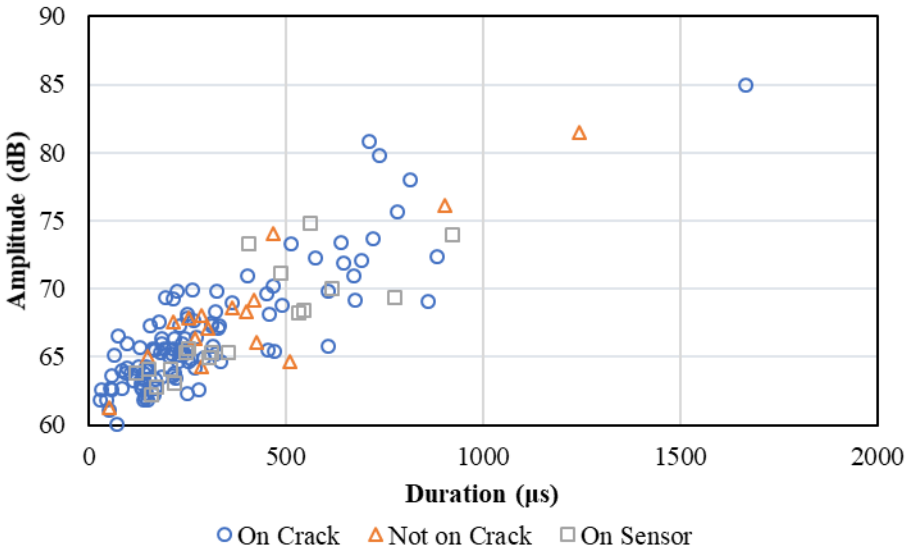

Figure 5.3: AE event duration vs. amplitude categorized by proximity to observed cracks

5.1.3.2 3-D Sensor Array

The laboratory three-point bending to failure test with the 3-D sensor array recorded a total of 111 AE events, Figure 5.4. The cracking took place on the left side of the beam, largely as shear cracking. No cracks appeared on the right side of the test beam. The location of the recorded AE events was almost entirely on the left side of the beam, coinciding with where all the cracks occurred.

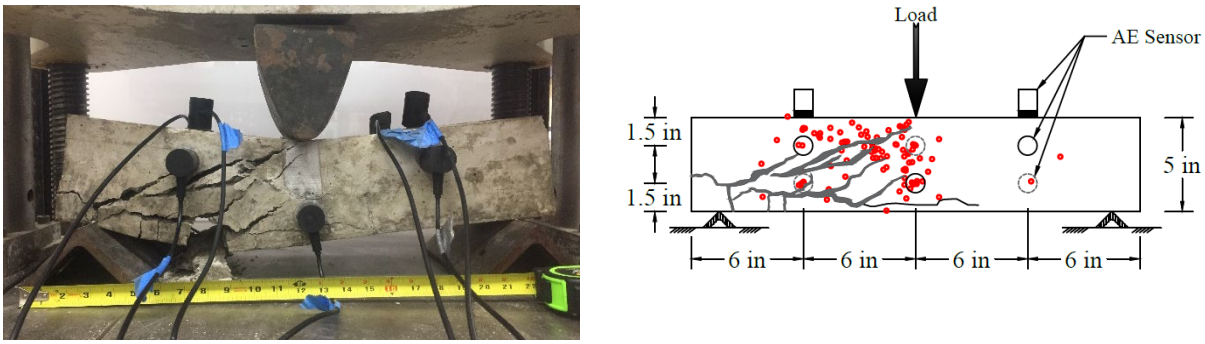

(a) *(b)*

Figure 5.4: Laboratory three-point bending 3-D sensor array. (a) Photograph of 3-D sensor array at the completion of testing, (b) Schematic of 3-D sensor array including AE event locations, sensors, and observed cracks

These tests indicated a strong correlation between observed cracks and recorded AE event locations. The 2-D planar sensor array configuration showed greater accuracy in locating surface cracks.

A possible reason for the discrepancy between the 2-D and 3-D sensor arrays stems from the differences in the AE event source-locating algorithms. The 2-D source-locating algorithm relies on surface wave speeds determined from pencil lead break tests. The 3-D source locating algorithm utilizes longitudinal, transverse, and surface wave velocities, with the speeds estimated from correlations with published values (Lee et al, 2016).

5.2 Summary of Conclusions

5.2.1 Conclusions and Future Work

Laboratory experiments on relatively small reinforced concrete beam specimens under pull-out and three-point bending yielded proof of concept and guidance on data acquisition setup parameters for field testing. These include:

1. Appropriate amplitude and duration filters to remove background noise;
2. Verification of wave mode velocities through pencil lead break tests;
3. Verification of correlation between AE events and observed cracks; and
4. Selection of appropriate sensor array.

Laboratory pull-out and three-point bending (flexure) testing yielded correlations between AE events and cracking and indicated that a 2-D planar sensor array was more accurate in AE event source location than a 3-D sensor array. One possibility for the difference in accuracy is the use of measured wave speed velocity used in the 2-D location algorithm versus the empirical relationship estimates of wave speed velocities used in the 3-D sensor array. Another possibility is the nature of the underlying algorithm and potential distortions from wave-speed inhomogeneities.

CHAPTER 6
ACOUSTIC EMISSION DATA COLLECTION AND RESULTS: FABRICATION

6.1 Overview

This chapter describes AE measurements of pre-fabricated and pre-stressed reinforced concrete Northeast Extreme Tee (NEXT) beams and Bulb Tee's during specific prefabrication processes including; detensioning and craned lifting from form beds.

6.2 NEXT Beam Testing

Moving the AE testing from the laboratory to full-sized pre-stressed and prefabricated concrete girders began with scouting observations of detensioning and crane movement operations. The observations indicated that it would be advantageous to have an untethered instrument package. This prompted modifications to the instrumentation to include a portable power supply and wireless remote network connection, which allow for untethered operations. The next step recorded the AE events of a NEXT beam during the detensioning processes and craned removal of the beam from the formwork deck and placement on wood blocks for additional finishing steps, curing and storage. The sensing configuration arranged eight AE sensors in a 2-D array on the top deck of the NEXT beam off-center towards one end of the deck, which had a skew of approximately 14 degrees. The placement of the sensor array was along lines running parallel and square to the sides of the beam. The intent of the sensor layout was to capture the AE events that may result from the release of energy and load transfer during the torch cutting of the steel tensioning strands within the NEXT beam. Steel armor boxes and 5-minute epoxy attached the sensors to the topside of the beam. The formwork geometry prevented attaching the sensors to the side of the beam and using 3-D estimates of event locations. Instead, the estimation of event locations used a 2-D plate model of the beam.

The instrumentation recorded 38 AE events during the detensioning process as illustrated in Figure 6.1. The torch cutting of pre-stressing strands was synchronized to cut wires from the same strand simultaneously on each side of the NEXT beam in a gradual process that sequentially releases the entire tension within that strand and transferring the load into the beam. The strand cut sequence followed a pattern that alternated sides of the beam cross section in an effort to balance the load transfers, in a manner similar to the pattern used to tighten wheel lug nuts. The loading exerted on the beam by strand cutting was less dynamic than originally anticipated, primarily due to the slow cutting of individual wire within the strands releasing only a relatively small amount of energy per cut. The recorded AE events tended to occur closer to the end of the NEXT beam with multiple events stacked onto one another and occurring along the underlying integral girder containing the tensioning strands.

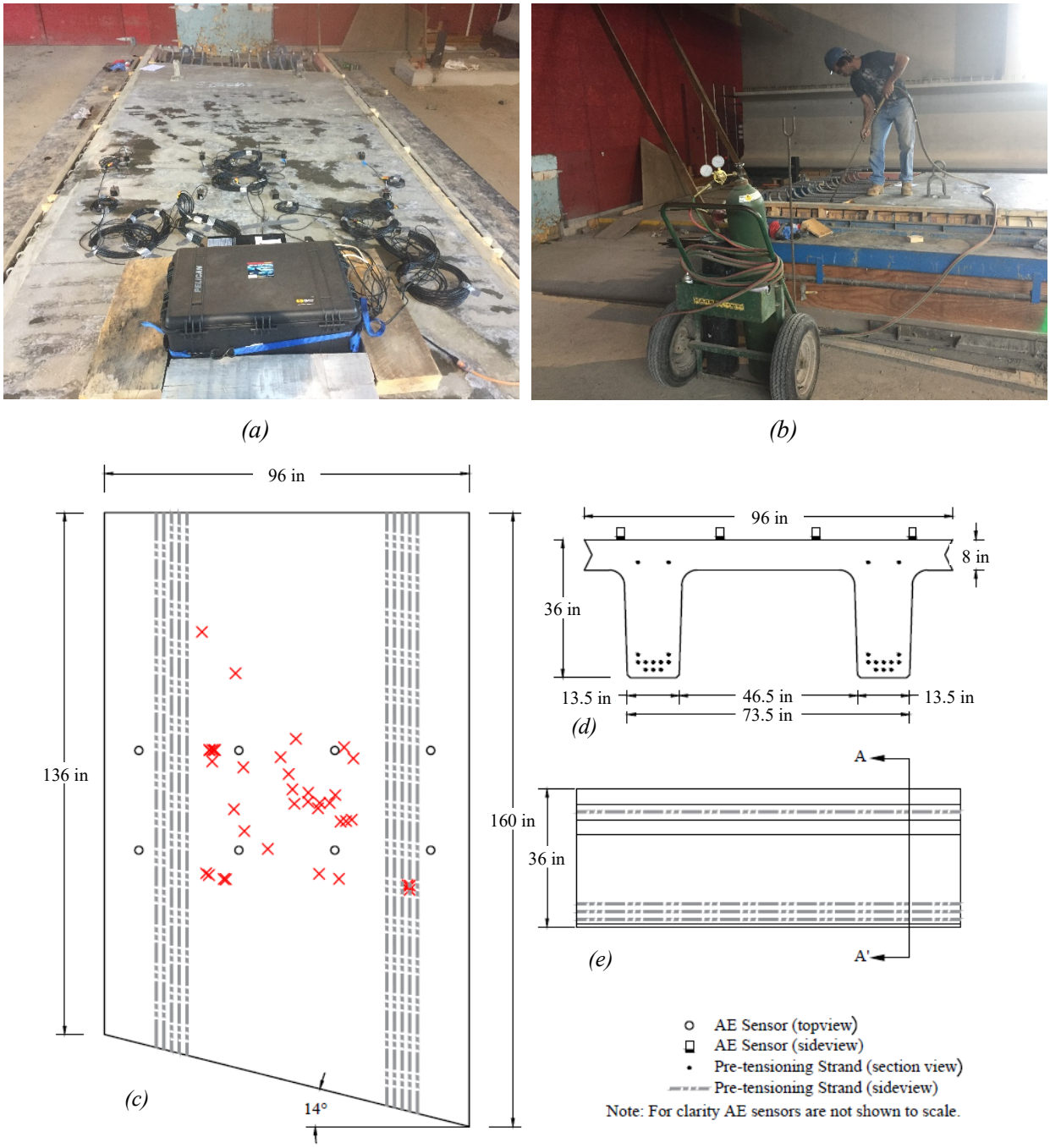

Figure 6.1: NEXT beam field testing of detensioning with 38 recorded events (a) field testing equipment setup, (b) torch cutting of pre-tensioning strands, (c) plan view of AE events on NEXT beam, (d) section view of NEXT beam, and (e) profile view of NEXT beam

The craned removal of the NEXT beam from the form bed produced twenty recorded AE events, Figure 6.2. Upon completion of detensioning, overhead tracked gantry cranes lifted the beams from the form decks. The lifting and movement processes stress the beam as it breaks loose from the form deck and

changes the vertical support to only four load points, two pairs of points at approximately quarter spans. Immediately after hoisting out of the form deck, the beam appeared to camber from an initially flat profile over roughly one minute, presumably due to tension stresses exerted by the embedded steel in the lower sections of the girder and the release of the geometric constraints imposed by the form deck. Cambering along with change of gravity load paths during hoisting may create areas of concentrated stress/strain. This is a period of interest for AE event monitoring, as cracking may occur.

AE event data collection during the detensioning and craned form removal of the NEXT beam were the first full-scale field data collection performed with the equipment and corresponding software. The results were 1) The instrumentation successfully recorded AE events, 2) the equipment alterations for wireless connectivity and portable power supply were successful, and 3) event locations loosely correlated with the integral girders during the detensioning process where the pre-tensioning strands were being cut, and. The collected AE data show that many AE events occurred during the craned removal of the NEXT beam from the formwork deck. It should be noted that the sensor placement near to one end of the girder was not ideal for AE event sensing during craned movements since it is likely that the maximum strains will occur midspan.

(a)

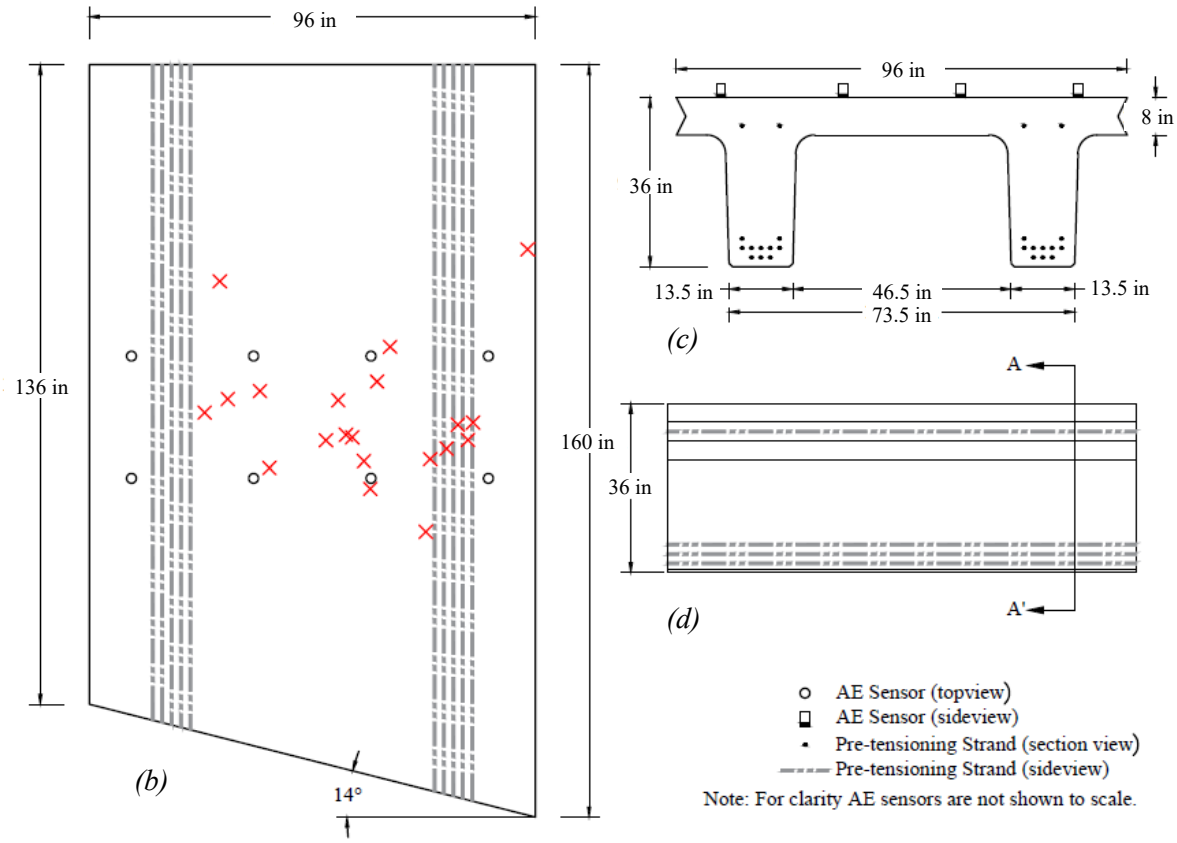

Figure 6.2: NEXT beam field testing of craned form removal with 20 recorded events (a) crane lifting, (b) plan view of AE events on NEXT beam, (c) section view of NEXT beam, and (d) profile view of NEXT beam

6.3 Northeast Bulb Tee Girder Testing

Additional fabrication facility field site investigations recorded AE events from the webs of two Bulb Tee girders during the detensioning processes, craned form removal, and end bulkhead removal.

The first sensor configuration placed eight sensors in a 3-D array, four sensors on each side of the web of the Bulb Tee, within the end zone transfer depth, estimated as 60 times the diameter of the pre-tensioning strands or 36-inches (914 mm) per 5.11.4.1 of AASHTO Bridge Design Specifications (PCINE-14-ABC, 2014). The intent of the sensor array placement was to focus AE data collection in an area predicted to have the greatest stress/strain transfer during loading from the release of the pre-tensioning strands by cutting with a torch. Metal armor boxes and 5-minute epoxy secured the sensors to the Bulb Tee girder. The data acquisition unit operated in an untethered wireless configuration. Estimation of AE event locations used a simplified model that included only the web of the Bulb Tee girder. The end zone of the Bulb Tee girder had three empty post tensioning tubes running roughly in the middle of the girder, each approximately 4-inches (100 mm) in diameter. End zone reinforcement pattern details include; six no. 5 rebar in the top flange running the length of the beam, fourteen no. 5 rebar in the web running the length of the beam, and four no. 6 and six no. 4 rebar in the bottom flange running the length of the beam. The end zones also had four stirrups in the end 11-inches (275 mm) of the Bulb Tee along with an additional seven no. 6 rebar spaced at 3-inches (75 mm) running perpendicular the Bulb Tee in both the top and bottom flanges behind the stirrups.

The detensioning process produced 466 recorded AE events, Figure 6.3. The detensioning process followed a synchronized single wire cutting of strands on both ends of the girder in an effort to distribute evenly the load transfer. The recorded AE events tended to occur within the end zone transfer depth. The AE event locations were dense in the area of the pre-tensioning strands in the web and less dense in areas furthest from the pre-tensioning strands. There were also noticeable conglomerates of events located directly at the sensor locations on the surface of the Bulb Tee. Visual observations detected and documented end zone cracking immediately after the completion of the detensioning process, Figure 6.3. End zone cracks ranged in length from 5-inches to 20-inches (127 mm to 508 mm).

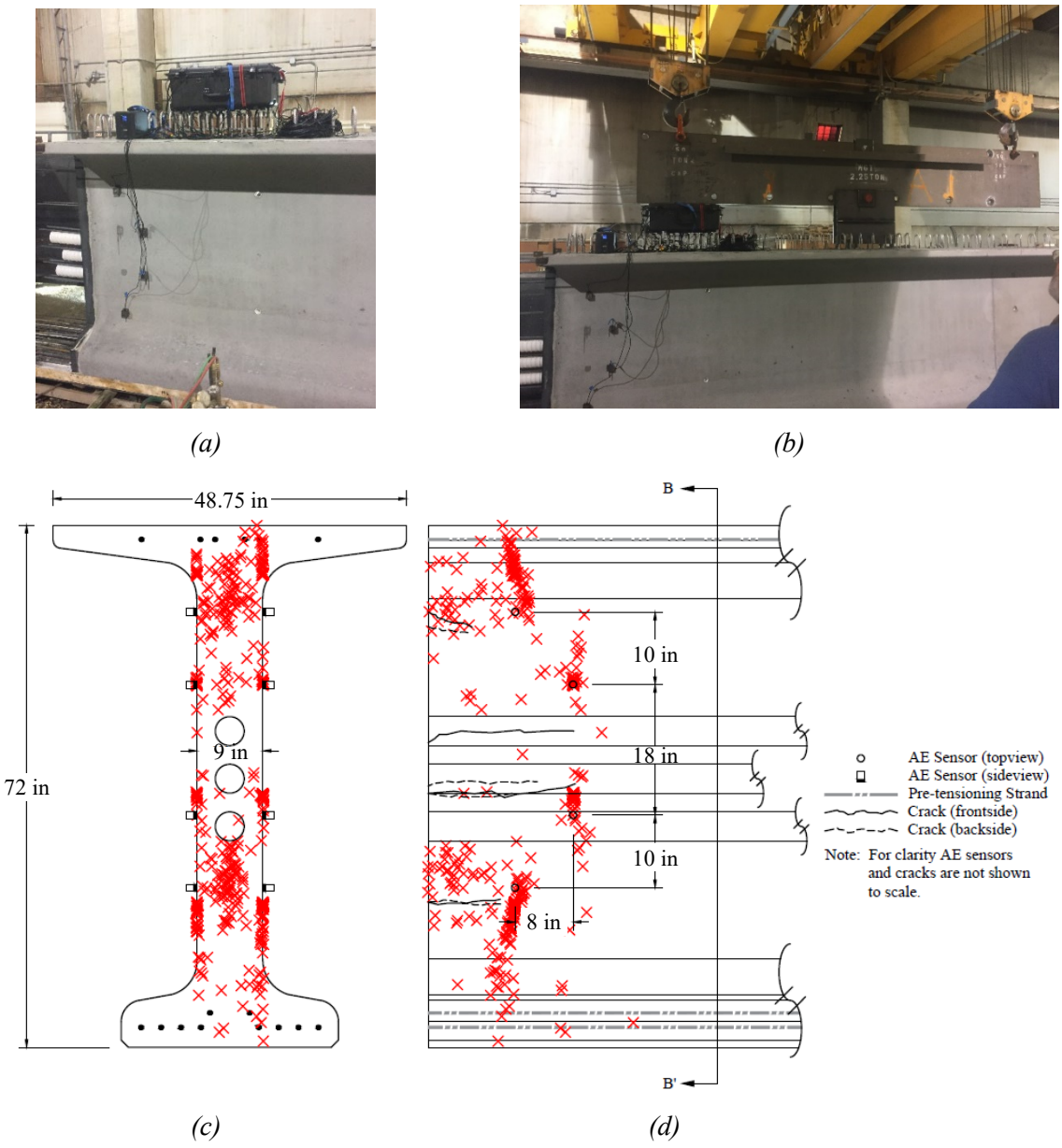

Figure 6.3: Bulb Tee beam 3D sensor array field testing of detensioning with 466 recorded events (a) AE equipment setup, (b) gantry crane connection to Bulb Tee, (c) section view of Bulb Tee beam, and (d) profile view of Bulb Tee beam

Event amplitude provides a means of further discrimination and possible interpretation. Figure 6.4 shows event amplitudes of Figure 6.3 with the dots color and size coded according to event amplitude. The amplitude plot of AE events shows a weak clustering pattern of AE events with high amplitudes (red: 90dB-100dB).

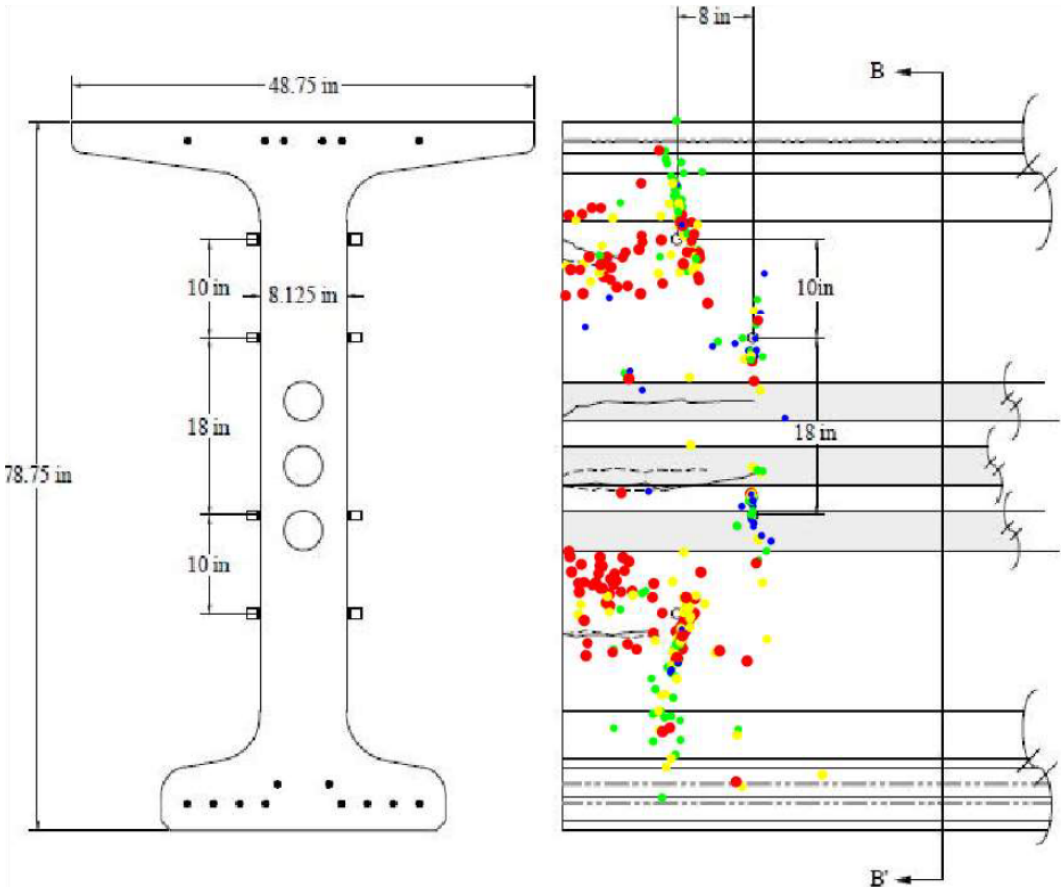

Figure 6.4: Bulb Tee beam 3D sensor array field testing of detensioning with 466 recorded events – AE measurements plotted by amplitude

Upon completion of detensioning, overhead tracked gantry cranes lifted the beams from the form decks and placed them roughly 50 feet (15 meters) away for storage and inspection. This process changes the geometric shape constraints on the beam and alters the internal load paths as it breaks loose from the form deck and rests on the two load point pairs of the gantry crane. Similar to the NEXT beam, the Bulb Tee beam appeared to camber slowly over about a minute due to the highly tensioned embedded steel. The cambering process has the potential for creating areas of concentrated stress/strain leading to cracking. The instruments recorded only 12 AE events during the craned onsite relocation from form to storage/inspection area. Again, if any cracking occurred, it was most likely near the center which would not be captured with the sensor array located near to the ends of the beam.

Bulkhead removal produced 383 AE events. The bulkhead is the end of the formwork that serves the dual purposes of containing the uncured cement as well as providing patterned openings for the reinforcing bar and pre-tensioning strands to pass through to the deadman anchors on either end of the Bulb Tee. Following movement of the beam to the storage/inspection location, a manual process using prybars

and hammers removes the bulkhead. Although bulkhead removal created many AE events, they were likely the result of hammering and prying. The cracks observed from detensioning did not grow during bulkhead removal.

The second sensor configuration placed eight sensors in a 2-D array, with all eight sensors located on one side of the web of the Bulb Tee, within the end zone transfer depth, estimated as 60 times the diameter of the pre-tensioning strands or 36-inches (914 mm) per 5.11.4.1 of AASHTO Bridge Design Specifications (PCINE-14-ABC, 2014). The intent of the sensor placement pattern was twofold; 1) to focus AE data collection in an area predicted to have the greatest stress/strain transfer during loading from the release of the torch cut pre-tensioning strands, and 2) to use an equilateral triangular grid that helps to optimize the performance of the triangulation algorithm and minimize on-sensor location anomalies (ASTM 3100-17, 2017). The sensor coupling method and end zone reinforcement were the same as in the first sensor configuration.

The detensioning process produced 960 recorded AE events, as illustrated in Figure 6.5. The detensioning process was similar to that of the first Bulb Tee 3-D sensor array test. ThisBulb Tee differed from the previous one in that it was a hammerhead (haunched) section with a deep bottom flange that increased in depth at midspan to meet a pier cap. The hammerhead sections used a different layout of reinforcement as well as pre-tensioning strand layout as depicted in Figure 6.5. The recorded AE events tended to occur within the end zone transfer depth and were concentrated towards the interior ends of the observed end zone cracking. The 2-D planar sensor array that formed a pattern of near-equilateral triangles showed a noticeable reduction in the conglomerates of events located directly at the sensor locations on the surface of the Bulb Tee as was observed with the first 3-D sensor array. Visual observations detected and documented end zone cracking immediately after the completion of the detensioning process as seen in Figure 6.5.a. End zone cracks ranged in length from 5-inches to 17-inches (127 mm to 432 mm).

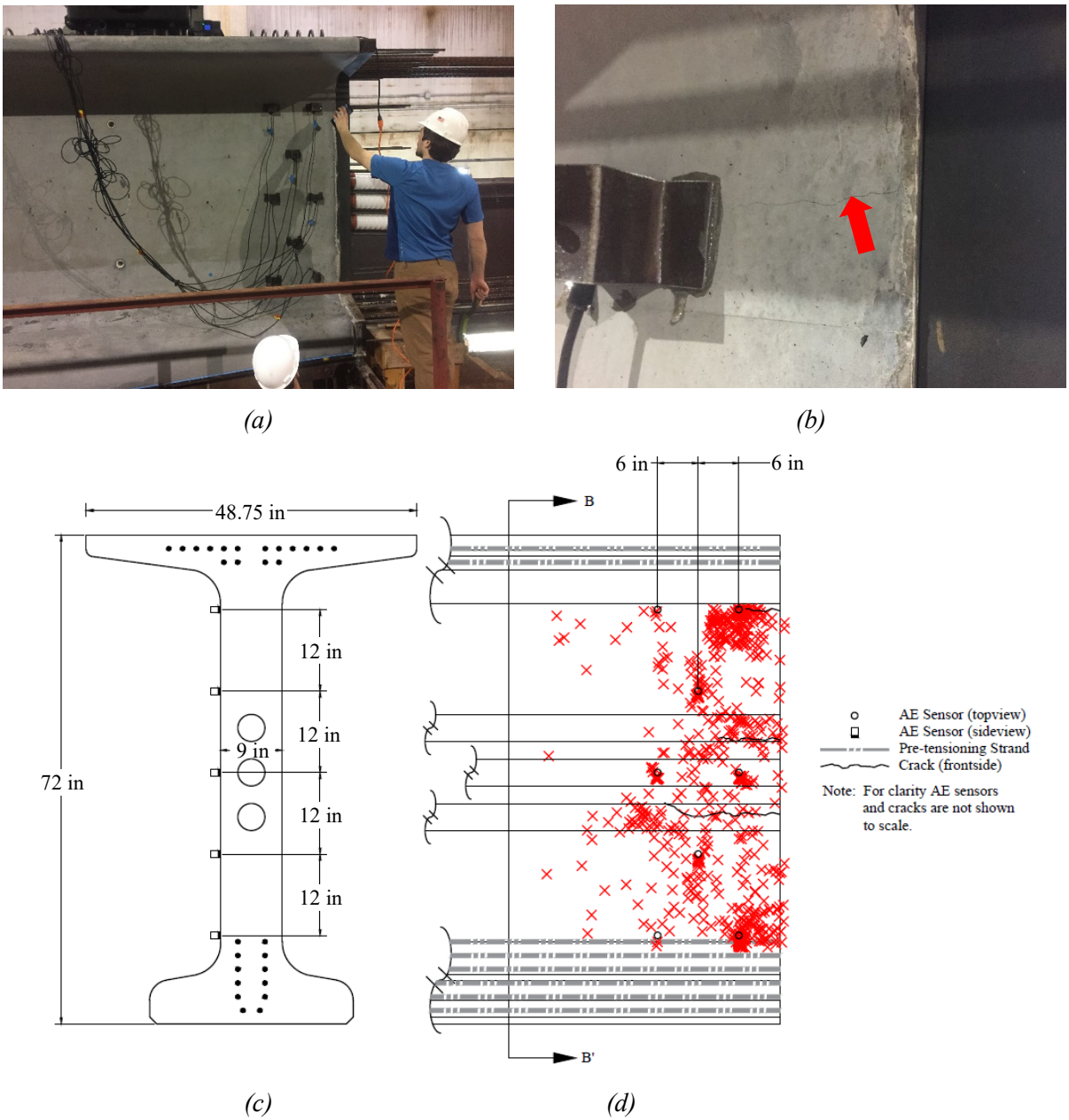

Figure 6.5: Hammerhead Bulb Tee girder 2D sensor array field testing of detensioning with 960 recorded events (a) AE equipment/sensor setup, (b) observed horizontal web crack, (c) section view of Bulb Tee beam, and (d) profile view of Bulb Tee girder

Figure 6.6 shows the same recorded AE events in Figure 6.5 were also plotted by amplitude coded by dot size and color. The amplitude plot of AE events shows a weak clustering pattern between AE events of different amplitudes. There there does not appear to be a clustering of AE events with similar frequency ranges.

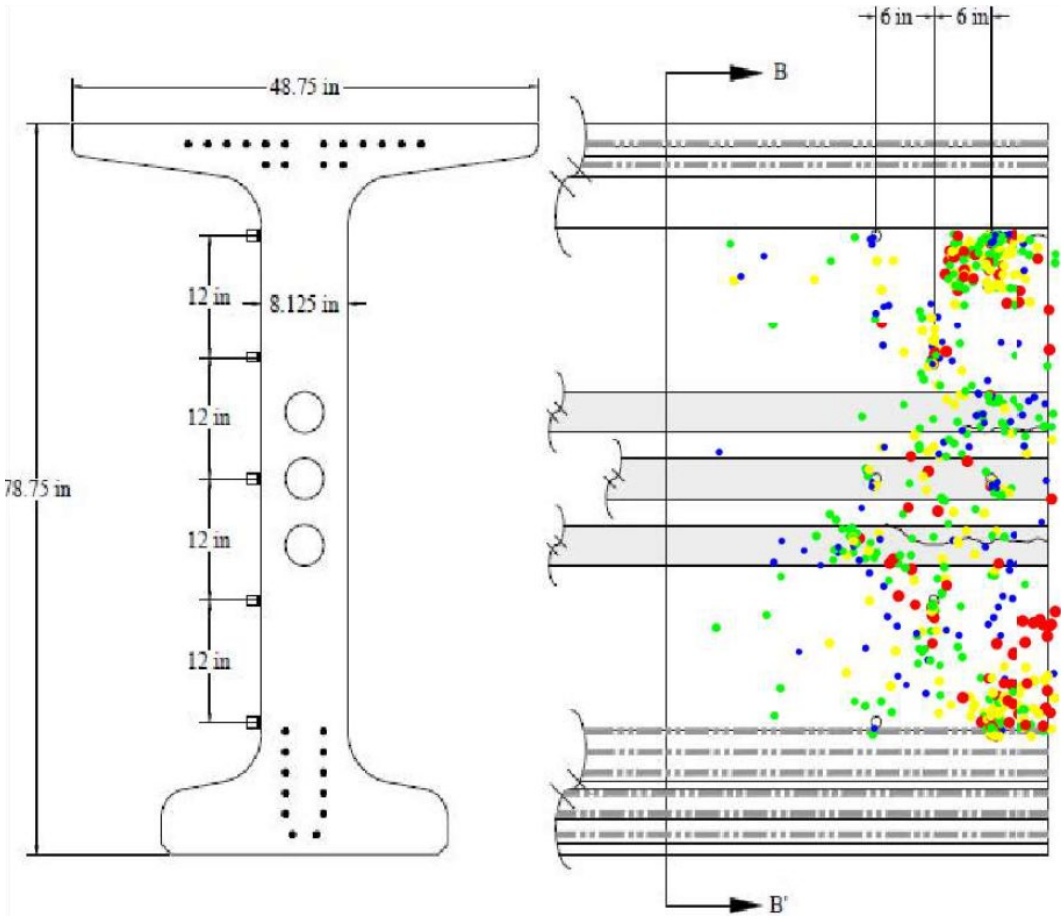

Blue: 60dB – 69dB Green: 70dB – 79dB Yellow: 80dB – 89dB Red: 90dB – 100dB

Figure 6.6: Bulb Tee beam 2D sensor array field testing of detensioning with 960 recorded events – AE measurements plotted by amplitude

Upon completion of detensioning, overhead tracked gantry cranes lifted the beams from the form decks and placed them roughly 50 feet (15 meters) away for storage and inspection. This process changes the geometric shape constraints on the beam and alters the internal load paths as it breaks loose from the form deck to rest on the two load point pairs of the gantry crane. Cambering may create areas of concentrated stress/strain leading to cracking. The instruments recorded only 16 AE events during the craned onsite relocation from form to storage/inspection area. Again, if any cracking occurred, it was most likely near the center which would not be captured with the sensor array located near to the ends of the beam. Observations of the hammerhead girder found little, if any, camber to occur when lifting the girder out of the form bed.

During this test bulkhead removal data were not collected due to timing limitations between detensioning and removal of the bulkhead.

6.4 Summary of Conclusions

6.4.1 Conclusions and Future Work

This chapter reports on results that demonstrate the viability of AE sensing in detecting and locating cracks in prefabricated pre-stressed concrete girders. AE field data collected from the Bulb Tee showed more recorded AE events during the torch cutting of pre-tensioning strands than for a similar process on the NEXT beam. This could be due to Bulb Tee having a thin web with three hollow post-tensioning tubes and dense packing of pre-stressing strands guiding the AE waves and reducing attenuation within the Bulb Tee girder. A key observation made during the detensioning processes was the appearance of horizontal cracks in the web of the Bulb Tee girder. The crack lengths ranged between 5-inches and 20-inches (127 mm and 508 mm) with vertical spacing between cracks ranging from 1.4-inches to 32-inches (35 mm to 813 mm), Table 6.1.

Table 6.1: Quantification of AE Events Versus Number of Observed Cracks During Detensioning and Craned Movement

Beam type	# of observed AE events during detensioning	# of observed AE events during craned form removal	# of observed cracks (crack lengths)
NEXT beam	38	20	0
Straight bulb tee	466	12	7 (5 inches-20 inches)
Haunched bulb tee	960	16	6 (5 inches-17 inches)

The observed end zone cracking occurred both within and outside of the region directly covered by the AE sensor array for the Bulb Tee girders beams and AE event location distributions indicate differences in between in the 3-D and 2-D sensor arrays.

AE event data collected from multiple fabrication processes including the detensioning of pre-tensioning strands embedded in NEXT beams and Bulb Tee's identified internal AE events indicative of crack nucleation. AE events recorded above the 60-dB amplitude pre-filter determined through laboratory testing may be indicative of internal cracking and provide an approximate estimate of crack location. Additionally, the AE monitoring determined which fabrication process is responsible for the most AE events, which could point to the critical fabrication processes responsible for crack nucleation. This is highlighted by the Bulb Tee beam field data that showed far more AE events occurred during the detensioning of the Bulb Tee than during the craned removal from its form bed.

Additional future work for this project includes AE source discrimination and data collection during transportation, installation, and service of full-scale NEXT beams and Bulb Tee girders.

CHAPTER 7
ACOUSTIC EMISSION DATA COLLECTION AND RESULTS: TRANSPORT

7.1 Overview

This chapter describes a series of acoustic emission (AE) measurements taken on prefabricated and pre-stressed concrete bridge girders during transport from the fabrication facility to the bridge site. The girders were New England Bulb Tee (NEBT) girders; fabricated at J.P. Carrara and Sons, Inc. in Middlebury, VT; and transported 160 miles (258 kilometers) to a bridge under construction in Rockingham, VT (Rockingham IM 091-1(66)). The testing began with visual observations of the transport process, followed by measurements on three girders – two straight and one hammerhead (haunch), running from June 14 to June 26, 2018. The measurement instruments consisted of an 8-channel array of AE transducers attached to the girders and connected to a central data acquisition unit strapped to the top of the girders and controlled via wireless telemetry by an operator in a chase vehicle. The data acquisition was largely successful. A preliminary analysis of the results indicates that the hammerhead girder produced significantly more AE events than the straight girders and transport maneuvers that tended to flex the girders by a differential change in elevation produced more events than traversing potholes. The girder movements did not produce any visible damage.

7.2 Pilot Transport AE Data Collection

7.2.1 Objective and Scope

The first transportation tests were a series of pilot tests to evaluate system configuration and operation. These pilot tests used two vehicles in a lead vehicle – chase vehicle configuration. The lead vehicle contained the AE test equipment a and small reinforced concrete block that simulated a large girder. The chase vehicle transported an operator with the system controller and a wireless connection to the lead vehicle. The tests ran on and around the UVM campus grounds. The goals of the tests were: 1) To evaluate potential equipment modifications and system configurations required for transport testing; and 2) To evaluate the connectivity range of the wireless router during transport.

7.2.2 Highway Sensor III Input Parameters

Mistras AEwin^{TM} Sensor Highway III monitoring system and associated AEwin^{TM} processing software allows for user-defined inputs to refine the collected AE events. The acquisition setup parameters, as listed in Table 7.1, followed specifications suggested by the manufacturer. Pencil lead break tests in

controlled laboratory specimens confirmed the validity of these parameters (Sause, 2011). Table 1 lists the input parameters.

Table 7.1: Mistras AEwin™ Sensor Highway III Input Parameters

Parameter		**Value**	**Units**
Threshold		60	decibel (dB)
Pre-amplifier Gain		26	decibel (dB)
Analog Filter	Lower Bounds	20	kilohertz (kHz)
	Upper Bounds	400	kilohertz (kHz)
Digital Filter	Lower Bounds	20	kilohertz (kHz)
	Upper Bounds	200	kilohertz (kHz)
Timing Parameters	Peak Definition Time (PDT)	200	microsecond (µs)
	Hit Definition Time (HDT)	800	microsecond (µs)
	Hit Lockout Time (HLT)	1,000	microsecond (µs)
	Maximum Hit Duration (MDT)	1,000	millisecond (ms)
Longitudinal Wave Velocity		13,083	feet per second (ft/sec)
Transverse Wave Velocity		7,833	feet per second (ft/sec)
Surface Wave Velocity		7,250	feet per second (ft/sec)

If the user-defined minimum sensor hits occur within the specified time duration parameters then the AEwin™ software collects fifteen features of the AE waveform signals including: 1) amplitude, 2) duration, 3) energy, 4) counts, 5) rise time, 6) peak frequency, 7) frequency centroid, 8) absolute energy, 9) signal strength, 10) initial frequency, 11) reverberation frequency, 12) counts-to-peak, 13) average signal level, 14) root mean square (RMS), and 15) average frequency.

7.2.3 Equipment Layout

The sensor configuration was with eight AE sensors in a 2-D array on the top surface of the concrete block of about 16.5-inch x 9.75-inch x 5.5-inch (419 mm x 248 mm x 140 mm), Figure 7.1. The sensors pattern formed a grid of near equilateral triangles. The mounting arrangement secured the sensors into prefabricated steel U-shaped brackets with 5-minute epoxy secured the brackets to the concrete block, Figure 7.2. Custom electronic alterations to the equipment provided standalone power with a UPS remote power manager and remote monitoring with a wireless network connection. Additionally, a remote-controlled electromechanical vibrator was secured to the concrete block with an adhesive tape, Figure 7.3. The purpose of the vibrator was to induce AE events during testing.

Figure 7.1 Pilot transport test AE equipment set-up

Figure 7.2 AE sensor connection to concrete block with U-shape brackets

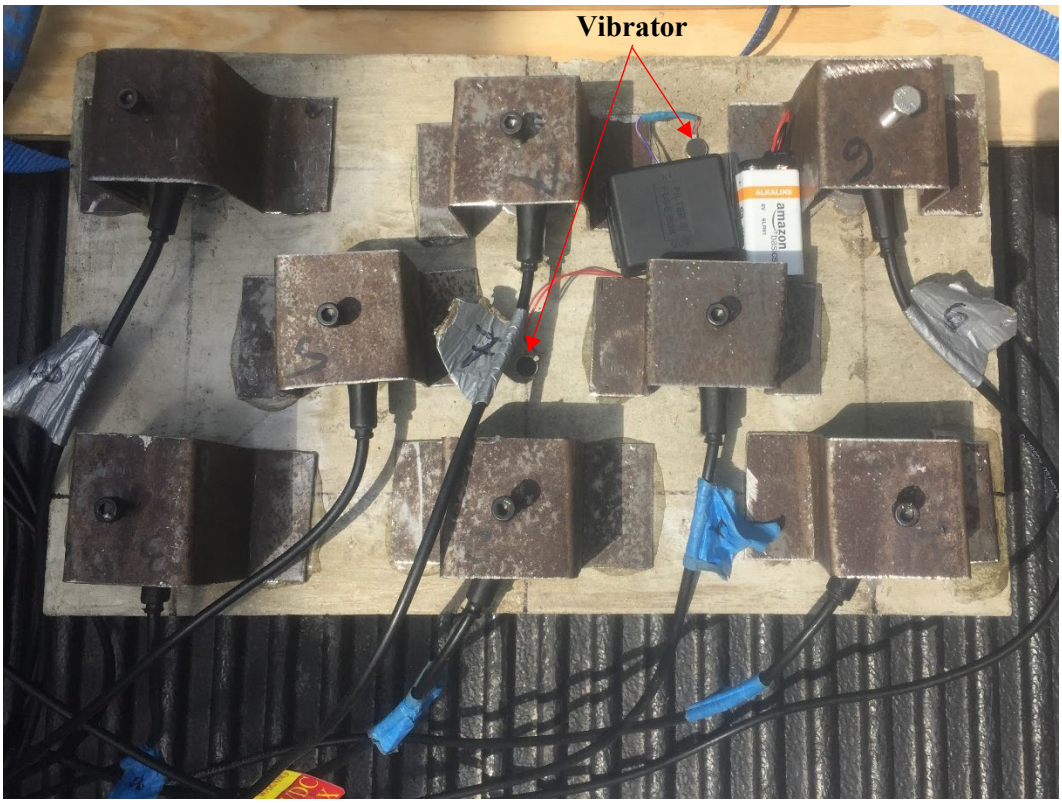

Figure 7.3 Pilot AE transport configuration showing concrete, electromechanical vibrator and transducer array, in bed of pickup truck

7.2.4 Data Collection Process Observations

The overall results of the pilot test were positive. Road vibrations induced AE events in the small-scale concrete block. A tailing vehicle with a laptop computer serving as a remote controller followed the truck on a test drive to determine the range of connectivity of the wireless router and receiver from the lead to tailing vehicle with the wireless router. The tail vehicle stopped, and the transport truck continued until connectivity was lost. The measured viable telemetry distance was 645 feet (197 meters). From the pilot transport test, it was clear that the portable power source needed to be changed from the available UPS to batteries for increased power duration, and that the remote telemetry configuration was capable of providing real-time updates of AE activity and for remote control of the test instruments during transport testing.

7.3 Northeast Bulb Tee Transport Observation

7.3.1 Objective and Scope

Field work started with a visit to J.P. Carrara & Sons, Inc. (Carrara) precast concrete plant located at 2464 Case Street, Middlebury, VT (Site), on June 14, 2018 to observe the loading and transport of NEBT girders from the plant to the drop location for the IM 091-1(66) I-91 bridge construction site in Rockingham,

VT. The intent was to identify opportunities and constraints for AE data collection during transport. Personnel from the University of Vermont, College of Engineering and Mathematical Sciences (UVM CEMS), (R. Worley and M. Pereira) observed transport of an NEBT during transport from Carrara's to the drop location, 160 miles (258 kilometers) away, in Rockingham, VT. Figure 7.4 shows the route, which followed the main highway (US 7) from Middlebury to Burlington, and then the interstate roads (I-189, I-89 and I-91) from Burlington to Rockingham.

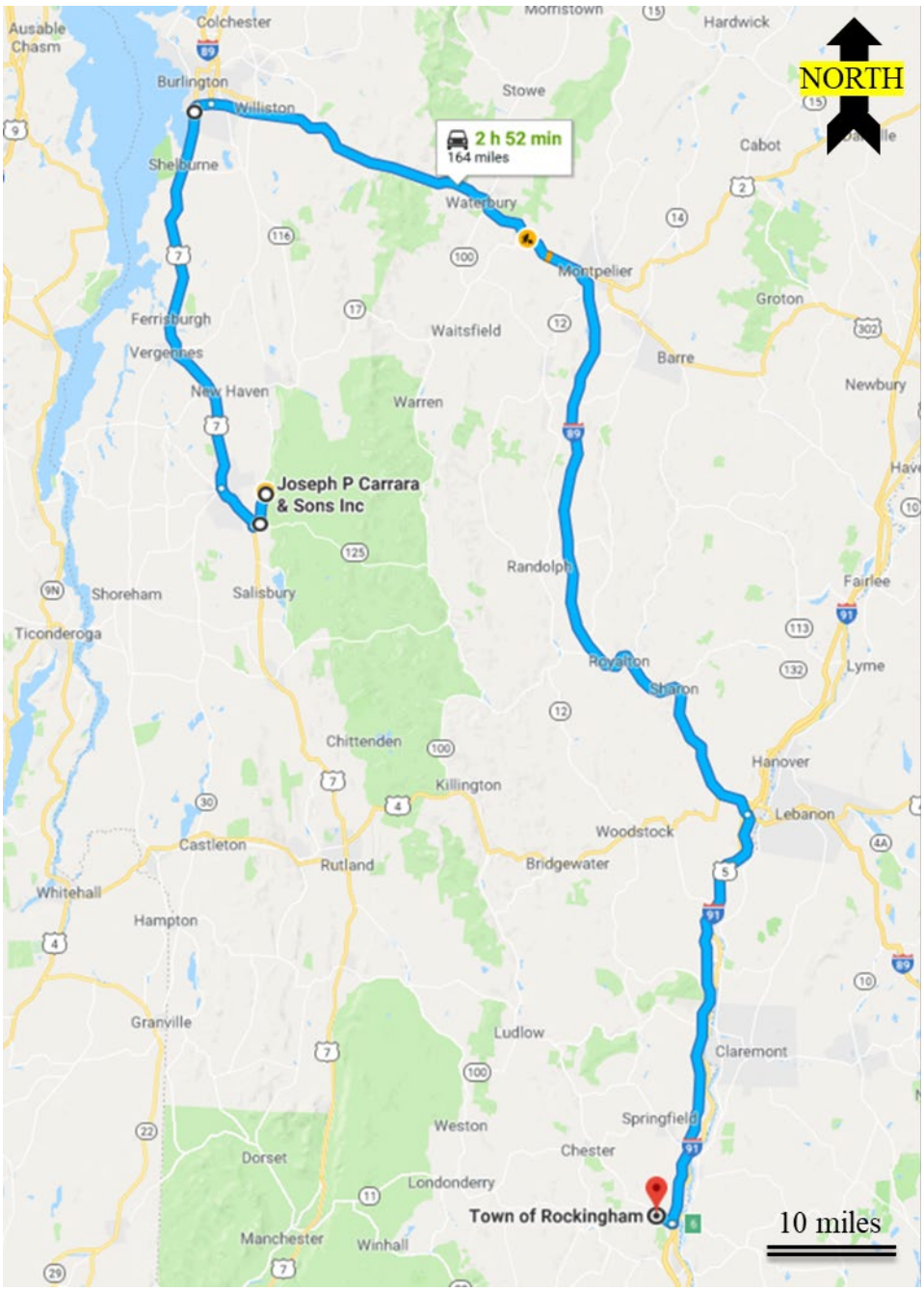

Figure 7.4: Travel route from J.P. Carrara & Sons Inc.in Miiddlebury, VT to the IM 091-1(66) I-91 bridge construction site in Rockingham, VT

7.3.2 Transport Process Observations

Transport of the NEBT girders is typically a 2-day process. The first day is at the fabrication facility and is for loading the girders onto the truck with gantry cranes. The second day begins at the fabrication facility, followed by transport to the bridge site and then unloading at the bridge site. The truck used for transport was a jeep and dolly rig that allowed for independent steering of the rear dolly by a trailing chase vehicle that follows during transport. Fabrication drawings include details for placement of the NEBT girder on the jeep and dolly. A system of chains, rachets, and steel bars secures the NEBT girder to the jeep and dolly.

On the second day, departure from Carrara's starts between 3:00am and 4:00am. The number of girders transported per day ranges between 1 and 3 with 15-minute gaps between departures of each beam to allow for traffic flow between each convoy. The convoy for each girder consists of a lead oversized vehicle escort, a lead police escort, the tractor with beam on a jeep, the rear steering vehicle (dolly), and finally a rear police escort. Each load requires a permit and must abide by local restrictions as well as state restrictions for times and conditions at which oversized loads are allowed to travel. Travel was not permitted during rain, fog, or on wet roads. Additionally, travel was not permitted between 7:00am and 8:00am as well as between 12:00pm and 1:00pm. If no issues arise during transport the travel from Carrara's in Middlebury to the drop site in Rockingham, VT takes approximately 4-hours for a hammerhead NEBT girder and approximately 3.5-hours for a straight section NEBT girder. Once at the drop site, the tractors detach from the loads and reattach to the empty jeep and dolly from the previous day's load, to be brought back to Carrara' for loading.

Observations of the transport indicated that there were multiple factors of concern for usage and placement of the AEwin™ Sensor Highway III and associated sensors. These factors were: 1) safely securing equipment; 2) clearance constraints from overhead powerlines; 3) exposing the equipment to weather; 4) maintaining wireless connectivity to the AEwin™ Sensor Highway III; 5. safety during placement and removal of the AEwin™ Sensor Highway III and associated sensors.

7.3.3 System Modifications

The observation of the girder transport identified a set of issues that required modification to both the equipment and attachment procedures. An outdoor-rated steel case houses the AEwin™ Sensor Highway III data acquisition system. Two 12V motorcycle batteries connected in parallel provided power to the AEwin™ Sensor Highway III and wireless router through modified electrical bus connections. Gorilla tape secured the wireless router to the AEwin™ Sensor Highway III steel housing. The placement of the steel housing was directly on the top of the NEBT girder in a gap between exposed deck attachment rebars. 2-inch (50 mm) wide heavy duty rachet straps looped all the way around the NEBT girder secured

the assembly in place. Overnight rain protection consisted of placing a waterproof back pack cover over the AEwin™ Sensor Highway III with wireless router and covering the AEwin™ Sensor Highway III and batteries with a tarp. The height of the placement required an extension ladder.

Attaching the AE sensors to the girder was a multistep procedure: 1.Secured U-shaped brackets to the beam with quick-setting epoxy, followed by a 5 to 10-minute curing cycle. 2. Applied high-vacuum silicone grease to the sensor wear plates. 3. Place the sensors in U-shape brackets and secure using the set screw. 4. Secure excess cable lengths to the exposed rebar with zip ties the top of the beam.

7.4 Straight Northeast Bulb Tee End Zone Data Collection (Transport Test 1)

7.4.1 Objective and Scope

The first NEBT transport test (TT1) collected AE data on the end zone of a straight NEBT girder. The sensor layout geometry matched that of the second NEBT detensioning girder test with a triangular grid placed at the end of the girder on one side of the web. Personnel from UVM CEMS, (R. Worley) collected the data from the NEBT girder during transport from the Carrara precast concrete plant in Middlebury, VT on June 22, 2018. Data were collected with a Mistras AEwin™ Sensor Highway III system and analyzed using the corresponding AEwin™ processing software. The AE data included the timing, waveform shape features, and triangulated location estimates of AE events. The AE data collection was continuous from the Carrara precast concrete plant in Middlebury, VT to the drop site at Rockingham, VT.

7.4.2 Equipment Layout

The placement of the AEwin™ Sensor Highway III was directly on the top of the NEBT girder, as described in Section 4.3. The sensor arrangement was eight AE transducers in a 2-dimensional array in the end zone (the end zone transfer depth is estimated as 60 times the diameter of the pre-tensioning strands or 36-inches per 5.11.4.1 of AASHTO Bridge Design Specifications) of the vertical web section of the NEBT girder. Since this particular girder was slated for placement on the outside of the deck, care was taken to place the transducers on an inward-facing side. This placement reduced the visibility of any residual stains left by the epoxy used for attaching the AE transducers. The selection of the sensor array configuration was to match that used previously in tests at the fabrication facility during detensioning and craned lifting. U-shaped brackets with set screws secured the sensors to the beam, as described in Section 4.3. Placing a tarp and waterproof back pack cover protected the equipment from rain. The equipment and covers remained in place overnight.

The first step the following morning was to remove the tarp and waterproof back pack covers and then to power on the equipment. The next step verifies connectivity and performance with a tap test. Upon

successful completion of the morning tests, an operator rode in the rear steer vehicle to stay close enough to the AE monitoring equipment and take notes during the transport test.

7.4.3 Representative Data Collection

AE event monitoring of the end zone of a straight section of a NEBT proceeded over the course of roughly 160 miles (258 kilometers) in transport from the fabrication location to the installation location. **The number of recorded AE events totaled 673.** Figure 7.5 shows the spatial distribution. The AE events tended to occur in the upper half of the web section of the NEBT. Figure 7.6 shows the recorded AE events from Figure 7.5 plotted by amplitude, with a coding by dot size and color. The amplitude plot of AE events show a weak clustering pattern between AE events of different amplitudes but there appears to be small pockets of low amplitude AE event clusters near the top of the beam. Travel along a secondary highway (US 7) from Middlebury, VT to Burlington, VT produced events at a higher rate than along the interstate (I-89 and I-91) from Burlington, VT to Rockingham, VT, Figure 7.4. An examination of the NEBT girder following transport found no new cracks and no new growth of the existing cracks.

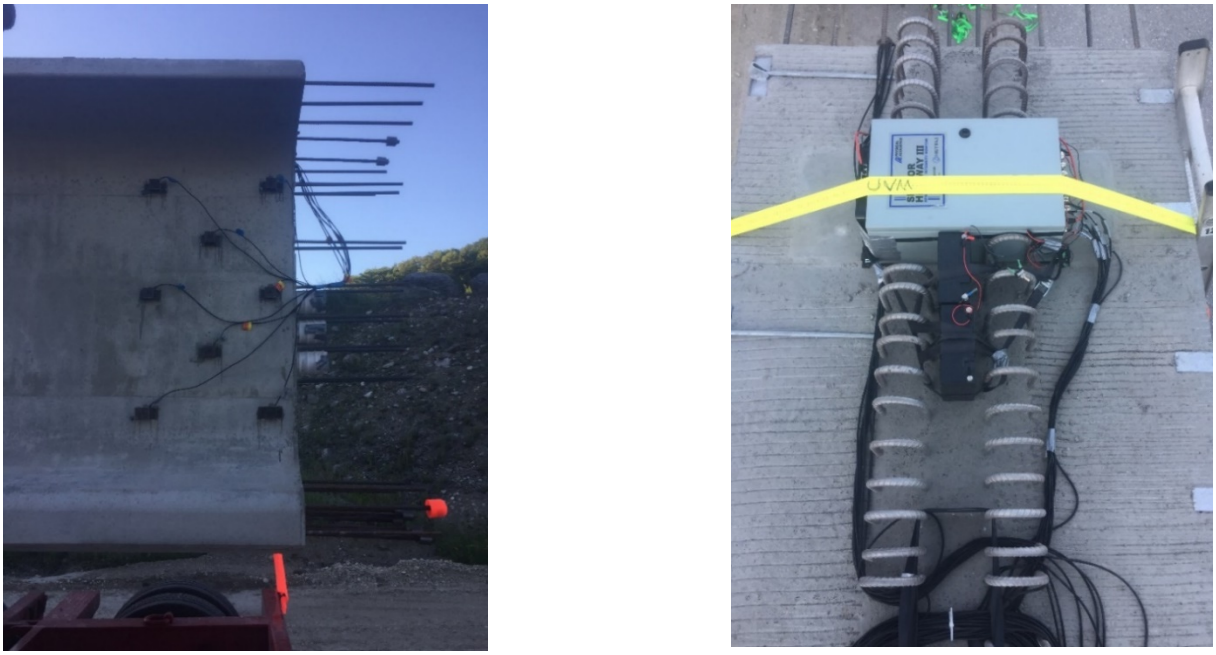

(a) *(b)*

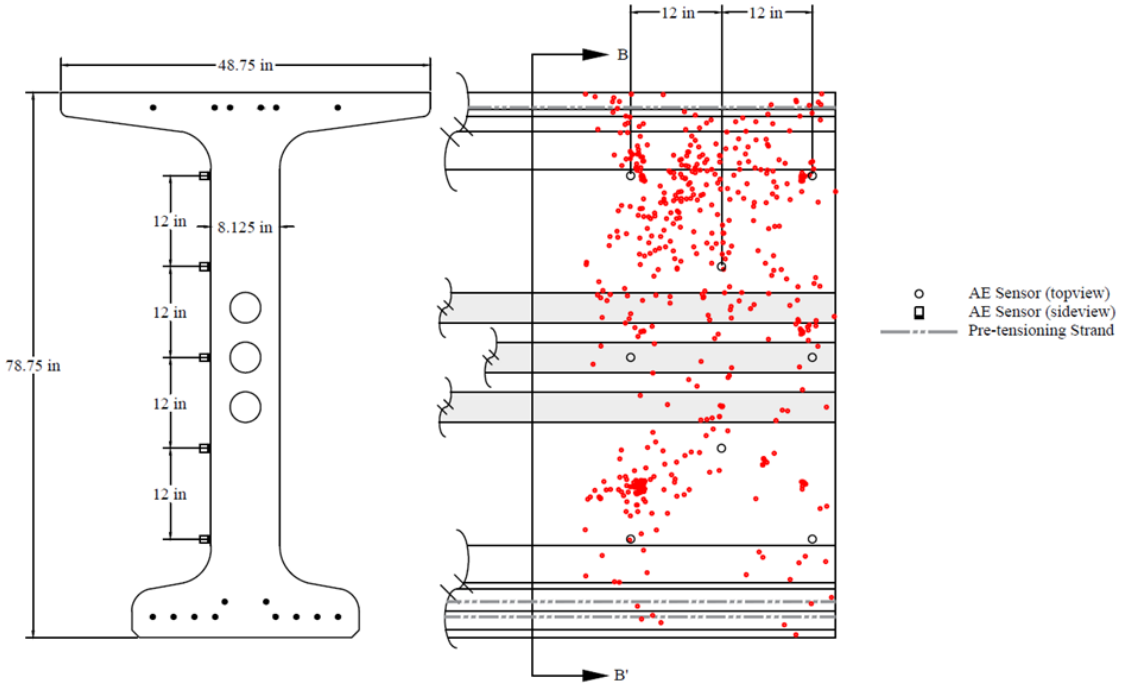

(c) *(d)*

Figure 7.5: Transport Test 1 – AE measurements of the end zone vertical web of a straight NEBT during transport with 673 recorded AE events. (a) Photograph of 2-D sensor array, (b) Photograph of equipment set-up, (c) Cross-section of NEBT tested, (d) Profile view of NEBT including AE event locations, sensors, and observed cracks.

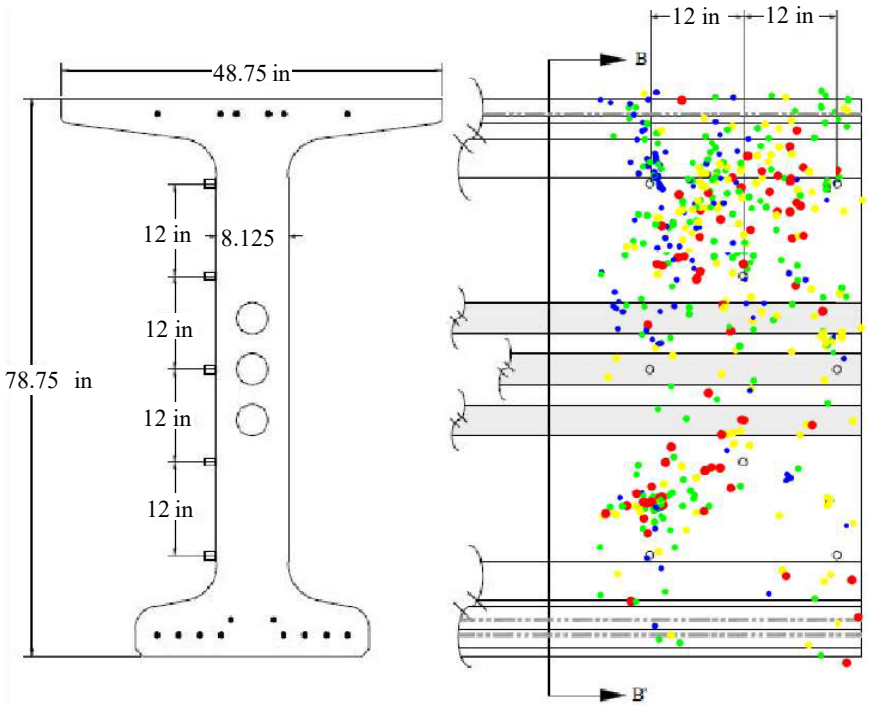

Blue: 60dB – 69dB Green: 70dB – 79dB Yellow: 80dB – 89dB Red: 90dB – 100dB

Figure 7.6: Transport Test 1 – AE measurements plotted by amplitude of the end zone vertical web of a straight NEBT during transport with 673 recorded AE events.

AE event data collection during transport included the time history of data collection. The AE event time histories were then plotted (Figure 7.7) in 5-minute intervals with respect to three different conditions; secondary/highway, interstate, or stopped. The AE event time histories for TT1 indicate a greater level of AE event occurrences when on secondary/highway roadways compared to AE event data collection on the interstate. Additionally, no AE events were collected during stops. The decreasing trend in the number of AE events with time could be representative of a breaking in period, i.e. the Kaiser effect, where AEs only occur when exceeding if the maximum previously experienced stress.

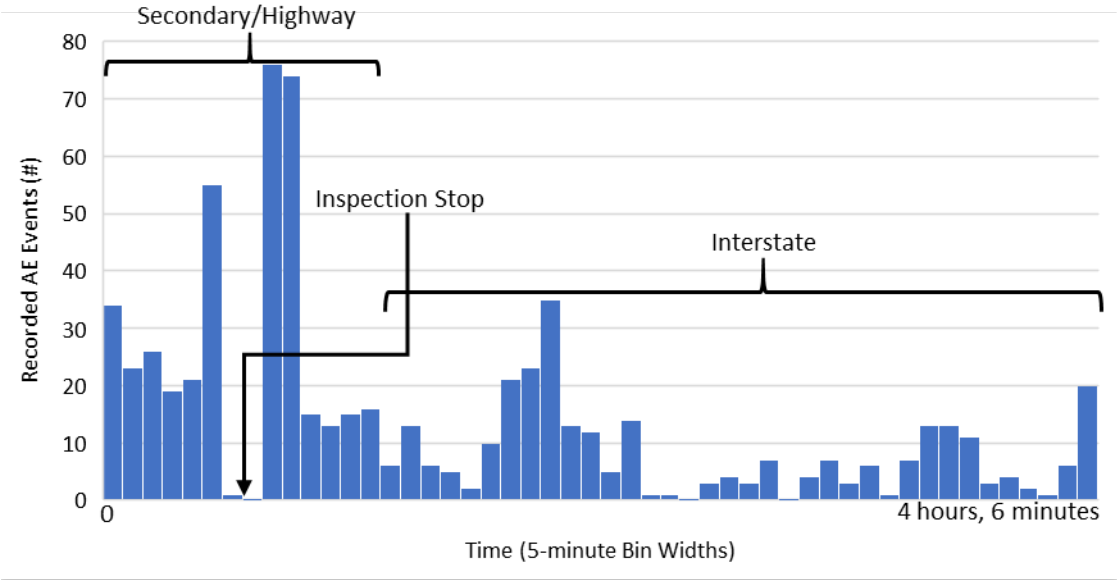

Figure 7.7: AE event density during transport testing of end zone region of straight NEBT, with a total event count of 623

7.4.4 Data Collection Process Observations

The AE event data collected during Transport Test 1 (TT1) had a sparse and diffuse distribution of locations as spaced on the vertical web. Observations by the data acquisition operator riding in the chase vehicle noted that the recorded AE events occurred mostly during vehicle maneuvers that tended to flex the girder, such as when cresting a hill, bottoming in a valley, and during tight turns or turns with abrupt movements. AE events did not appear to occur when hitting a pothole in the road or driving over a rumble strip. This suggests that the recorded AE events recorded may be largely due to a release of internal energy and not due external energy injected into the girder by roadway conditions.

Finite element modeling of the stresses in the girder may lead to a better understanding of the source of these recorded AE events. The modeling used the ANSYS R18.2 academic version. The finite element model (FEM) was a quasi-static model and used quarter beam symmetry to reduce the number of nodes and elements and associated computational effort. The material properties were standard values for concrete properties in the ANSYS database. Application of an equivalent shearing force accounted for the pre-stressing load from the pre-tensioning strands. Additionally, to model for bouncing and deflections of the beam during transport, the model was assessed with a gravity load of 1g down and 1g up. The finite element models in Figure 7.8 and Figure 7.9 show a relatively even stress distribution at the end zone which corresponds to the relatively evenly dispersed AE events recorded at the end zone during transport.

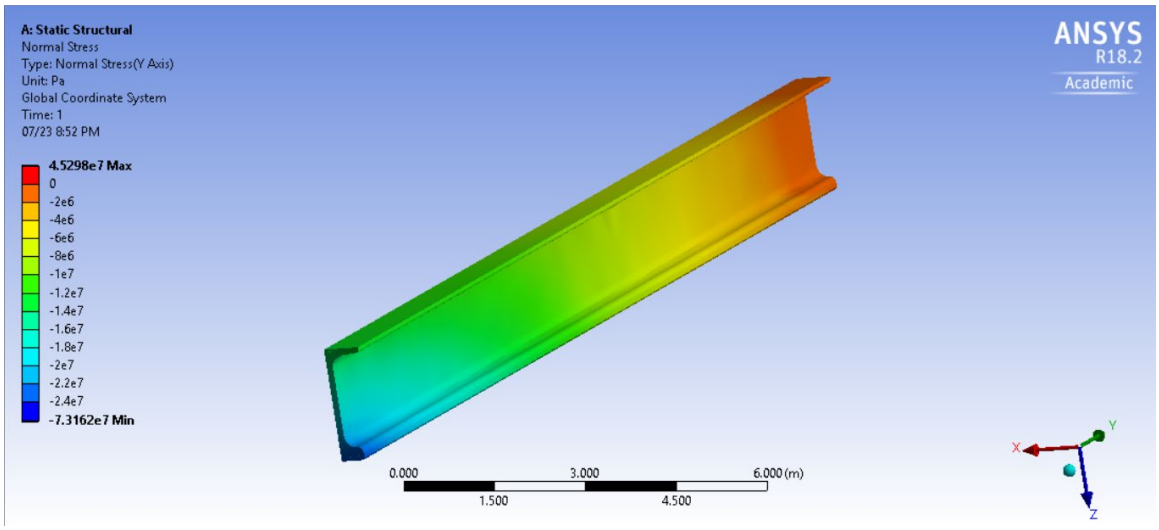

Figure 7.8: FEM quarter straight NEBT stress distribution with 1g down, left side corresponds to mid-span and right side corresponds to the end zone

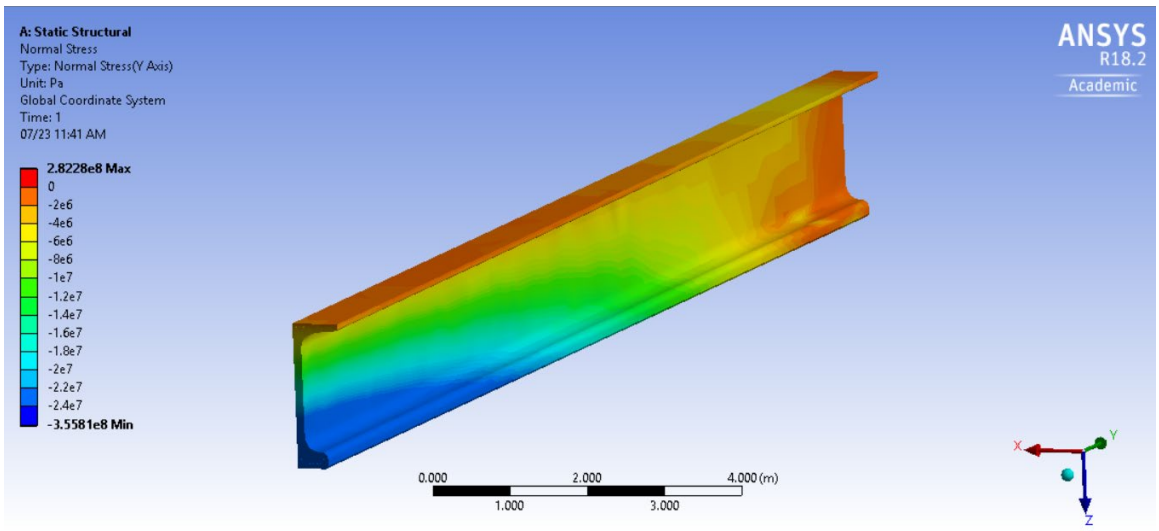

Figure 7.9: FEM quarter straight NEBT stress distribution with 1g up, left side corresponds to mid-span and right side corresponds to the end zone

7.5 Straight Northeast Bulb Tee Mid-Span Data Collection (Transport Test 2)

7.5.1 Objective and Scope

This was the second transport test (TT2). The girder was a straight NEBT. The AE data collection zone was the vertical web of the girder at midspan. Personnel from UVM CEMS, (R. Worley) collected data from an NEBT girder during transport from the Carrara precast concrete plant in Middlebury, VT on June 25, 2018. An Mistras AEwin^{TM} Sensor Highway III data acquisition system collected and stored the data. Subsequent processing used AEwin^{TM} software. The AE data included the timing, waveform shape

features, and triangulated location estimates of AE events. AE data collection proceeded continuously from the Carrara precast concrete plant in Middlebury, VT to the drop site at Rockingham, VT.

7.5.2 Equipment Layout

The placement of the AEwin^{TM} Sensor Highway III system was directly on the top of the NEBT girder, as described in Section 4.3. The sensor arrangement placed eight AE transducers in a 2-dimensional triangular grid array in the mid-span of the vertical web section of the NEBT girder. U-shaped brackets with set screws secured the sensors to the beam. Placing a tarp and waterproof back pack cover protected the equipment from rain. The equipment and covers remained in place overnight.

The first step the following morning was to remove the tarp and waterproof back pack covers and then to power on the equipment. The next step verified connectivity and performance with a tap test. Upon completion of the morning final test and setup, an operator rode in the rear steer vehicle to stay close enough to the AE monitoring equipment and take notes during the transport test.

7.5.3 Representative Data Collection

The sensor configuration of the second transport test was a 2-D planar triangular grid array placed mid-span of the straight section NEBT, Figure 7.10. **The number of recorded AE events totaled 2,628**. The recorded AE events tended to occur in the upper half of the web section of the NEBT. Travel along a secondary highway (US 7) from Middlebury to Burlington produced events at a slightly higher rate than along the interstate (I-89 and I-91) from Burlington to Rockingham, Figure 7.4. Visual observation found that no new cracks formed and the existing cracks did not grow during transport.

(a)

(b)

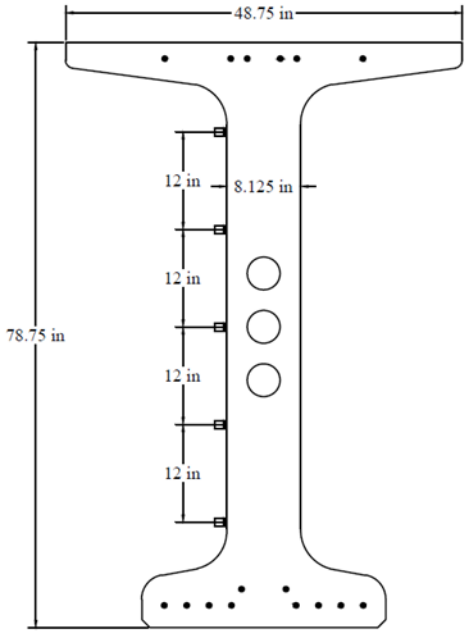

(c)

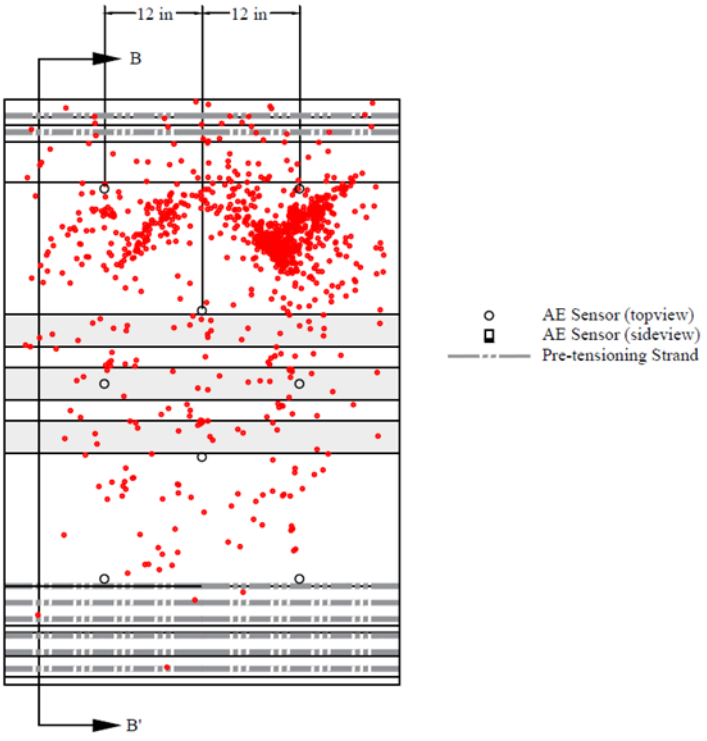

(d)

Figure 7.10: Transport Test 2 – AE measurements of the mid-span vertical web of a straight NEBT during transport with 2,628 recorded AE events. (a) Photograph of 2-D sensor array, (b) Photograph of equipment set-up, (c) Cross-section of NEBT tested, (d) Profile view of NEBT including AE event locations, sensors, and observed cracks

Figure 7.11 shows the recorded events of Figure 7.10 plotted by amplitude coded as dot size and color. The amplitude plot of AE events show a clustering of medium medium-high amplitude AE events (yellow: 80dB – 89dB) in the upper right portion of the NEBT girder with a high concentration of low amplitude (blue: 60dB – 69dB) and medium-low amplitude AE events (green: 70dB – 79dB) AE events are concentrated in the upper third of the NEBT girder. High amplitude AE events (red: 90dB – 99dB) are infrequent and not clustered, but diffuse, in location.

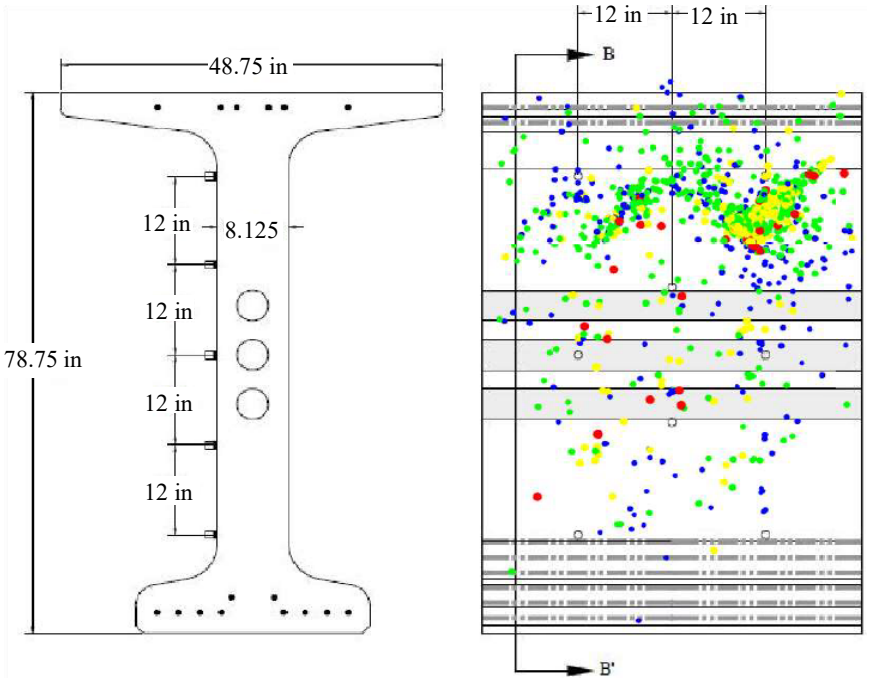

Blue: 60dB – 69dB Green: 70dB – 79dB Yellow: 80dB – 89dB Red: 90dB – 100dB

Figure 7.11: Transport Test 2 – AE measurements plotted by amplitude of the end zone vertical web of a straight NEBT during transport with 2,628 recorded AE events.

The AE event time histories collected during TT2 and plotted in Figure 7.12, indicate a greater level of event occurrences when on secondary/highway roadways than on the interstate. Additionally, no AE events were collected during stops. Although there still is a decreasing trend in the number of AE events with time; this decreasing trend is less distinct than identified in TT1.

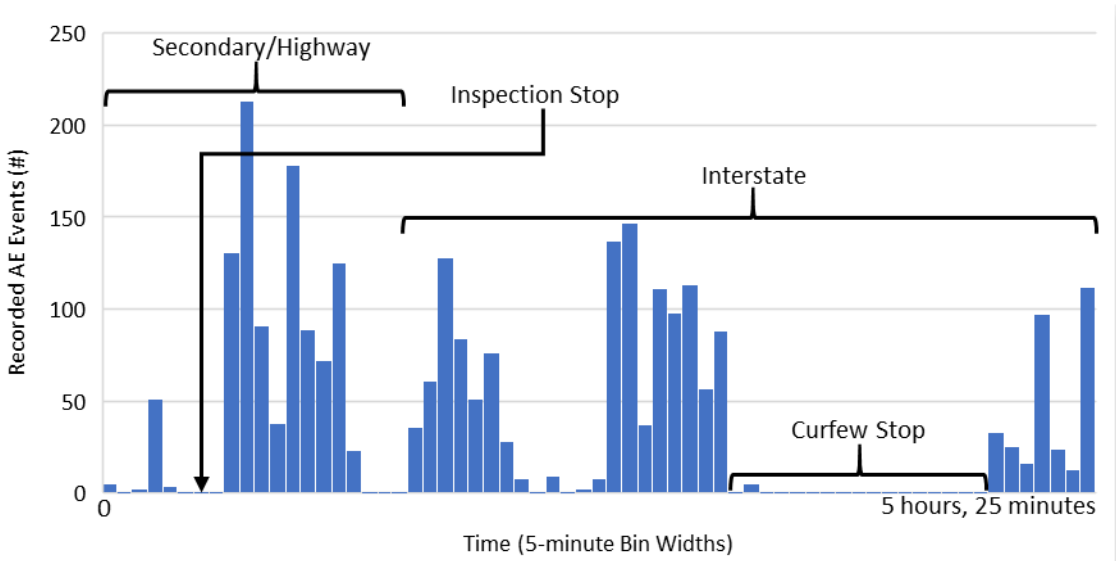

Figure 7.12: AE event density during transport testing of middle zone region of straight NEBT, with a total event count of 2,628

7.5.4 Data Collection Process Observations

AE field transport data collected from the middle zone of a straight NEBT section were densely-spaced and concentrated in the upper region of the beam. The events occurred mostly during flexure-inducing vehicle maneuvers, such as when cresting a hill, bottoming in a valley, and during tight turns or turns with abrupt movements. Hitting a pothole in the road or driving over a rumble strip did not induce many AE events. This suggests that the recorded AE events may be due to internal energy release and not the injection of external energy from roadway conditions.

A finite element model using ANSYS R18.2 academic version calculated the stress distribution in the girder with the goal of determining if regions high stress correspond to the locations of AE events. The finite element model (FEM) was quasi-static and used quarter beam symmetry to reduce the number of nodes and elements and associated computational effort. The model used the same standard concrete material properties as for Transport Test 1 and approximated the action of the pre-stressing strands as a shearing force. Additionally, to model for bouncing and deflections of the beam during transport, the model was assessed with a gravity load of 1g down and 1g up. The finite element model results shown in Figure 7.13 and Figure 7.14 indicate stress distributions commensurate with the recorded AE event distributions. Further confirmation comes from an examination of the shear and moment diagram for the beam during transport and nominal in-service loading, Figure 7.15 and 7.16. The FEM shows a compression at the bottom of the beam moving toward tension at the top of the beam which corresponds to the recorded AE events being in the upper regions on the middle zone of the straight NEBT during transport. This stress distribution with the top of the beam in tension and the bottom of the beam in compression is due to a

vertically asymmetric distribution of pre-stressing strands, with more strands in the bulb at the bottom. This distribution of pre-stressing gives the beam a slight camber.

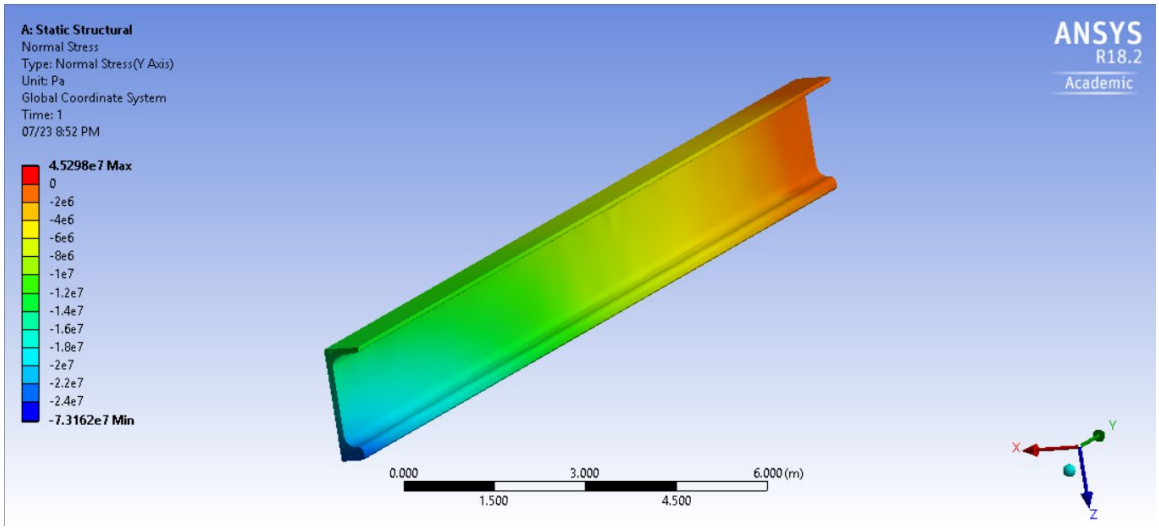

Figure 7.13: FEM quarter straight NEBT stress distribution with 1g down, left side corresponds to mid-span and right side corresponds to the end zone

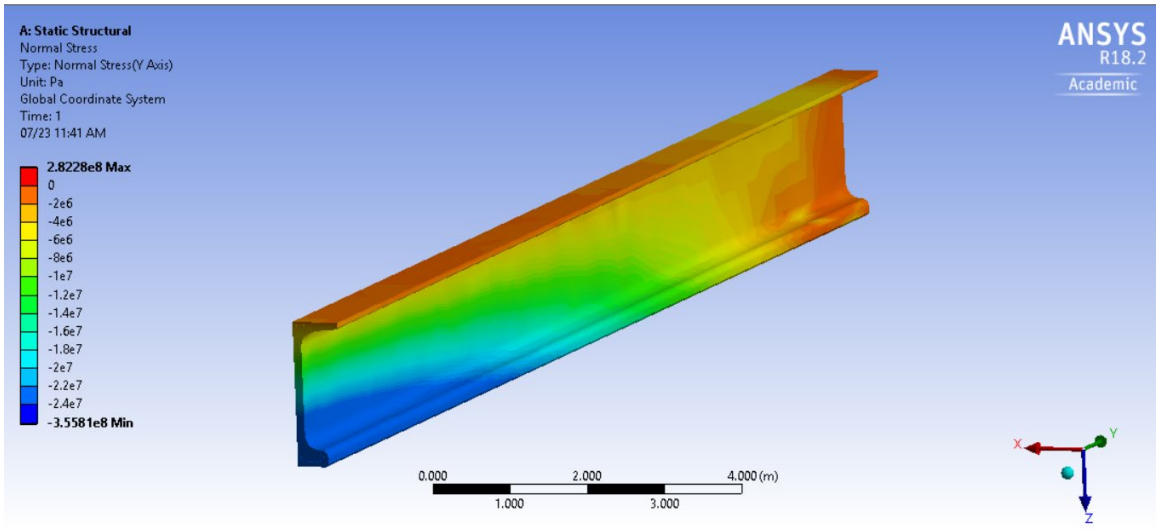

Figure 7.14: FEM quarter straight NEBT stress distribution with 1g up, left side corresponds to mid-span and right side corresponds to the end zone

The shear and bending moment diagrams of the straight span NEBT girders during transport as illustrated in Figure 7.15, are similar to the shear and bending moment diagrams of the straight span NEBT girders during in-service loading as illustrated in Figure 7.16.

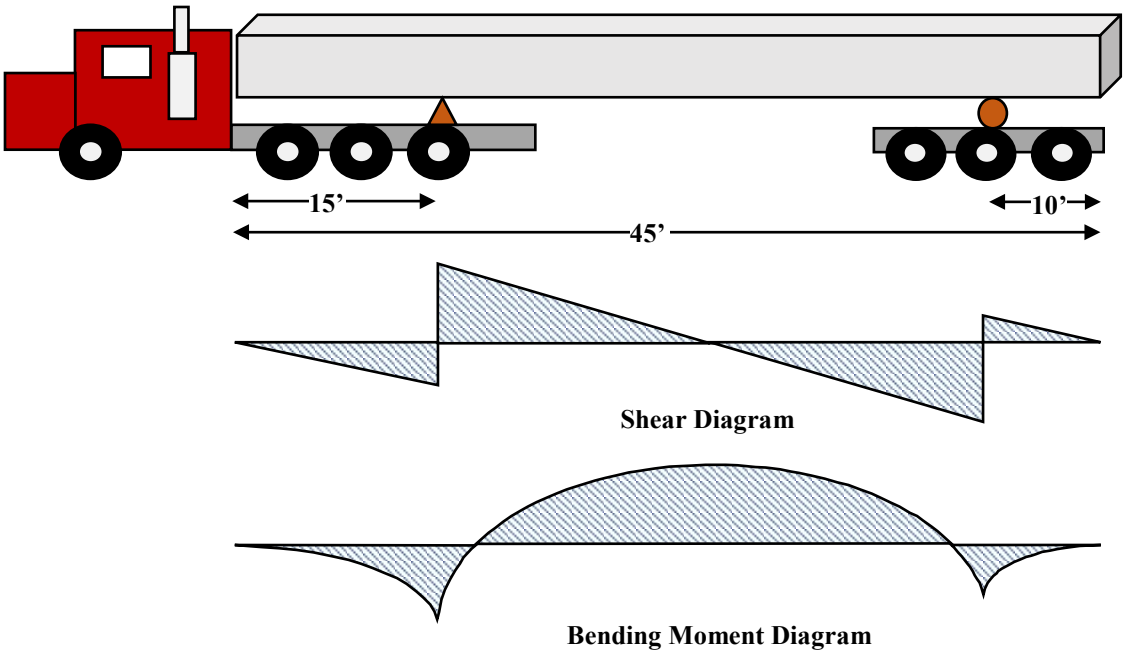

Figure 7.15: Straight span NEBT shear and bending moment diagrams during transport

The locations that are in opposite loading between in-service loading and transport are at the end zones. This may be indicative of the end zone AE event patterns during transport.

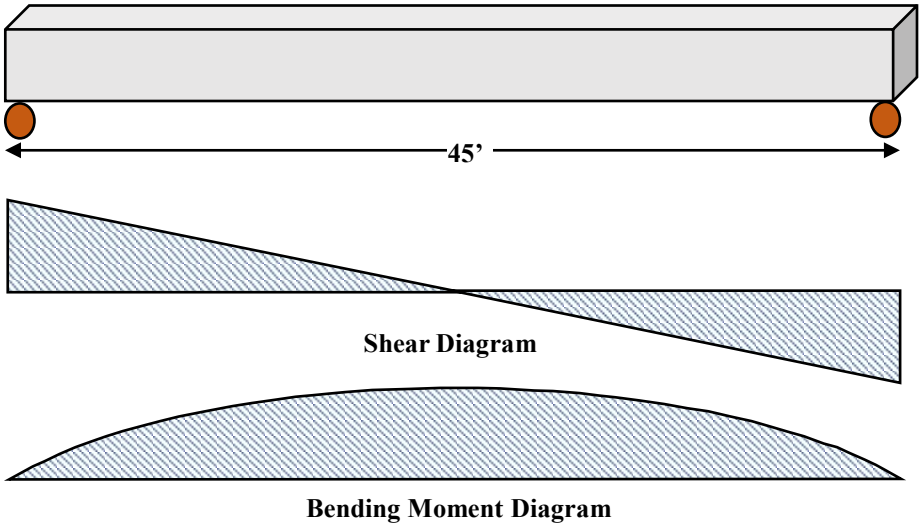

Figure 7.16: Straight span NEBT shear and bending moment diagrams during in-service loading

7.6 Hammerhead Northeast Bulb Tee Mid-Span Data Collection (Transport Test 3)

7.6.1 Objective and Scope

This was the third transport test (TT3). The girder was a hammerhead (haunch) NEBT. The AE data collection zone was the vertical web of the girder at midspan. Personnel from UVM CEMS, (R. Worley) collected the data from a the NEBT girder during transport from the Carrara precast concrete plant

in Middlebury, VT on June 26, 2018. A Mistras AEwin™ Sensor Highway III data acquisition system collected the data for analysis with the corresponding AEwin™ processing software. The AE data included the timing, waveform shape features and triangulated location estimates of AE events. The AE data were collected continuously from the Carrara precast concrete plant in Middlebury, VT to the drop site at Rockingham, VT.

7.6.2 Equipment Layout

The placement of the AEwin™ Sensor Highway III system was directly on the top of the NEBT girder, as described in Section 4.3. The sensor arrangement placed eight AE transducers in a 2-dimensional array in the mid-span of the vertical web section of the NEBT girder. U-shaped brackets with set screws secured the sensors to the beam. Placing a tarp and waterproof back pack cover protected the equipment from rain. The equipment and covers remained in place overnight.

The first step the following morning was to remove the tarp and waterproof back pack covers and then to power on the equipment. The next step verified connectivity and performance with a tap test. Upon successful completion of the morning tests and final setup, an operator rode in the rear steer vehicle to stay close enough to the AE monitoring equipment and take notes during the transport test.

7.6.3 Representative Data Collection

The sensing configuration for the third transport test used a 2-D planar triangular sensor array placed on the vertical web of the mid-span of a hammerhead NEBT girder (Figure 7.17). During transport, the truck supports the girder at both ends, approximately in a simple support configuration. Following installation on the bridge, the support conditions change to a fixed cantilever support mid-span on a column and free at the ends.

The monitoring of the middle region of a hammerhead NEBT ran over the course of roughly 160 miles (258 kilometers) in transport from the fabrication location to the installation location. **The number of recorded AE events totaled 91,723.** The recorded AE events tended to occur in the lower two thirds of the web section of the NEBT modeled. Travel along a secondary highway (US 7) from Middlebury to Burlington produced events at a slightly higher rate than along the interstate (I-89 and I-91) from Burlington to Rockingham, Figure 7.4. A visual observation of the girder found no new cracks or growth of existing cracks during transport.

(a)

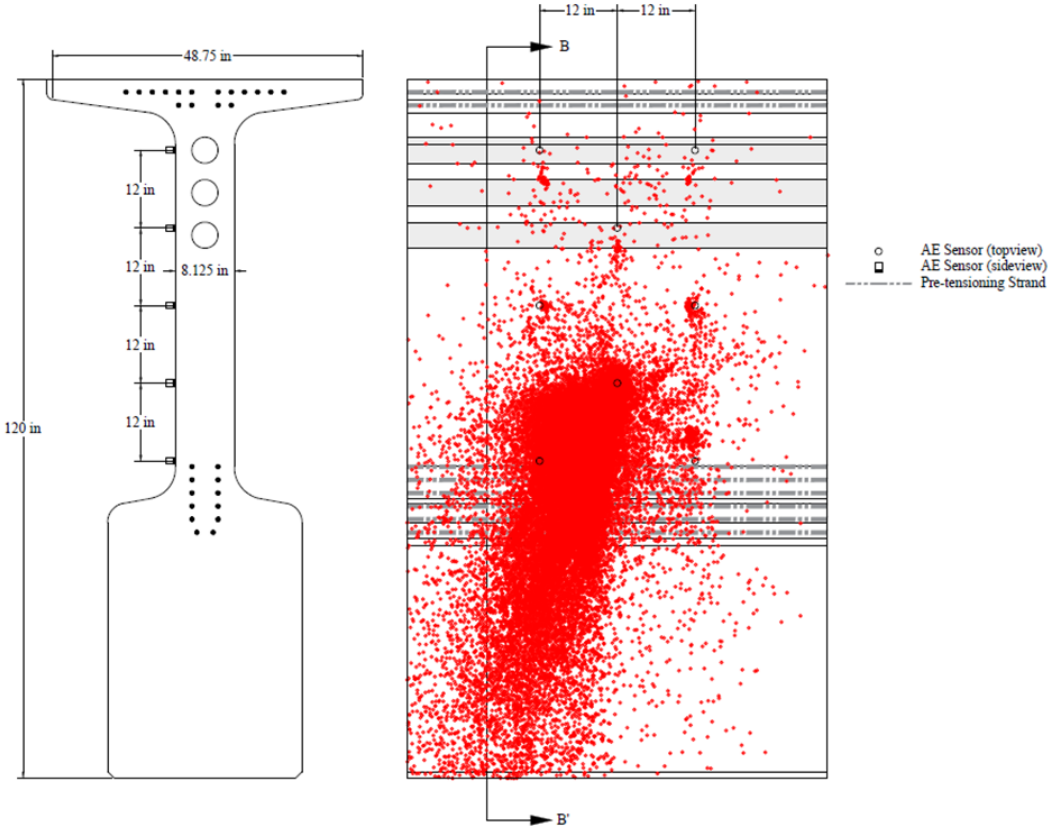

(b) (c)

Figure 7.17: Transport Test 3 – AE measurements of the mid-span vertical web of a hammerhead NEBT during transport with 91,723 recorded AE events. (a) Photograph of girder on truck with 2-D sensor array and equipment set-up, (b) Mid-span cross-section of tested NEBT, (c) Profile view of NEBT including AE event locations and sensors. Note that the post-tensioning strand ducts are at a higher location in the mid-span cross sections of (b) and (c) than at the end zone as shown emerging from the end of the section face in (a).

The recorded AE events are depicted in Figure 7.17 were also plotted by amplitude as shown in Figure 7.18. The amplitude plot of AE events shows a high concentration of low amplitude (blue: 60dB – 69dB), medium-low amplitude (green: 70dB – 79dB), and medium-high amplitude AE events (yellow: 80dB – 89dB) AE events in the "belly" of the NEBT girder with high amplitude (red: 90dB – 99dB) AE events being limited in quantity and diffuse.

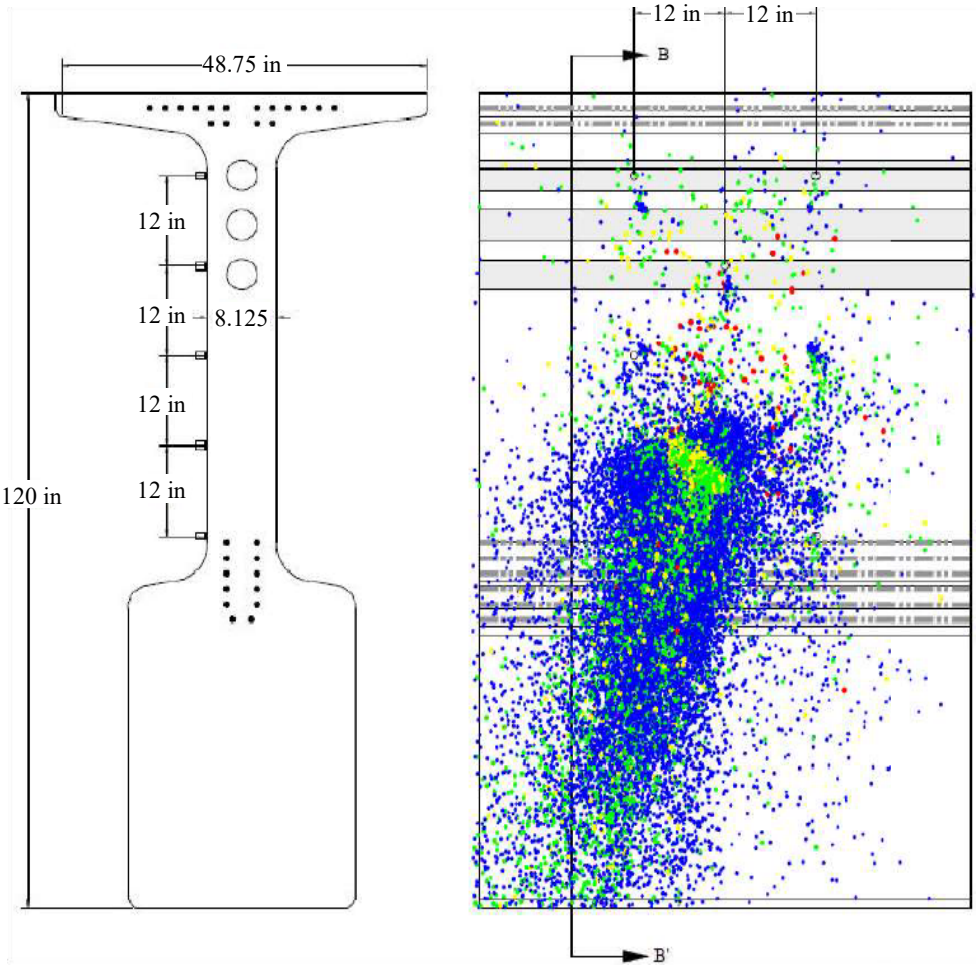

Figure 7.18: Transport Test 3 – AE measurements plotted by amplitude of the end zone vertical web of a straight NEBT during transport with 91,723 recorded AE events.

The AE event time histories collected during TT3 and plotted in Figure 7.19, indicate a greater level of AE event occurrences when on the interstate than on the secondary/highway roadways. This is the opposite of what was observed during TT1 and TT2. This could be due to the difference in geometries, stress distributions, and loading between the straight NEBT sections and hammerhead NEBT sections. Additionally, during stops no AE events appeared.

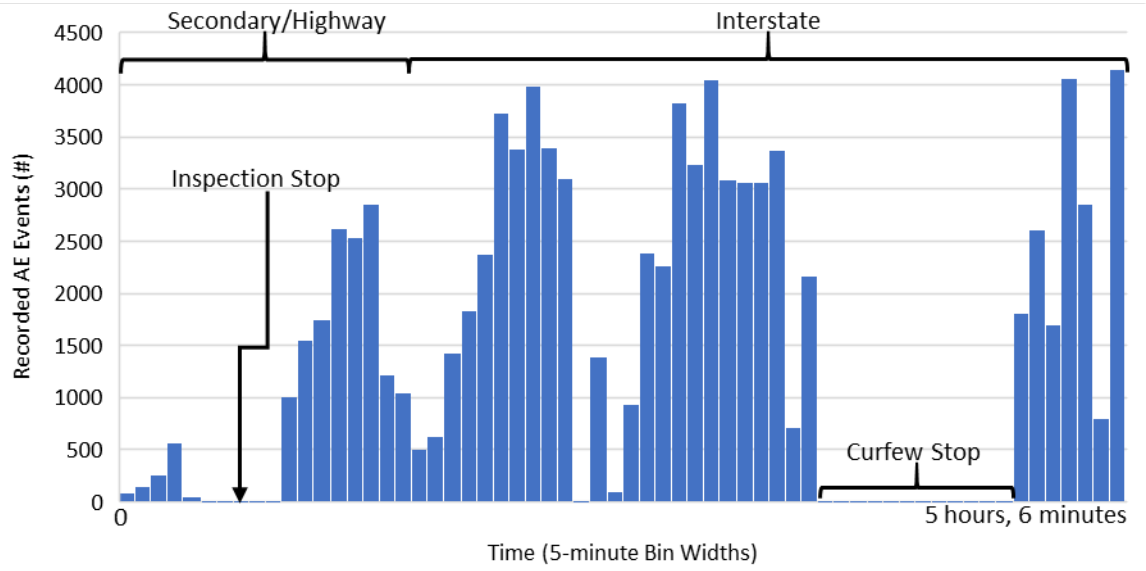

Figure 7.19: AE event density during transport testing of middle zone region of hammerhead NEBT, with a total event count of 91,723

7.6.4 Data Collection Process Observations

AE field transport data were collected from the middle zone of a hammerhead NEBT. AE event data collected from the middle zone of the hammer head NEBT were abundant and concentrated in the low region or "belly" of the beam. It was noted during transport that the occurrence of AE events was similar to that of Transport Test 1 and 2. The events occurred mostly during flexure-inducing vehicle maneuvers, such as when cresting a hill, bottoming in a valley, and during tight turns or turns with abrupt movements. Hitting a pothole in the road or driving over a rumble strip did not induce many AE events. This suggests that the recorded AE events may be due to internal energy release and not the injection of external energy from roadway conditions.

A finite element model using ANSYS R18.2 academic version calculated the stress distribution in the girder with the goal of determining if regions high stress correspond to the locations of AE events. The finite element model (FEM) was quasi-static and used quarter beam symmetry to reduce the number of nodes and elements and associated computational effort. The model used the same standard concrete material properties as for Transport Test 1 and approximated the action of the pre-stressing strands as a shearing force. Additionally, to model for bouncing and deflections of the beam during transport, the model used with a gravity load of 1g down and 1g up. The finite element models shown in Figures 7.20 and 7.21 indicate stress distributions commensurate with the recorded AE event distributions. Further confirmation comes from an examination of the shear and moment diagrams, Figure 7.22 and 7.23. The FEM shows a compression at the top of the beam moving toward tension at the bottom of the beam which corresponds to the recorded AE events being in the lower regions on the middle zone of the hammerhead NEBT during

transport. This stress distribution with the top of the beam in compression and the bottom of the beam in tension is due to the mass of the "belly" of the hammerhead NEBT overpowering the pre-stress that would otherwise make the beam camber. This reflects the design of the hammerhead NEBT as it will sit on a pier cap supported at the middle, essentially reversing the moment distribution. Only during craning and transport does the hammerhead NEBT experience this type of loading and stress distribution.

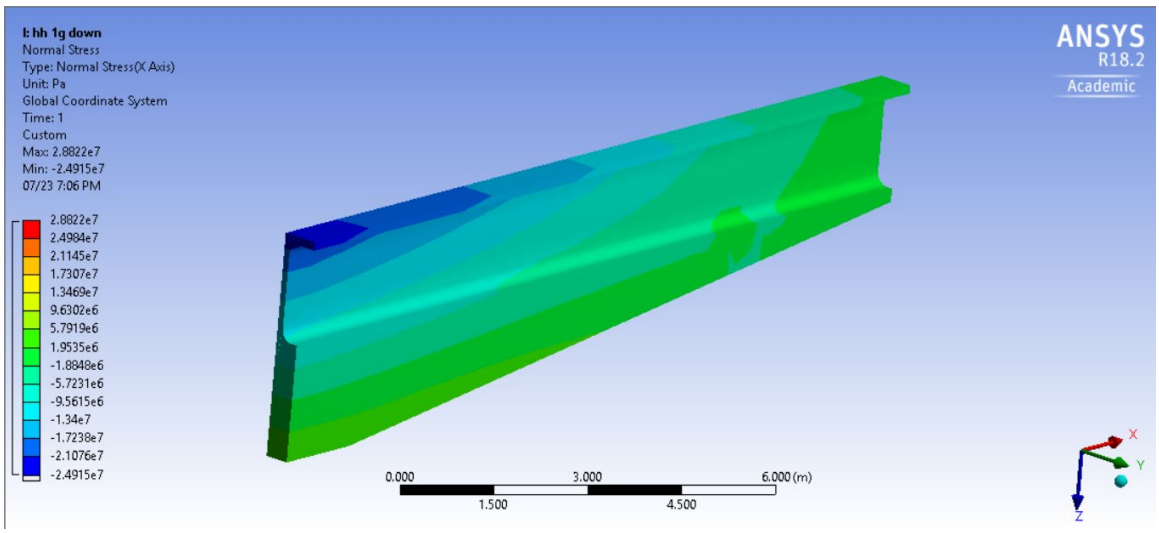

Figure 7.20: FEM quarter hammerhead NEBT stress distribution with 1g down, left side corresponds to mid-span and right side corresponds to the end zone

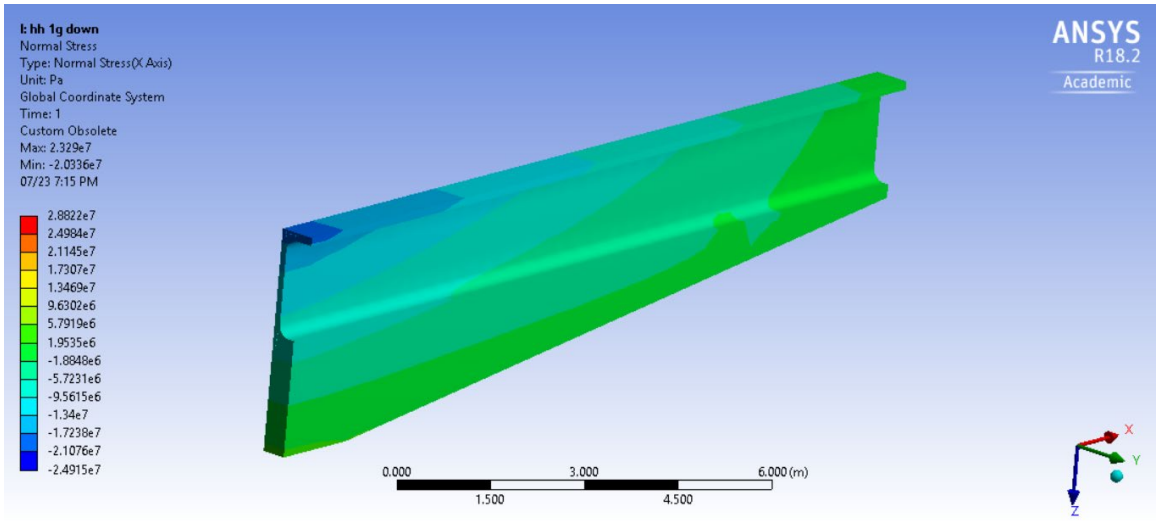

Figure 7.21: FEM quarter hammerhead NEBT stress distribution with 1g up, left side corresponds to mid-span and right side corresponds to the end zone

The shears and bending moments of the hammerhead span NEBT girders during transport as illustrated in Figure 7.22, are largely opposite to the shears and bending moments during in-service

loading as illustrated in Figure 7.23. This makes the transport process for the hammerhead span NEBT girders of particular interest because the hammerhead NEBT girders experience a unique stress pattern that is the opposite of the intended in-service design.

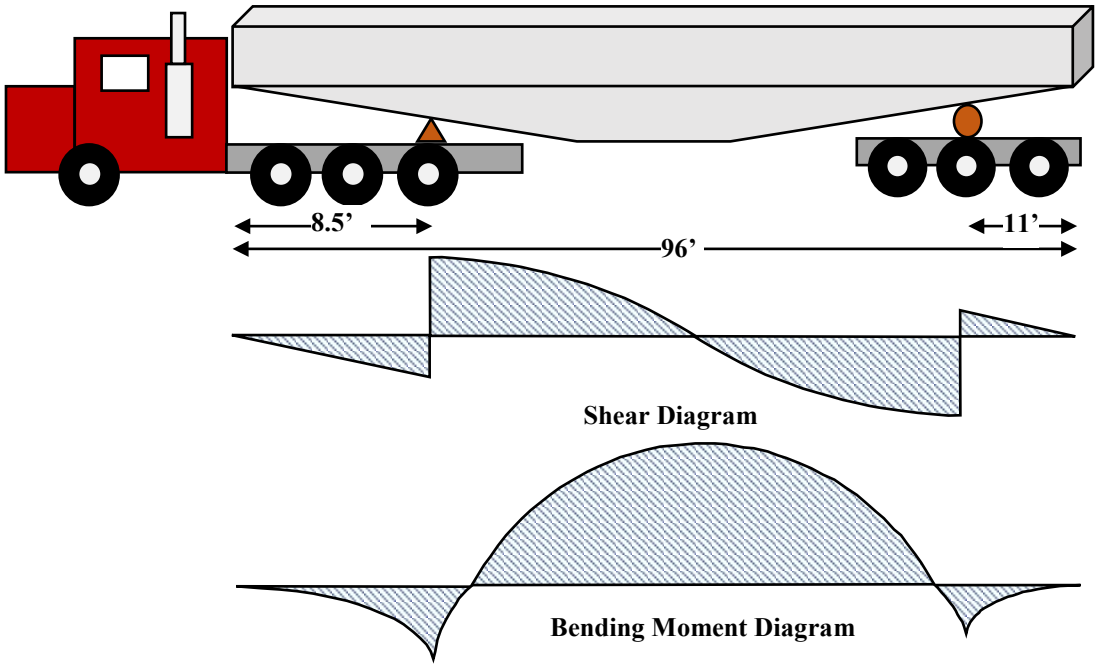

Figure 7.22: Hammerhead span NEBT shear and bending moment diagrams during transport

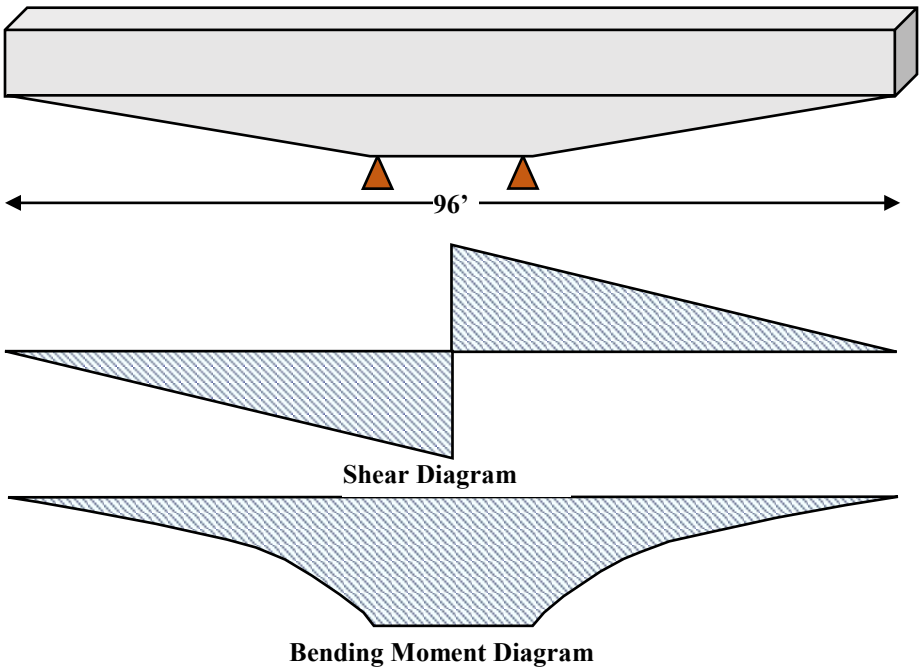

Figure 7.23: Hammerhead span NEBT shear and bending moment diagrams during in-service loading

7.7 Summary of Conclusions

7.7.1 Conclusions and Future Work

This chapter presents AE measurements during transport of full-scale Northeast Bulb Tee (NEBT) girders. The results indicate that AE sensing is a potential practical QA/QC process for PBES elements. The tests confirm the ability to collect AE data on prefabricated girders during transport. While there were no notable occurrences of damage or other QA/QC issues observed during transport, the recorded AE event distributions from the girder correspond to regions predicted by finite element modeling and simple shear/moment analysis to experience elevated stress levels. These results open the possibility for using the AE transport data to identify cracking and related damage that occurs during transport.

7.7.2 Northeast Bulb Tee Field Testing

Field testing during transport of full-scale Northeast Bulb Tee (NEBT) girders produced the following findings:

1. The AE test equipment required modest levels of custom modification for the transport tests.
2. The test equipment performed flawlessly during the tests and did not sustain any visible or notable damage.
3. Differences in AE event patterns were observed between end zone and middle zone regions along with between straight sections and hammerhead sections, Table 7.1.
4. Large quantities of AE events were recorded without correlation to observed cracks during transport.
5. Finite element modeling indicates areas of high stress corresponding to areas of dense AE event locations.
6. Additional data sets are required for statistical clustering and logistical regressions to define an AE event feature signature of cracks from other AE event source types.

Table 7.1: Quantification of AE Events Versus Girder Type and Sensor Array Location During NEBT Detensioning and Craned Movement

Girder type	Sensor array location	# of observed AE events during transport	Damage Observed
Straight Bulb Tee	End span	623	None
Straight Bulb Tee	Mid span	2,628	None
Haunched Bulb Tee	Mid span	91,723	None

Field tests on NEBT's provided an abundance of AE event data during critical stages of the fabrication and transportation processes. AE event data appeared both when cracking was observed and when cracking was not observed. A finite element stress analysis identified regions of high stress that corresponded to regions of high AE event activity. No cracking or other damage appeared at these locations Continued work on AE event source discrimination to identify the feature signatures related to cracking, regions of high stress, or otherwise requires additional data sets. This work has set the foundation for understanding when cracks tend to occur, where the key areas to concentrate sensors are, and what processes are of the highest stress to the NEBT's prior to service.

CHAPTER 8
PROPOSED METHODOLOGY FOR QUALITY ASSURANCE/QUALITY CONTROL ACCEPT AND REJECT CRITERIA

8.1 Potential Use of Existing Damage Assessment Methods

8.1.1 Background

The basis for most of the currently-available methods for damage assessment of reinforced concrete is to collect and analyze of experimental data sets from tests using cyclic loading, often in an increasing pattern up to failure. In this vein, the Felicity ratio and Load-Calm ratios assess damage by examining AE activity in increasing loading-unloading cycles. Exceptions to the requirement for cyclic loading experiments are event counting and frequency analysis. An additional issue is the need for large data sets due to the inherent experimental scatter that characterizes most concrete fracture studies.

The fabrication and transport processes for Northeast Extreme Tee (NEXT) beams and Northeast Bulb Tee (NEBT) girders include; detensioning, craned form removal, and transport. These processes are single loading events (detensioning and craned form removal) or random/variable loading events (transport). The resulting data do not readily fit into a cyclic load testing framework. These differences in loading require modifying current damage assessment methods for use as a QA/QC procedure for the fabrication and transport events studied as part of this project. Due a reliance on cyclic loading, damage assessments based on Felicity ratios and Load-Calm ratios are not directly applicable to these cases. Event-counting, parametric analysis, b-value analysis, and frequency analysis have better potential for adaptation for use in single loading events or inconsistent/variable loading.

8.1.2 Adapted Parametric Feature Analysis

A feature-based analysis extracts and then records a set of features from each AE event waveform. The features include but are not limited to amplitude, duration, counts-to-peak, and peak frequency. In a cyclic load-unloading regime, the correlation between RA values (risetime/peak amplitude) and the average frequency (kHz) are established damage indicators. Single event threshold values have yet to be established. It is hypothesized from the analysis of AE data during laboratory and field testing thus far that the use of statistical methods such as logistical analyses or multivariate analyses can establish feature threshold identifiers that would allow for the classification of a single AE event by damage or no damage and what was the source of the AE event. To establish this feature analysis for “fingerprinting” of recorded AE events requires a larger AE data set than what has been established as part of this study. A large AE data

set of repeated testing is needed in conjunction with damage observations to establish not only the feature identifiers of different AE sources and levels of damage but also to establish reliability and typical variance for the prescribed AE event fingerprint.

8.1.3 B-value and Frequency Analysis

The b-value and frequency analyses were both developed as damage assessment tools but provide two very different interpretations of damage. The b-value analysis provides an assessment of the severity of damage while the frequency analysis provides a source of damage. Although the b-value analysis is a statistical regression of the AE event peak amplitudes and can be calculated for the loading cycle only or a complete loading-unloading cycle, it is hypothesized that if a large enough historical b-value data set calculated from loading events was established, that lower and upper bounds for acceptable b-values could be established to assess the severity of damage. Once the damage severity is established from the b-value analysis the frequency analysis can be implemented to determine the source of damage. The frequency analysis flow chart as currently established will need revision to describe damage sources that are specific to damage modes possible during fabrication and transport processes for Northeast Extreme Tee (NEXT) beams and Northeast Bulb Tee (NEBT) girders. Similar to the parametric analysis, lower bounds for b-values and verification of the frequency analysis flow chart, along with the suitably small variance requires a large AE data set of repeated tests is needed in conjunction with damage observations to establishing the upper and lower bounds.

8.1.4 Potential AE Damage Assessment Methods

Spatial representations of AE data collected during both laboratory and field testing yielded AE event locations that tended to cluster in areas of high stress or cracking and were diffuse in areas where no damage was observed. A correlation is hypothesized to be made between the number of concentrated AE events to an acceptable level of damage similar to the ASTM standard for AE testing of composite fuel tanks. AE technology has been proven to reliably detect material failure of composite fuel tanks and as such is an acceptable QA/QC technology for industry practice (ASTM E2191/E2191M-16). The use of AE sensing as a QA/QC procedure in composite fuel tanks is a measure of cumulative recorded AE events over a prescribed amplitude threshold during a pressure test where the tank pressure incrementally increased with specific holding times between each pressure increase. If the number of recorded events exceeds a threshold, then the part is either slated for further examination (10,000 events) or rejected (50,000 events). Although only the detensioning process mirrors step loading, the same principle of increased AE activity as an indicator of stress and damage could applied to many loading scenarios. Similar to the parametric and b-value/frequency analyses, a large AE data set of repeated testing is needed in conjunction with

damage observations to establish an AE event density threshold to determine if the beam should be accepted or rejected but also to establish reliability and typical variance for the proposed AE event density method along with the variance of strength of the material being tested.

8.2 Proposed Multi-Step Procedure

A systematic future work effort would be multistep; 1. Conduct realistic laboratory tests of beams with embedded defects so that they experience early and controlled damage and failure; 2. Identify the AE signatures of these failures; 3. Modify AE technique to improve sensitivity and selectivity of damage recognition; 4. Repeat these tests in small pilot study to determine the experimental scatter of detection versus damage; 5. Analyze pilot test data to determine the statistical power of the technique and estimate the number of tests needed to establish validity of tests; 6. Conduct sufficient number of repeat tests to identify sensitivity and selectivity in the form of Receiver Operating Characteristic (ROC) curves; 7. Identify field conditions prone to damage that is of concern and estimate the rate and severity of occurrence. This may be end zone cracking, delaminations, debonding, etc. 8. Combine information from the above steps to conduct a longitudinal study with sufficient number of repeats to obtain sufficient statistical power to justify setting an accept/reject threshold based on AE readings. Future work would be to conduct an appropriately-sized laboratory testing regimen over an extended period on a single type of commonly produced beam or girder to build a large AE database for all processes that are associated with cracking or high strain events. Once a sufficient AE database is established with visual observations of damage, conditions, and element performs; the three potential AE damage assessment techniques can be implemented and compared to determine the effectiveness for use as accept/reject criterion.

Potential laboratory tests include; 1. Prestressed beam with diffuse cracking, 2. Beam with excess prestress that induces end cracking, 3. Beam with a crack prone mix. Summary of Conclusions

8.3 Conclusions and Future Work

This study focuses on the development of accept/reject criteria for full-scale prefabricated and pre-stressed, reinforced concrete Northeast Extreme Tee (NEXT) beams and Northeast Bulb Tee (NEBT) girders based on Acoustical Emission (AE) monitoring as a Quality Assurance/Quality Control (QA/QC) procedure during the detensioning, craned form removal, and transport processes. Although there are many published damage assessment techniques for reinforced concrete, these techniques are based on cyclic loading and are not compatible with loading conditions observed during the fabrication and transport of the NEXT and NEBT beams. Loading of the full-scale prefabricated and pre-stressed, reinforced concrete NEXT beams and NEBT girders is either a single near-instantaneous event or a variable self-weight loading

event. Of the five common reinforced concrete damage assessment techniques (felicity ratio; parametric analysis; load-calm ratio; b-value analysis; frequency analysis) only the parametric, b-value, and frequency analyses were determined to be adaptable to the field loading conditions experienced by the NEXT and NEBT beams during fabrication and transport.

Of existing AE data damage assessment techniques, there is one with potential for use in the loading scenarios observed in this project and two with potential for use in conjunction with one another. Additionally, from AE data collected and analyzed as part of this study a third damage assessment technique is hypothesized. The three potential damage assessment methods are;

1. The use of a parametric analysis using AE event waveform features to develop algorithms relating the unique features to observed damage types and severities;
2. To build a database of b-value's (using the published b-value damage assessment technique) for specific beams and processes. The database would indicate the upper and lower bounds for a typical b-value and therefore establish the upper and lower limits for accepting/rejecting the beam. Additionally, the frequency analysis would then be used to identify the AE source or damage type that lead to the rejection of the beam;
3. Based on AE data collected and analyses from laboratory and field testing, AE events tended to have dense clustered near the location of observed. It is hypothesized a damage assessment could be performed based on AE event clustering density. The frequency analysis would then be used to identify the AE source or damage type.

In the case with all three of the potential accept/reject damage assessment techniques, large AE data sets are needed for each beam type, reinforcement pattern, pre-tensioning strand pattern, and concrete mixture. Data sets need to include instances of varying observed damage from no damage to major damage in order to establish the lower and upper limits of acceptable AE emissions. It is not possible to establish accept/reject criteria based on the current AE event database; however, the current database has presented a new and unique possibility for damage assessment as well as validated the efficacy of AE technology as a potential Quality Assurance/Quality Control (QA/QC) procedure in locating the sources of AE events associated with cracking or high strain events.

Of existing AE data damage assessment techniques, at least four have potential utility in the loading scenarios as observed in this project:

1. Event counting – If the number of recorded events above a preset amplitude threshold exceed the number specified for that loading period, the part is set aside for closer examination, or reject. In situations where the loading is not cyclic, but stationary random, it may be possible to extend this technique to a Load-Calm ratio method based on whether the number of events increases or decreases as

the loading continues. Increasing event counts would correspond to increasing damage. Decreasing event counts would correspond to the part initially undergoing a break-in period with high event counts, followed by a minimal damage under the same loading condition.

2. The use of a parametric analysis using AE event waveform features to develop algorithms relating the unique features to observed damage types and severities.

3. To build a database of b-value's (using the published b-value damage assessment technique) for specific beams and processes. The database would indicate the upper and lower bounds for a typical b-value and therefore establish the upper and lower limits for accepting/rejecting the beam. Additionally, the frequency analysis would then be used to identify the AE source or damage type that lead to the rejection of the beam.

4. Based on AE data collected and analyses from laboratory and field testing, AE events tended to have dense clustered near the location of observed. It is hypothesized a damage assessment could be performed based on AE event clustering density. Once damage established the frequency analysis would then be used to identify the AE source or damage type.

In the case with all four of the potential accept/reject damage assessment techniques, large AE data sets are needed for each beam type, reinforcement pattern, pre-tensioning strand pattern, and concrete mixture. Data sets need to include instances of varying observed damage from no damage to major damage in order to establish the lower and upper limits of acceptable AE emissions. It is not possible to establish accept/reject criterion based on the currently limited AE event database; however, the current database has presented a framework for damage assessment as well as validated the efficacy of AE technology as a potential Quality Assurance/Quality Control (QA/QC) procedure in locating the sources of AE events associated with cracking or high strain events.

CHAPTER 9
ACOUSTIC EMISSION MONITORING EQUIPMENT REUSE AND FUTURE DEVELOPMENT RECOMMENDATIONS

9.1 Overview

This chapter describes the functionality and reusability of the acoustic emission (AE) monitoring equipment for future VTrans relevant research and structural assessments. The use of the equipment to date has primarily been to research the potential for AE measurements as part of a Quality Assurance/Quality Control (QA/QC) procedures for precast pretensioned concrete girders used in bridges. Proposed future work includes additional laboratory testing, fabrication processes monitoring, transport monitoring, construction site beam placement monitoring and long-term service use monitoring. These continued and additional AE data collection scenarios are recommended to provide larger data sets for developing future QA/QC standards and to complete AE monitoring during the complete life cycle of a full-scale prefabricated and pre-stressed, reinforced concrete; 1) fabrication, 2) transport/construction, 3) service use.

9.1.1 Current AE Monitoring Equipment

The AE monitoring equipment used in this study was an 8-Channel Mistras AEwin™ Sensor Highway III monitoring system, associated AEwin™ processing software, and an eight PK6I sensor array. The design and configuration of this measurement system is for field testing of civil infrastructure. The setup and selection followed the manufacturers' recommendations and ASTM standards (ASTM E1316-18a, 2018; ASTM E3100-17, 2016; Physical Acoustics, 2018). The PK6I sensor is a medium-frequency, resonant AE sensor with an integral, ultra-low noise, low-power, filtered 26 dB preamplifier, which can drive up to 200 meters of cable and operates at a resonant frequency of 60 kHz frequency (Physical Acoustics, 2018). The Mistras AEwin™ Sensor Highway III monitoring system can expand up to 32 high speed AE and over 100 slower speed channels with supplemental transducer. A NEMA-4 enclosure houses the AEwin™ Sensor Highway III, allowing for outdoor use. The system has wireless (WiFi) and Ethernet 10/100/1000 BT communications interfaces. An AE monitoring schematic along with an image of the Mistras AEwin™ Sensor Highway III appear in Figures 9.1 and 9.2. Table 9.1 lists the specific equipment items acquired as part of the Mistras AEwin™ Sensor Highway III system.

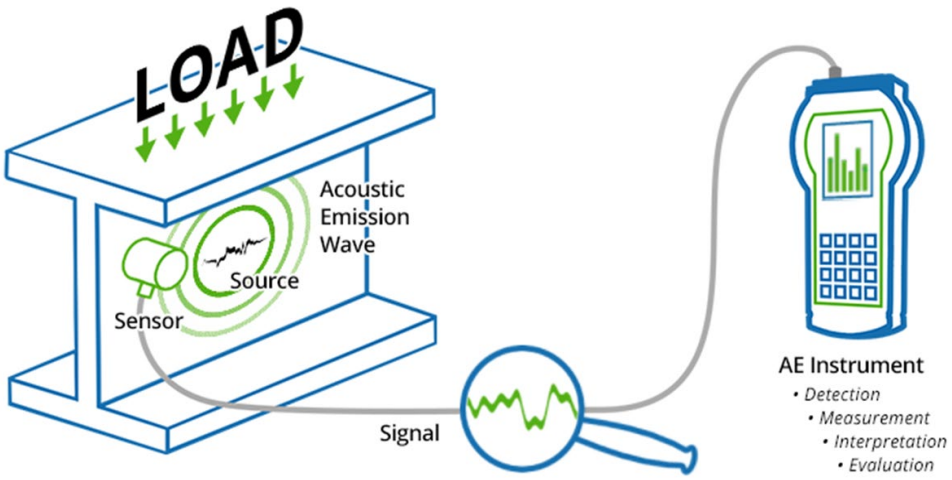

Figure 9.1: AE monitoring process schematic (Physical Acoustics, 2018)

Figure 9.2: Mistras AEwin™ Sensor Highway III (Physical Acoustics, 2018)

Table 9.1: Mistras AEwin™ Sensor Highway III System Parts

Item	Model and Description	Quantity
1	PN# SHIII-8, SHIII-8, Smart Remote Monitoring, 8-channel Sensor Highway III system is a full, stand-Alone AE system for unattended monitoring in outdoor environments. System Includes; Outdoor weatherproof case (18" x 12" x 6"), one 8-channel AE board, 8 single-ended parametric inputs, remote reboot, Windows 7 Operating system, AEwin installed and licensed for 8 channels, Ethernet	1

	connectivity to a factory network or Internet, 110/220VAC or 9 - 28 VDC power at 15 watts.	
2	PN# PK6I-5015, PK6I, Low Power Sensor, 60 kHz with Integral Preamp and SMA Connector for Sensor Highway	8
3	PN# 1234-4002-30, 1234-SMA/BNC-30, Signal Cable, RG58 SMA-BNC 30 Meters	8
4	PN# 9380-7003-2, AE-WIN 2D-LOC, FULL PLANAR, 2 DIMENSION LOCATION	1
5	PN# 9380-7003-9, AE WIN 3D-LOC, 3 DIMENSIONAL LOCATION SOFTWARE OPT	1

Mistras AEwin™ Sensor Highway III monitoring system and associated AEwin™ processing software allows for user-defined inputs to refine the collected AE events. The acquisition setup parameters, as listed in Table 1, followed that specified by the manufacturer. Pencil lead break tests in controlled laboratory specimens confirmed the validity of these parameters (Sause, 2011). These input parameters are found in Table 9.2.

Table 9.2: Mistras AEwin™ Sensor Highway III Input Parameters

Parameter		**Value**	**Units**
Threshold		60	decibel (dB)
Pre-amplifier Gain		26	decibel (dB)
Analog Filter	Lower Bounds	20	kilohertz (kHz)
	Upper Bounds	400	kilohertz (kHz)
Digital Filter	Lower Bounds	20	kilohertz (kHz)
	Upper Bounds	200	kilohertz (kHz)
Timing Parameters	Peak Definition Time (PDT)	200	microsecond (µs)
	Hit Definition Time (HDT)	800	microsecond (µs)
	Hit Lockout Time (HLT)	1,000	microsecond (µs)
	Maximum Hit Duration (MDT)	1,000	millisecond (ms)
Longitudinal Wave Velocity		13,083	feet per second (ft/sec)
Transverse Wave Velocity		7,833	feet per second (ft/sec)
Surface Wave Velocity		7,250	feet per second (ft/sec)

If the user-defined minimum sensor hits occur within the specified time duration parameters then the AEwin™ software processes the waveforms to extract and record fifteen features of the AE waveform signals including: 1) amplitude, 2) duration, 3) energy, 4) counts, 5) rise time, 6) peak frequency, 7) frequency centroid, 8) absolute energy, 9) signal strength, 10) initial frequency, 11) reverberation frequency, 12) counts-to-peak, 13) average signal level, 14) root mean square (RMS), and 15) average frequency.

9.2 Demonstrated AE Test Capabilities

9.2.1 Laboratory Testing

This section describes a series of laboratory tests performed to verify the efficacy of the AE monitoring equipment to be used for crack detecting in reinforced concrete with the intent to apply laboratory observations and methodologies to future full-scale filed tests. This section also provides observations of the performance of the current Mistras AEwin™ Sensor Highway III monitoring system and recommendations for system alterations/modifications for future laboratory AE data collection.

9.2.2 AE Event Locating

Alternative strategies for event location using non-parametric machine learning algorithms were investigated. Currently, the Mistras AEwin™ locating algorithm assumes a homogeneous specimen, where the wave speed is constant; that exists a linear path across the material between the source and the piezoelectric sensor; and that the first AE signal is due to the p-wave. Such model leads to the solution of a nonlinear system of equations with the Nelder-Mead simplex optimization algorithm (Physical Acoustics, 2018). However, the presence of large aggregates, reinforcing rebars, and tubes in the concrete part break these assumptions, as they may lead to scattering, or a linear path between the source and the receiver may not exist. Furthermore, geometrical nonlinearities will break the assumption of a direct linear path. The wave travel speed varies depending on the wave type and is not known with accuracy for each specimen a priori.

To circumvent such limitations, inspired on successful applications on composite materials (Baxter et al., 2007), a locating strategy based on difference of time of arrival mapping, or ΔT-mapping, coupled with a nonlinear regression method called Gaussian Process (GP) is being investigated. The ΔT-mapping process consists of mapping the difference in time of arrivals between each couple of sensors by performing a pencil-lead break test over a predetermined grid (Hensman et al., 2010). When a part has been mapped, then, when in service, any given set of time of arrivals will lead to possible source regions in each ΔT-map.

By superposing these possible regions, the event source location can be determined. Notice that this method does not require any material properties or part geometry knowledge and could prove more accurate and robust for NEXT beam applications. Interpolation fills in the points that are out of the grid using GPs, a non-parametric machine learning algorithm. Furthermore, we introduce a weighting on the ΔT-maps based on the underlying uncertainty given by the GP and on the wave maximum amplitude at each sensor. Points of the map where variance is high get penalized. Maps are balanced based on the received amplitude at each sensor.

The experimental setup consists of 4 resonant (150kHz) AE sensors, with pre-amp set to 40 dB. The goal of this first experiment was to benchmark the ΔT-map with the currently used locating algorithm. A concrete block of 0.41x0.25x0.14 m was fabricated, and 62 points have been mapped on its face, with another 4 points taken for performance evaluation, as shown in Figure 9.3. At each point, 10 pencil-lead break tests were performed, and the average value was taken for both the ΔT-mapping and the Nelder-Mead simplex algorithm calculation.

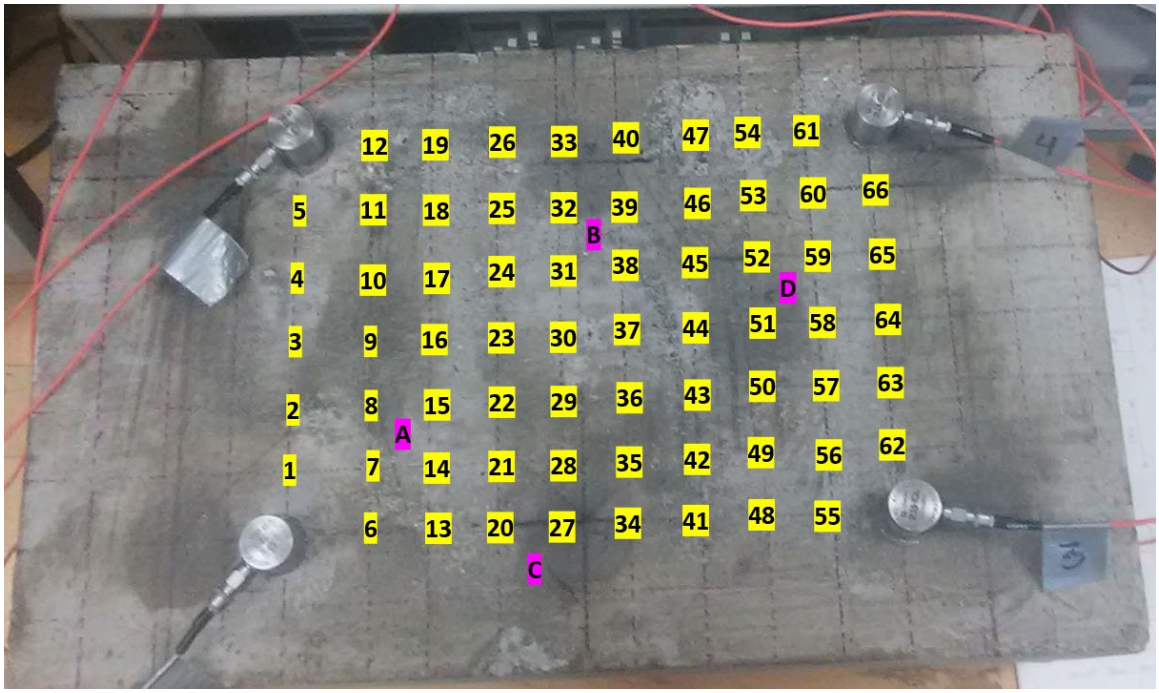

Figure 9.3: Concrete block face with 62 grid points (yellow) and 4 test points (magenta)

The mapped ΔTs and the corresponding GP interpolation are shown in Figure 9.4 to 9.8 show the true event location (green), the AEWin^{TM} system location (red) and the ΔT-map location (magenta).

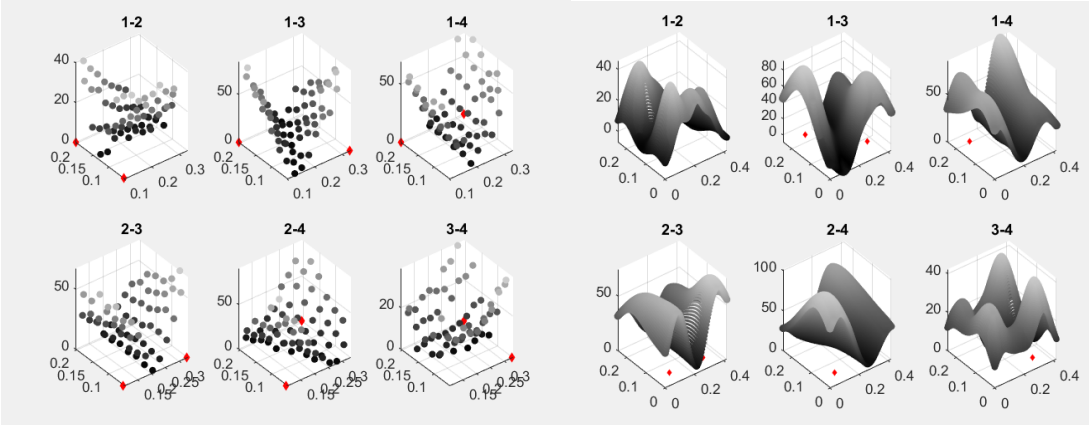

Figure 9.4: Experimental ΔT-map at the grid points (left) and interpolated values (right) given by the GP

This scenario satifies the AEWin™ algorithm assumptions. Both perform well. New concrete specimen that include rebar and PVC pipes have been fabricated, but experiments are still ongoing. Under such scenario, the Δ*T*-map approach is expected to be superior to the current locating system.

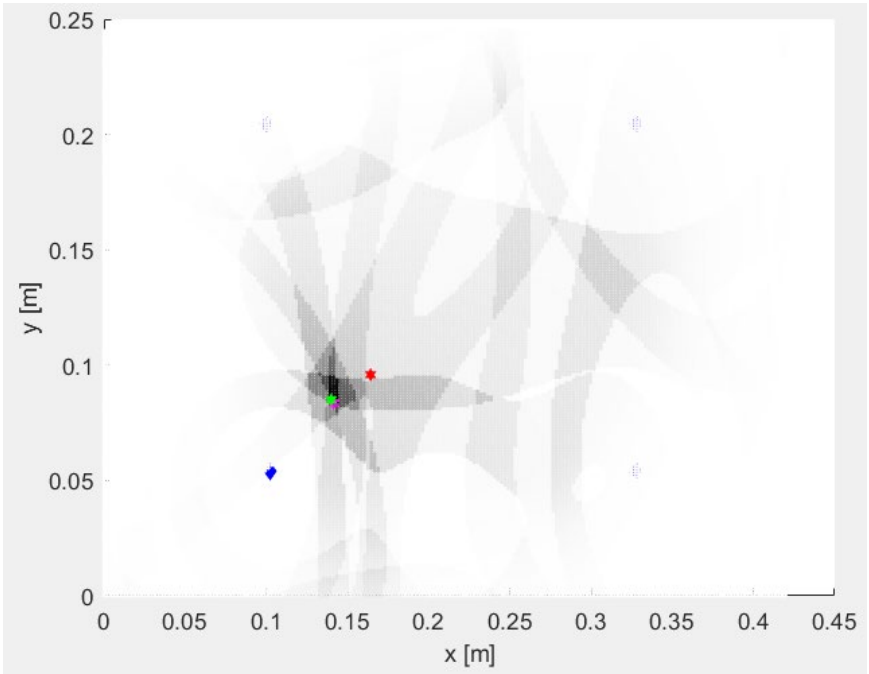

Figure 9.5: Test point A, the true location and the ΔT-map location are superposed

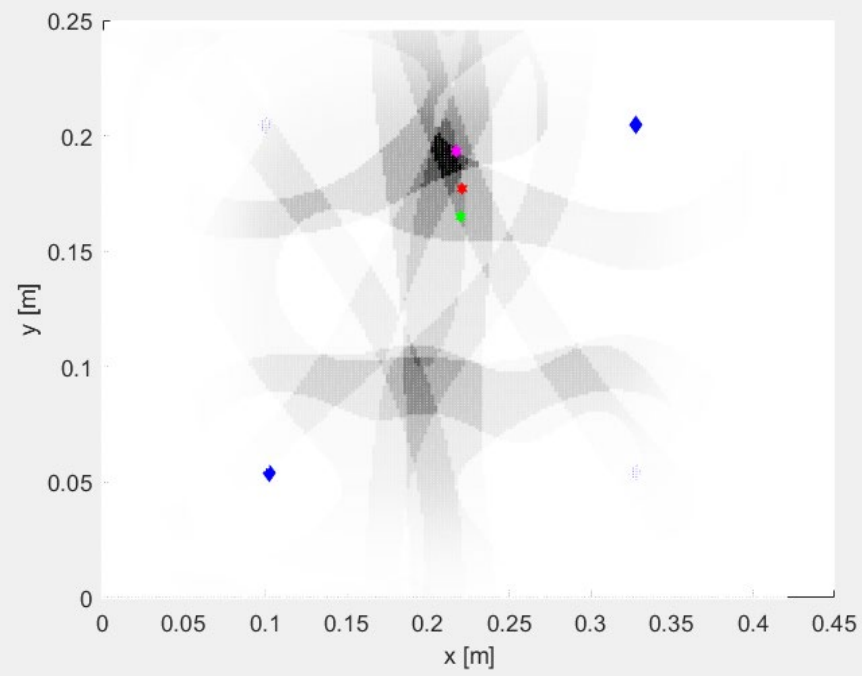

Figure 9.6: Test point B, in this case the AEWin system performed better

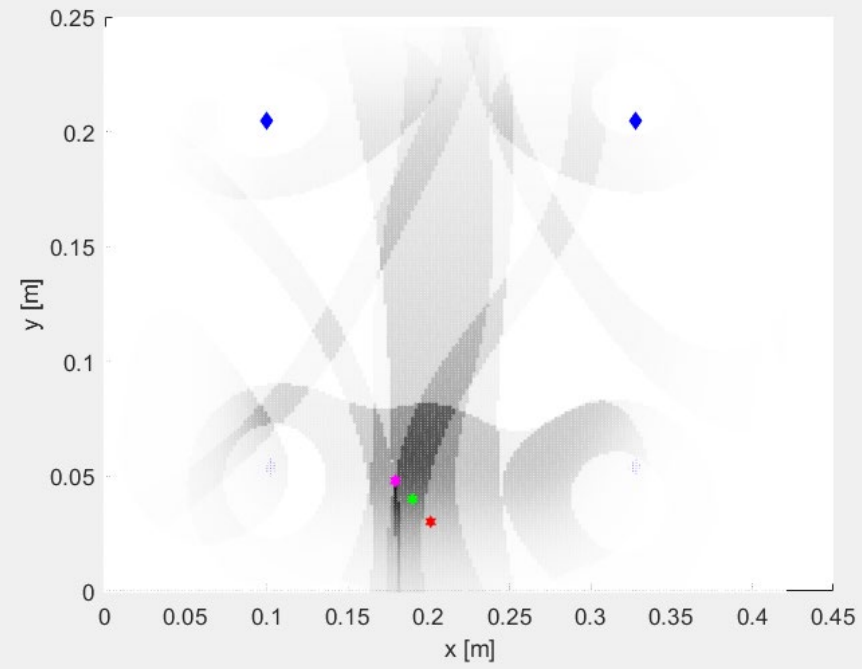

Figure 9.7: Test point C, both methods show similar performance

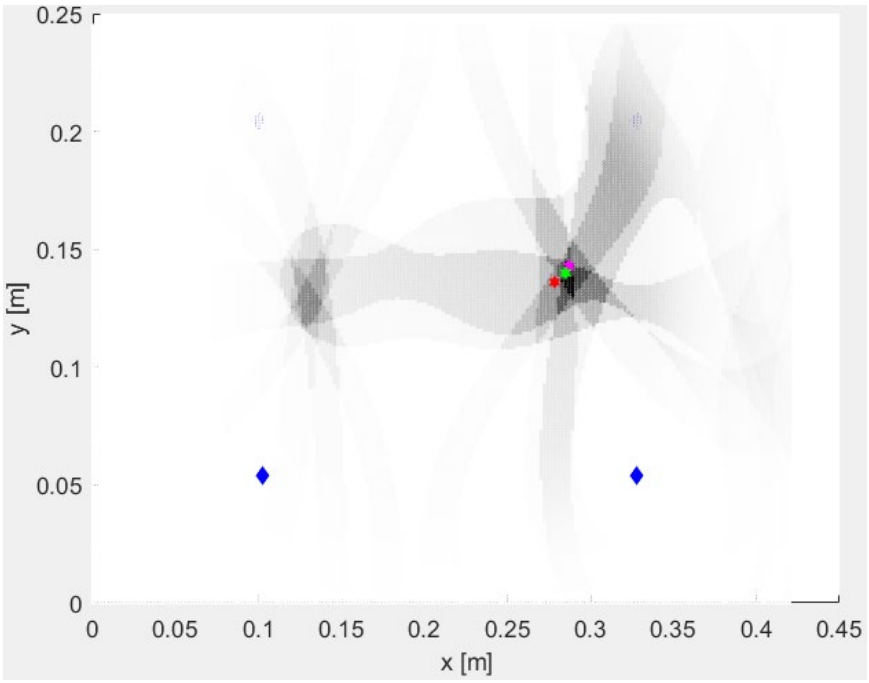

Figure 9.8: Test point D, both methods show similar performance

9.2.3 Pull-Out AE Monitoring

AE monitoring of laboratory pull-out tests were performed in a controlled laboratory environment with limited spatial and time constraints. Observations of AE data collection from pull-out tests performed with a Tinius Olsen static tension material testing machine indicated that the unmodified Mistras AEwin™ Sensor Highway III monitoring system with wired broadband AE sensors was adequate for these tests. The orientation of the AE sensor placement and dislodging of AE sensors at rupture showed potential to damage the AE sensors by impacting the tension test machine or by being hit from dislodged concrete. A mechanism to maintain connection between the AE sensor wear-plates and the concrete as well as to protect the AE sensors from damage was needed. To assist with these concerns, two types of metal armor/fastening devices were fabricated. The first metal armor/fastener was made from cut sections of square hollow stock large enough for the AE sensor to be inserted into. A hole drilled and tapped on one side allowed for the installation of a set screw to hold the AE sensor in place. Epoxy adhesive attached the metal armor/fasteners to the concrete surface. This design succeeded in both protecting the AE sensors during testing and maintained contact to the concrete surface. However, concerns that the metal between AE sensor wear plate and the concrete surface could distort the AE signals prompted a new approach; U-shaped brackets with two ears on each side to epoxy to the concrete surface were fabricated from metal sheet stock. Again, these U-shaped brackets had a hole drilled and tapped for a set screw to pressure the AE sensor against the concrete surface.

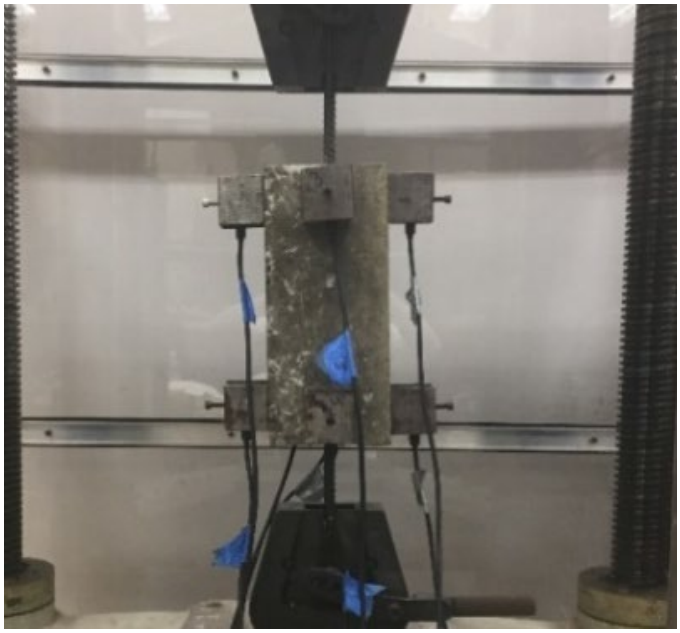

Figure 9.3: Laboratory acoustical emission pull-out testing

9.2.4 Three-Point Bending AE Monitoring

Observations of AE data collection from three-point bending tests performed using a Tinius Olsen static tension material testing machine indicated that the unmodified Mistras AEwin™ Sensor Highway III monitoring system with wired broadband AE sensors was adequate for these tests. Additionally, unlike the pull-out tests, the three-point bending tests were control loaded creating a less violent failure and therefore sensor protection was not required for these tests. The duration of tests was short enough that the sensors were simply adhered to the concrete surface with high vacuum grease.

(a) (b)

Figure 9.4: Laboratory acoustical emission three-point bending (flexure) tests (a) 2-D sensor array and (b) 3-D sensor array

9.2.5 Void Detection

An array of AE sensors can locate a source by triangulating the time of arrival of waves. Voids in the solid will distort the waves. This opens up the possibility of inverse tomographic methods for determining void size and location by measuring the waves as they arrive from known sources, Figure 9.5.a. Voids also affect the frequency of standing acoustic waves, typically by reducing the wavelengths and increasing the frequencies – an affect readily measured by active acoustic methods, Figure 9.5.b.

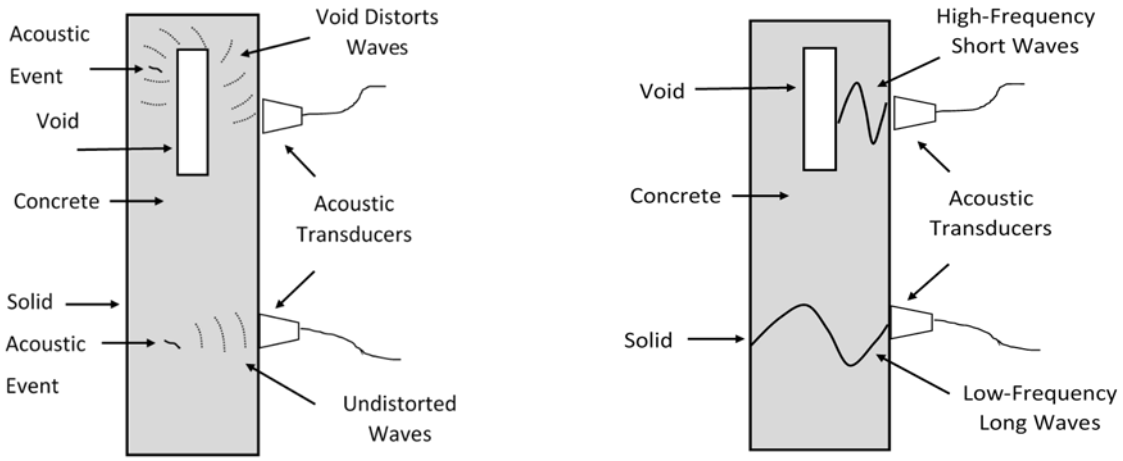

(a) *(b)*

Figure 9.5: Effects of voids on acoustic waves (a) distortion of propagation and (b) alteration of frequency of standing waves

Proof-of-concept tests determined if in-house AE test equipment could detect voids, using a small reinforced concrete beam (30 x 5 x 5 in^3) with internal voids created with a plastic bottle and Styrofoam inserts, 9.6.a. Frequency sweeps using AE transducers with one operated as an active source and the other operating as a receiver appear as the setup in 9.6.b, data from solid beam 9.6.c and data from section with void 9.6.d. The section with the void sustains a high-frequency standing wave as suggested in 9.5.b. 9.7.a shows the same beam undergoing ground penetrating radar (GPR) tests. The GPR B-scan traces indicate the likely location of a void. A conclusion from this test is that AE and GPR testing can detect this relatively large void. It should be noted that in this case, the GPR does not have to penetrate through a dense mesh of reinforcing, as is common in prestressed girders and is commonly a challenge for GPR imaging.

(a)

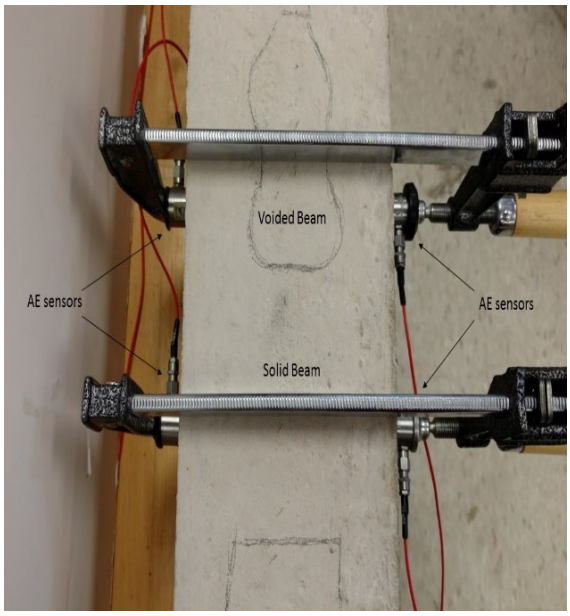

(b)

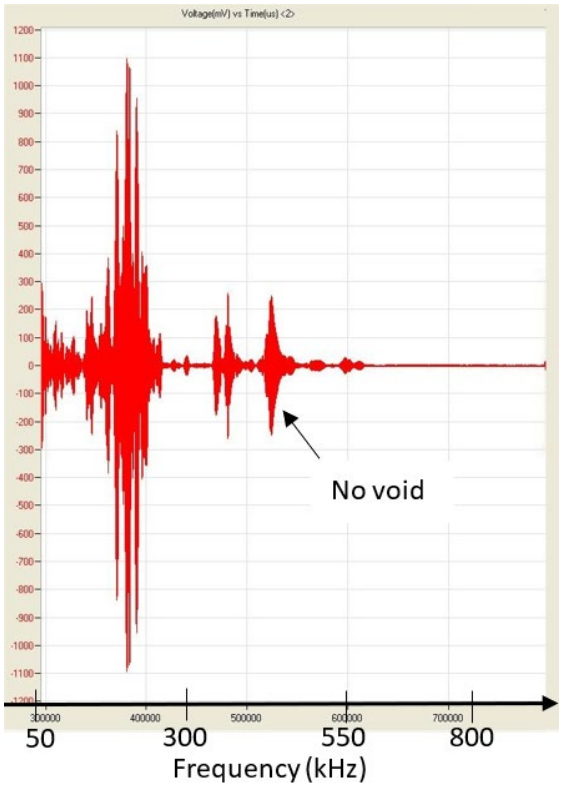

(c)

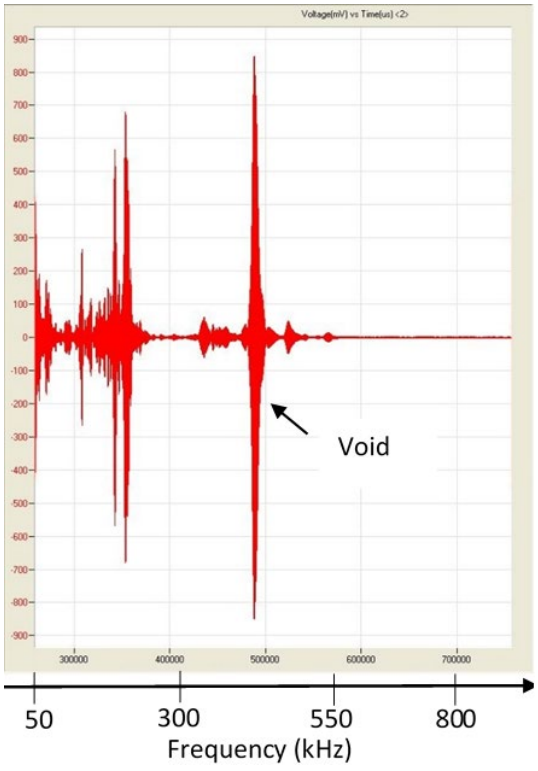

(d)

Figure 9.6: Active acoustic detection of voids in laboratory beam: (a) Formwork and void inserts prior to fabrication, (b) Acoustic transducer setup, (c) Frequency content of standing waves in solid section, (d) Frequency content of standing waves in section with void – note addition of high frequency waves at approx. 400 kHz.

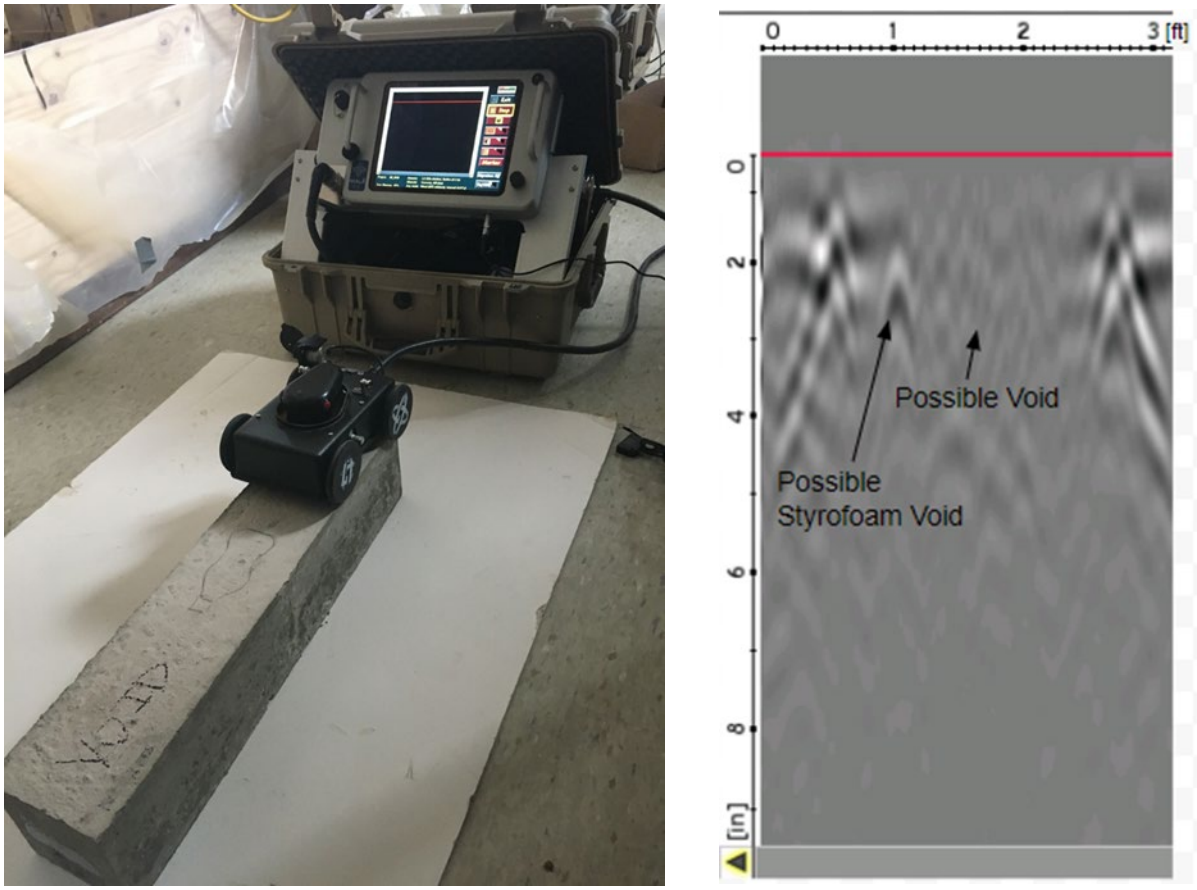

(a) (b)

Figure 9.7: Ground penetrating radar test of beam in 9.6: (a) Test setup and (b) B-scan showing possible void

9.3 Field Testing

9.3.1 Detensioning AE Monitoring

AE monitoring field tests of NEXT beams and NEBT girders during detensioning were performed on Site and were bound by multiple constrained including time, spatial, access, and distance. As to not disturb or slow the fabrication processes; it was paramount to deploy the Mistras AEwin^{TM} Sensor Highway III monitoring system, collect data, and remove the system without disturbing or delaying any fabrication processes. This required four alterations to the existing system:

1. Portable power supply – Used an Uninterruptible Power Supply (UPS) to allow for untethered and portable power to the Mistras AEwin^{TM} Sensor Highway III.
2. Wireless remote access to the Mistras AEwin^{TM} Sensor Highway III – Used an external wireless router to allow for remote connection to a laptop so that AE monitoring personnel were able to stay a safe distance away from fabrication activities while live streaming the data collection.
3. AE sensor protection/fasteners – Used the metal armor/fasteners fabricated as part of previous laboratory testing.
4. Physical protection of the entire system – Placed the entire unit and wireless router inside a pelican case for additional protection of the AE monitoring equipment.

Figure 9.8 shows the equipment on top of a NEXT beam in the Carrara fabrication plant, along with the detensioning operation. Figure 9.9 shows the equipment in place and testing of the end of a Northeast Bulb Tee girder.

(a) (b)

Figure 9.8: NEXT beam field testing of detensioning (a) field testing equipment setup, (b) torch cutting of pre-tensioning strands

(a) (b)

Figure 9.9: Northeast Bulb Tee girder field testing of detensioning (a) AE equipment/sensor setup, (b) observed horizontal web crack

9.3.2 Craned Form Removal AE Monitoring

AE monitoring filed tests of NEXT beams and NEBT girders during craned form removal collected data on site. The operating conditions and constraints were the same as the detensioning process with the addition of an increased telemetry distance when lifting and craning the beam from the form bed to the finishing area. Equipment modifications described in the above Section 3.2.1 Detensioning AE Monitoring were adequate to power the monitoring system, maintain connectivity during data collection, and protect the AE sensors during craned removal from the form bed, Figure 9.10 and 9.11.

Figure 9.10: NEXT beam field testing of craned form removal

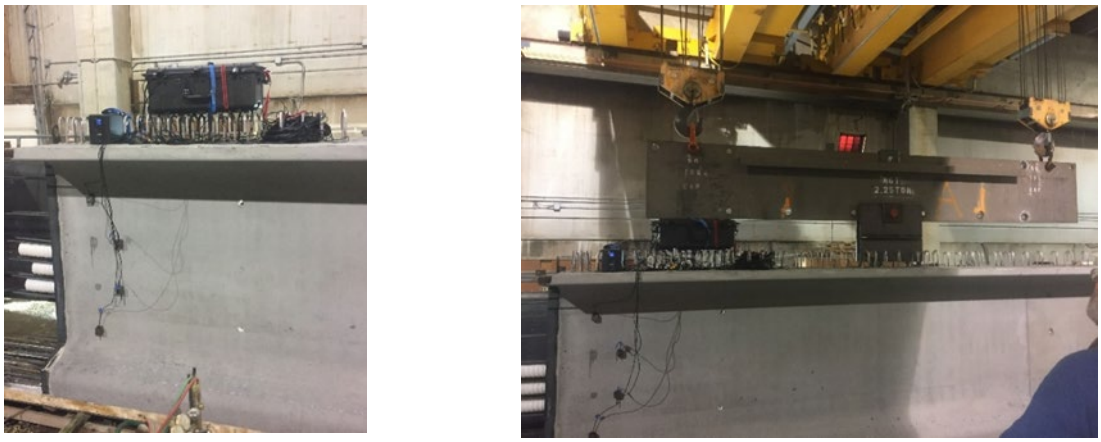

(a) (b)

Figure 9.11: Northeast Bulb Tee beam field testing of detensioning (a) AE equipment setup, (b) gantry crane connection to Northeast Bulb Tee

9.3.3 Transport AE Monitoring

The NEBT girders were the only ones evaluated with measurements during transport. Some factors of concern were:

1. Safely securing equipment;
2. Clearance constraints from overhead powerlines;
3. Exposing the equipment to weather;
4. Maintaining wireless connectivity to the AEwin™ Sensor Highway III;
5. Safety during placement and removal of the AEwin™ Sensor Highway III and associated sensors.

Modifications to both the equipment and attachment procedure mitigated these concerns. The AEwin™ Sensor Highway III which is in an outdoor rated metal housing, was placed directly on the top of the NEBT girder between deck rebar. Gorilla tape secured the wireless router to the outside of the AEwin™ Sensor Highway III. Additional modifications to the AEwin™ Sensor Highway III and wireless router were to receive power from two motorcycle batteries connected in parallel. The placement of this assembly was on top of the NEBT girder using an extension ladder and secured to the NEBT girder with 2-inch wide heavy duty rachet straps looped all the way around the NEBT girder, Figure 9.12. U-shaped brackets with set screws secured the sensors to the beam by: 1. Adhering the U-shaped brackets to the beam with quick setting epoxy and allowing adequate time to harden; 2. Applying high vacuum silicone grease to the sensor wear plates; 3. Placing the sensors in the U-shape brackets and secured with a set screw. Zip ties secured excess cable lengths to the exposed rebar on the top of the beam. Placing a waterproof back pack cover

over the AEwin™ Sensor Highway III with wireless router and a tarp over the AEwin™ Sensor Highway III and batteries protected the instruments from rain.

(a) (b) (c)

(d)

Figure 9.12: Northeast Bulb Tee beam transport testing (a) straight section end zone testing, (b) straight section middle zone testing, (c) AE transport equipment set-up, and (d) hammerhead section middle zone testing

9.4 Reuse and Future Work

9.4.1 Objective and Scope

The purpose of this section is to explore options of reuse of the AE monitoring equipment for future work in AE monitoring and data collection with respect to laboratory testing on relatively small reinforced concrete beams and in the field on full-scale prefabricated and pre-stressed, reinforced concrete Northeast extreme tee (NEXT) beams and Northeast Bulb Tee (NEBT) girders. Proposed future work includes additional laboratory testing, fabrication processes monitoring, and transport monitoring as well as the introduction for AE monitoring during beam placement and long-term service use monitoring. These continued and additional AE data collection scenarios are recommended to provide larger data sets for developing future QA/QC standards and to complete AE monitoring during the complete life cycle of a full-scale prefabricated and pre-stressed, reinforced concrete; 1) fabrication, 2) transport/construction, 3) service use.

9.4.2 Additional Data Collection Recommendations

This section provides detailed recommendations for additional AE monitoring and newly proposed AE monitoring.

9.4.3 Additional Laboratory AE Data Collection

Much of the focus of previous research on AE monitoring of reinforced concrete is centered around cyclic loading. Because of this, many of the statistical interpretation and damage assessment algorithms have been developed to require AE data from cycles of loading and unloading over time or with increasing load. Since most of the fabrication processes are single loading event cases, the cracking/damage assessment algorithms currently published are not valid. To develop these algorithms additional laboratory AE data collection would focus on:

1. Creating laboratory scale reinforced concrete beams that mimic full-scale beams in both geometry and reinforcement patterns;
2. Performing cycling loading-unloading to establish parametric AE event waveform criteria for cracking and damage based current published methods;
3. Collect parametric AE event waveform data during loading to failure of the laboratory beams in manners simulating field fabrication processes (i.e. compression testing, three-point flexure testing, and pull-out testing);

4. Establish correlations between parametric AE event data collected in items 2 and 3 to develop cracking/damage algorithms for single loading event cases.

The above laboratory testing would require, for each simulated beam type, a minimum of three cyclic loading tests to establish base line criteria, three sets of three-point flexure tests using a 2D sensor array, three sets of three-point flexure tests using a 3D sensor array, three sets of compression tests using a 3D sensor array, and three sets of pull-out tests using a 3D sensor array.

9.4.4 Additional Fabrication AE Data Collection

AE data collection during fabrication of full-scale prefabricated and pre-stressed, reinforced concrete Northeast Extreme Tee (NEXT) beams and Northeast Bulb Tee (NEBT) girders focused on detensioning and craned removal from the formwork. The AE data collected during fabrication lacks replication since each successive data collection event changed various aspects as the AE collection team honed the methodology. At a minimum three replicate tests on each beam type should be performed. In addition, three replicate tests during the craned removal from the formwork with the AE sensor array is moved from the end-zone region to the middle region of the beams would fill-in the database.

Upon competition of these additional tests, AE data collects would then be analyses for comparison to algorithms developed from additional laboratory testing described in Section 5.2.1 Additional Laboratory AE Data Collection.

9.4.5 Additional Transport AE Data Collection

Current AE data collection during transport is limited to Northeast Bulb Tee (NEBT) girders and one test each of the end zone of a straight span beam, middle zone of a straight span beam, and middle zone of a hammerhead beam. This limited data set was due to timing constraints of beam transport for the Rockingham I-91 bridge construction project. Only three data collection events were possible and rather than repeat data collection, it was decided to collect different data sets in areas that would experience different stress distributions and magnitudes. It would be of interest to complete two additional replicate tests of the three already perform AE data collections during transport next construction season when the southbound bridge is constructed. Similarly, this would allow for a minimum of three AE data sets during transport for each of the beam regions tested; allowing for the development of algorithms to assess cracking/damage of beams during transport.

9.4.6 AE Monitoring During Beam Placement

AE monitoring during beam placement was not performed during this project due to time constraints and needed coordination with the contractor. The Rockingham I-91 bridge construction project included the craned placement of NEBT girders from the staging area into to place on the abutments/bents. Since the placement of the NEBT's used a crane, there were safety concerns and coordination issues to disconnect and retrieve the AE monitoring equipment and sensors after placement. Ideally, the AE monitoring equipment would stay in-place from transport testing and would allow for consistency in AE data collection between transport AE data collection and placement AE data collection.

9.4.7 Long-Term Service Use AE Monitoring

AE monitoring of long-term service use was not performed during previous AE testing due to project scope, limited data storage space, and the need for a continuous power supply. AE monitoring of long-term service use would require additional AE channels to incorporate more AE sensors to provide a larger study area. Long-term service use monitoring would also require either cloud access for data storage or a larger hard drive for AE data storage. Additionally, either a cabled power source or solar power source would be required along with a battery back-up to provide continuous, uninterrupted AE data collection. Long-term monitoring at an exterior girder, interior girder, middle span, and end span would be recommended for data collection to cover all regions of the bridge.

9.5 Summary of Conclusions and Equipment Modifications

9.5.1 Conclusions and Recommendations

This report focused on the effectiveness of the AE monitoring equipment used as part of a study into the efficacy of AE sensing as a potential Quality Assurance/Quality Control (QA/QC) procedure in locating the sources of AE events during laboratory testing on relatively small reinforced concrete beams and in the field on full-scale prefabricated and pre-stressed, reinforced concrete Northeast extreme tee (NEXT) beams and Northeast Bulb Tee (NEBT) girders during detensioning, craned form removal, and transport processes. Laboratory and field tests each presented unique challenges and constrains for the space, deployment, timing, and collection of AE event data which required modifications to the Mistras AEwin^{TM} Sensor Highway III monitoring system. These alterations included:

1. Portable power supply (7-hour minimum supply life);
2. Wireless router for remote connection to the Mistras AEwin^{TM} Sensor Highway III;

3. Metal AE sensor armor/fasteners

Although these modifications allowed for the completion of laboratory and field tests for this study, further improvements and modifications for future testing could: increase resolution, increase monitoring areas, speed deployment and breakdown, reduce the physical efforts of deployment, and increase uniformity between deployments. These improvements and modifications with a total cost of about $11,000 include;

1. Quick connect portable and rechargeable power supply (7-hour minimum supply life);
2. Integrated long range wireless router housed in the NEMA-4 rated enclosure;
3. Remote wireless AE sensors;
4. Additional AE sensors (additional 24 sensors to fill the current 32 channel capacity);

Additionally, the time allotted, project scope, and fabrication schedules left a large amount of additional testing to be desired. These tests include additional detensioning, craned removal from formwork, and transport monitoring as well as the introduction for AE monitoring during beam placement and long-term service use monitoring.

CHAPTER 10

CONCLUSIONS AND FUTURE RECOMMENDATIONS

This project has a variety of goals that were achieved through a mapped path of project objectives; designed to test the efficacy of AE sensing technologies use as a Quality Assurance/Quality Control (QA/QC) procedure for the fabrication and transport of pre-fabricated and pre-stressed, reinforced concrete beams and girders. Conclusions indicate that AE sensing may be practical QA/QC process for PBES elements as there is observational correlation to observed cracks and AE event locations as well as the AE instrumentation being portable and deployable enough to collect data during both the fabrication and transportation processes. The tests conducted in this study largely validate the methodology and procedures for data collection., However, the development specific accept/reject criteria for use as a QA/QC procedure requires additional data collection.

10.1 Conclusions from AE Laboratory Testing

Laboratory experiments on relatively small reinforced concrete beam specimens under pull-out and three-point bending yielded proof of concept and guidance on data acquisition setup parameters for field testing. These include:

1. Appropriate amplitude and duration filters to remove background noise;
2. Verification of wave mode velocities through pencil lead break tests;
3. Verification of correlation between AE events and observed cracks; and
4. Selection of appropriate sensor array.

Laboratory pull-out and three-point bending (flexure) testing yielded correlations between AE events and cracking and indicated that a 2-D planar sensor array was more accurate in AE event source location than a 3-D sensor array. One possibility for the difference in accuracy is the use of measured wave speed velocity used in the 2-D location algorithm versus the empirical relationship estimates of wave speed velocities used in the 3-D sensor array.

10.2 Conclusions from AE Fabrication Testing

This chapter demonstrates the viability of AE sensing in detecting and locating cracks in prefabricated pre-stressed concrete girders used as PBES in ABC, which could potentially be used as a QA/QC technique. AE field data collected from the Bulb Tee showed more recorded AE events during the torch cutting of pre-tensioning strands than for the same process on the NEXT beam. This could be due to the thin web and dense packing of pre-stressing strands guiding the AE waves and reducing attenuation

within the Bulb Tee girder. A key observation made during the detensioning processes was the appearance of horizontal cracks in the web of the Bulb Tee girder. The crack lengths ranged between 127 mm and 508 mm with vertical spacing between cracks ranging from 35 mm to 813 mm, as quantified in Table 1.

Table 10.1: Quantification of AE Events Versus Number of Observed Cracks

Beam type	# of observed AE events during detensioning	# of observed AE events during craned form removal	# of observed cracks (crack lengths)
NEXT beam	38	20	0
Straight bulb tee	466	12	7 (127mm-508mm)
Haunched bulb tee	960	16	6 (127mm-432mm)

The observed end zone cracking occurred both within and outside of the region directly covered by the AE sensor array for the Bulb Tee girders beams and AE event location distributions indicate differences between the 3-D and 2-D sensor arrays.

AE event data collected from multiple fabrication processes including the detensioning of pre-tensioning strands embedded in NEXT beams and Bulb Tee's yielded internal AE events indicative of crack nucleation. AE events recorded above the 60-dB amplitude pre-filter determined through laboratory testing may be indicative of internal cracking and provide an approximation of crack location. Additionally, the AE monitoring determined which fabrication process is responsible for the most AE events, which could point to the critical fabrication processes responsible for crack nucleation. A is highlight is the Bulb Tee beam field data that showed far more AE events occurred during the detensioning of the Bulb Tee than during the craned removal from its form bed.

Although, AE technology has been proven to reliably detect material failure of composite materials such as composite fuel tanks and as such is an acceptable QA/QC technology for industry practice (ASTM E2191/E2191M-16, 2016), it is not yet a proven technique for use with pre-tensioned, pre-cast concrete as an acceptable QA/QC technology for industry practice. Additionally, future work includes AE source discrimination and data collection during transportation, installation, and service of full-scale NEXT beams and Bulb Tee girders.

10.3 Conclusions from AE Transport Testing

Field testing during transport of full-scale Northeast Bulb Tee (NEBT) girders produced the following findings:

1. The AE test equipment required modest levels of custom modification for the transport tests.
2. The test equipment performed flawlessly during the tests and did not sustain any visible or notable damage.

3. Differences in AE event patterns were observed between end zone and middle zone regions along with between straight sections and hammerhead sections.
4. Large quantities of AE events were recorded without correlation to observed cracks during transport.
5. Finite element modeling indicates areas of high stress corresponding to areas of dense AE event locations.
6. Additional data sets are required for statistical clustering and logistical regressions to define an AE event feature signature of cracks from other AE event source types.

Field tests on NEBT's provided an abundance of AE event data during critical stages of the fabrication and transportation processes. AE event data were collected when cracking was observed and when cracking was not observed. Through the use of a finite element model it was concluded that AE events tend to occur in areas of high stress and the presence of AE events does not necessarily indicate the occurrence of cracking. Continued work on AE event source discrimination to identify the feature signatures related to cracking, regions of high stress, or otherwise is still an ongoing process and requires additional data sets; however, this work has set the foundation for understanding when cracks tend to occur, where the key areas to concentrate sensors are, and what processes are of the highest stress to the NEBT's prior to service.

10.4 Conclusions for Proposed Accept and Reject Criteria

This study focuses on the development of accept/reject criteria for full-scale prefabricated and pre-stressed, reinforced concrete Northeast Extreme Tee (NEXT) beams and Northeast Bulb Tee (NEBT) girders based on Acoustical Emission (AE) monitoring as a Quality Assurance/Quality Control (QA/QC) procedure during the detensioning, craned form removal, and transport processes. Although there are many published damage assessment techniques for reinforced concrete, these techniques are based on cyclic loading and are not compatible with loading conditions observed during the fabrication and transport of the NEXT and NEBT beams. Loading of the full-scale prefabricated and pre-stressed, reinforced concrete NEXT beams and NEBT girders is either a single near-instantaneous event or a variable self-weight loading event. Of the five common reinforced concrete damage assessment techniques (felicity ratio; parametric analysis; load-calm ratio; b-value analysis; frequency analysis) only the parametric, b-value, and frequency analyses were determined to be adaptable to the field loading conditions experienced by the NEXT and NEBT beams during fabrication and transport.

The three potential damage assessment methods are;

1. The use of a parametric analysis using AE event waveform features to develop algorithms relating the unique features to observed damage types and severities;
2. To build a database of b-value's (using the published b-value damage assessment technique) for specific beams and processes. The database would indicate the upper and lower bounds for a typical b-value and therefore establish the upper and lower limits for accepting/rejecting the beam. Additionally, the frequency analysis would then be used to identify the AE source or damage type that lead to the rejection of the beam;
3. Based on AE data collected and analyses from laboratory and field testing, AE events tended to have dense clustered near the location of observed. It is hypothesized a damage assessment could be performed based on AE event clustering density. Once damage established the frequency analysis would then be used to identify the AE source or damage type.

In the case with all three of the potential accept/reject damage assessment techniques, large AE data sets are needed for each beam type, reinforcement pattern, pre-tensioning strand pattern, and concrete mixture. Data sets need to include instances of varying observed damage from no damage to major damage in order to establish the lower and upper limits of acceptable AE emissions. It is not possible to establish accept/reject criterion based on the currently limited AE event database; however, the current database has presented a new and unique possibility for damage assessment as well as validated the efficacy of AE technology as a potential Quality Assurance/Quality Control (QA/QC) procedure in locating the sources of AE events associated with cracking or high strain events.

Future work would be to conduct a large laboratory testing regimen over an extended period of time on a single type of commonly produced beam or girder to build a large AE database for all processes that are associated with cracking or high strain events. Once a large AE database is established with visual observations of damage, conditions, and element performs; the three potential AE damage assessment techniques can be implemented and compared to determine the effectiveness for use as accept/reject criterion.

10.5 Conclusions for AE Monitoring Equipment Reuse and Future Development

Laboratory and field tests each presented unique challenges and constraints for the space, deployment, timing, and collection of AE event data which required modifications to the Mistras AEwin^{TM} Sensor Highway III monitoring system. These alterations included:

1. Portable power supply (7-hour minimum supply life);

2. Wireless router for remote connection to the Mistras AEwin™ Sensor Highway III;
3. Metal AE sensor armor/fasteners

Although these modifications allowed for the completion of laboratory and field tests for this study, further improvements and modifications are warranted for future testing to: increase resolution, increase monitoring areas, speed deployment and breakdown, reduce the physical efforts of deployment, and increase uniformity between deployments. These improvements and modifications include;

1. Quick connect portable and rechargeable power supply (7-hour minimum supply life);
2. Integrated long range wireless router housed in the NEMA-4 rated enclosure;
3. Remote wireless AE sensors;
4. Additional AE sensors (additional 24 sensors to fill the current 32 channel capacity);

Items 1 and 2 can be easily purchased and retrofitted to the current Mistras AEwin™ Sensor Highway III monitoring system. Item 3 is not yet a product offered by the current Mistras AEwin™ Sensor Highway III manufacturer, but the technology does exist through different providers. Item 4 can be purchased through the manufacturer of the Mistras AEwin™ Sensor Highway III monitoring system. The price for an addition 24 AE sensors identical to the current eight sensor array is $406 per sensor totaling $9,744 for 24 sensors, based on a 2016 quotation.

Additionally, the time allotted, project scope, and fabrication schedules left a large amount of additional testing to be desired. These tests include additional detensioning, craned removal from formwork, and transport monitoring as well as the introduction for AE monitoring during beam placement and long-term service use monitoring.

REFERENCES

Acoustic Emission Testing. (n.d.), NDT Resource Center, <https://www.nde-ed.org > (Jul. 14, 2018).

ARCHES Strategic Targeted Research Project. *Assessment and Rehabilitation of Central European Highway Structures – Annex C: The acoustic Emission Method*, pp. C-21 – C-32. 2009.

ASTM E1316-18a, Standard Terminology for Nondestructive Examinations, ASTM International, West Conshohocken, PA, 2018, www.astm.org

ASTM E2191 / E2191M-16, Standard Practice for Examination of Gas-Filled Filament-Wound Composite Pressure Vessels Using Acoustic Emission, ASTM International, West Conshohocken, PA, 2016, www.astm.org

ASTM E3100-17, Standard Guide for Acoustic Emission Examination of Concrete Structures, ASTM International, West Conshohocken, PA, 2017, www.astm.org

Aysal, U. (n.d.). "*The Piezoelectric Effect*." Academia.edu - Share research, PZT Application Manual, <http://www.academia.edu/9056282/PZT_Application_Manual_The_Piezoelectric_Effect> (Sep. 18, 2018).

Baxter, M. G., Pullin, R., Holford, K. M., and Evans, S. L. (2007). "Delta T source location for acoustic emission." *Mechanical Systems and Signal Processing*, 21(3), 1512–1520.

Chen HL, He Y. (2001) "Analysis of Acoustic Surface Waveguide for AE Monitoring of Concrete Beams" J Eng Mech, V 127, N 1

ElBatanouny, M. K., Larosche, A., Mazzoleni, P., Ziehl, P. H., Matta, F., and Zappa, E., *Identification of Cracking Mechanisms in Scaled FRP Reinforced Concrete Beams using Acoustic Emission*, Experimental Mechanics, vol. 54, no. 1, pp. 69–82, Jan. 2014.

Grosse, C. U., and Ohtsu, M. (2008). *Acoustic emission testing: [basics for research, applications in civil engineering*. Springer, Berlin.

Hasenkamp, C. J., Badie, S. S., Tuan, C. Y., and Tadros, M. K., *Sources of End Zone Cracking of Pretensioned Concrete Girders*, 2008.

Head M, Efe S, Grose S, Drumgoole J, Lajubutu O, Wright R, Hansboro T. (2015) "Durability Assessment of Prefabricated Bridge Elements and Systems" Final Report, MD-13-SP309B4E, Maryland State Highway Administration, Office of Policy & Research, 707 North Calvert Street, Baltimore MD 21202

Hensman, J., Mills, R., Pierce, S. G., Worden, K., and Eaton, M. (2010). "Locating acoustic emission sources in complex structures using Gaussian processes." *Mechanical Systems and Signal Processing*, 24(1), 211–223.

Huang Q, Nissen GL. (1997) "Structural Health Monitoring of DC-XA LH2 Tank Using Acoustic Emission" Structural Health Monitoring Current Status and Perspectives, Technomic Publishing, Lancaster

Huston D., Structural Sensing Health Monitoring and Prognosis, CRC Taylor & Francis, Boca Raton, FL, 2011.

Kaphle, M, Tan ACC, Thambiratnam, DP and Chan, THT, *Effective discrimination of acoustic emission source signals for structural health monitoring, in Advances in Structural Engineering*, 15(5): 707-716. 2012a

Kaphle, M, Tan ACC, Thambiratnam, DP and Chan, THT, *Identification of acoustic emission wave modes for accurate source location in plate-like structures, in Structural Control and Health Monitoring* 19(2): 187-198. 2012b

Krautkrämer, J. and Krautkrämer, H., *Ultrasonic Testing by Determination of Material Properties*, in Ultrasonic Testing of Materials, Springer, Berlin, Heidelberg, 1990, pp. 528–550.

Landis EN, Baillon L. (2002) "Experiments to Relate Acoustic Emission Energy to Fracture Energy of Concrete" J Eng Mech, V 128, 6

Lee, Y. H. and Oh, T., *The Measurement of P-, S-, and R-Wave Velocities to Evaluate the Condition of Reinforced and Pre-stressed Concrete Slabs*, Advances in Materials Science and Engineering, 2016.

MoDOT (2018). "*751.22 P/S Concrete I Girders. 751.22 P/S Concrete I Girders*," Engineering Policy Guide.

NJIT Online RSS, *"MSCE Articles."* (n.d.). , <https://graduatedegrees.online.njit.edu/msce-articles/an-introduction-to-pre-stressed-concrete/> (Sep. 18, 2018).

Okumus P., Kristam R. P., and Arancibia M. D., "*Sources of Crack Growth in Pretensioned Concrete-Bridge Girder Anchorage Zones after Detensioning*," *J. Bridge Eng.*, vol. 21, no. 10, p. 04016072, Oct. 2016.

Okumus, P. and Olivia, M. G., *Evaluation of crack control methods for end zone cracking in pre-stressed concrete bridge girders*, PCI J., pp. 91–105, SPR 2013.

Physical Acoustics. *Sensor Highway III Product Data Sheet*, MISTRAS Group, Inc., Princeton, NJ. 2018

Precast/Pre-stressed Concrete Institute Northeast. *Guidelines for Accelerated Bridge Construction Using Precast/Pre-stressed Concrete Elements Including Guideline Details*, 2nd Edition, pp. 1–48. 2014.

Ronanki V. S., Burkhalter D. I., Aaleti S., Song W., and Richardson J. A., "*Experimental and analytical investigation of end zone cracking in BT-78 girders*," *Eng. Struct.*, vol. 151, pp. 503–517, Nov. 2017.

Sause, M. G. R. (n.d.). *Investigation of Pencil-Lead Breaks as Acoustic Emission Sources*, Journal of Acoustical Emmision (29)., pp. 184-196, 2011.

Steel Auto Industries, "*Supervision of Pre-stressing*" |, <http://www.steelautoindustries.com/supervision-of-pre-stressing/> (Sep. 18, 2018).

Tensi, H., *The Kaiser-Effect and its Scientific Background*. Journal of Acoustic Emission, 22, pp.S1-S16. 2004.

Tuan C. Y., Yehia S. A., Jongpitaksseel N., and Tadros M. K., "*End zone reinforcement for pretensioned concrete girders*," *PCI journal*, vol. 49, no. 3, p. 68, 2004.

Vallen, H. (2009). "*AE Testing Fundamentals, Equipment, Applications*." NDT.net, 7(9).

Vejvoda M. F., (2018) “Post-tensioning vs. Pre-tensioning,” Post-tensioning Institute – NPCA Education – PTI Seminar.

VTrans (2015) “VTrans Strategic Plan Mission, Vision, Goals and Objectives” Vermont Agency of Transportation, Montpelier, VT

Worley II, R. L., Dewoolkar, M. M., Xia T., Farrell R., Orfeo D., Burns D., Huston D. R., (2018) *Acoustic emission sensing for crack monitoring in prefabricated and pre-stressed reinforced concrete bridge girders*, ASCE Journal of Bridge Engineering, Special Edition, (Submitted).